AGE-RELATED CHANGES OF OCULAR DIMENSIONS IN WHITE LEGHORN CHICKEN WITH ADDITIONAL INSIGHTS ON AN OCULAR HYPERTENSION MODEL IN THE CHICKEN

A thesis presented to the graduate faculty of
New England College of Optometry in partial fulfillment
of the requirements for the degree of Master of Science

Jennifer L. Choi, O.D.

December, 2013

© Jennifer Choi
All rights reserved

The author hereby grants New England College of Optometry permission to reproduce and to distribute publicly paper and electronic copies of the thesis document in whole or in part.

AGE-RELATED CHANGES OF OCULAR DIMENSIONS IN WHITE LEGHORN CHICKEN WITH ADDITIONAL INSIGHTS ON AN OCULAR HYPERTENSION MODEL IN THE CHICKEN

Jennifer L. Choi, O.D.

This manuscript has been read and accepted by the
Thesis Committee in satisfaction of the
thesis requirement for the degree of Master of Science

12-04-13
Date

Stacey S. Choi, Ph.D.
Graduate Faculty Advisor

Steven Koevary, Ph.D.
Thesis Committee Member

Frank Thorn, O.D., Ph.D.
Thesis Committee Member

Radouil Tzekov, M.D., Ph.D.
Thesis Committee Member

12-12-13
Date

Nancy J. Coletta, O.D., Ph.D.
Director of Graduate Studies

New England College of Optometry

Abstract

AGE-RELATED CHANGES OF OCULAR DIMENSIONS IN WHITE LEGHORN CHICKEN WITH ADDITIONAL INSIGHTS ON AN OCULAR HYPERTENSION MODEL IN THE CHICKEN

Jennifer L. Choi

New England College of Optometry, 2013

Purpose. While chickens have been used to study physiological optical properties of the eye and conditions such as myopia, there is limited information on the growth of ocular dimensions in chicken over an extended period of time and a lack of in vivo studies that investigated the potential of the chicken as a model of ocular hypertension or glaucoma. Therefore, we investigated the dynamics of eye growth (age range: 21-107 days), and the potential of the chicken as an experimental animal model of elevated intraocular pressure (IOP) and glaucoma, using ultrasound imaging and spectral domain optical coherence tomography (SD-OCT).

Methods. In chicken, eyes without any injections and those with anterior chamber injections of saline were used to study growth of ocular parameters, while other eyes were subjected to anterior chamber injections of microbeads in an attempt to increase IOP. Twenty chickens (12-110 days old) were divided into control animals (no injections in either eye (n = 3); injection with saline in one eye only (n = 2)), while the rest of the animals were subjected to one of 13 combinations of doses and types of magnetic and/or non-magnetic microbead injections into the anterior chamber angle in both eyes (n = 3) or one eye with the other eye used as a control (n = 12: 5 eyes (saline solution injected); 7 eyes (no injections)). For estimation of eye growth parameters, A-scan ultrasound biometry (35 MHz) was used to

measure corneal thickness (CrT), anterior chamber depth (ACD), lens thickness (LT), vitreous chamber depth (VCD), retinal thickness (RT), and choroidal thickness (ChT) in all non-injected eye(s) and one saline control animal. Refractive error (RE) was monitored in non-injected control eye(s). SD-OCT was used to measure retinal nerve fiber layer (RNFL) and total retinal thickness (RT) near the optic disc in all non-injected animals and in one animal that had an elevation in IOP. IOP was monitored in all eyes.

Results. Several parameters (CrT, LT, VCD and axial length (AL)) showed exponential growth with 95% maturation occurring within the observed time frame and predicted complete maturation by ~ 1 year of age, while ACD was predicted to continue to deepen beyond one year post-hatching. ChT and RE appeared stable over time. RT (at the visual axis, 0.5 to 2.5 degrees eccentricity from the optic disc), and RNFL thickness (0.5 to 2.5 degrees) were also stable in both control animals and in one animal that had a transient elevation in IOP. Growth equations were determined. Out of 15 microbead injected animals, elevation of IOP with a clear visual axis was achieved in two animals with magnetic microbeads, resulting in an elevation of 5- 8 mm Hg (3 - 7 days). Saline injections in one animal resulted in a decrease in LT in the injected eye. No effect on IOP was observed in any of the 7 saline injected eyes.

Conclusions. A comprehensive description of the growth pattern of ocular structures in White Leghorn chicken during the period 21-107 days post-hatching is provided and discussed in the context of other studies. The feasibility of IOP elevation via magnetic microbeads injections into the anterior chamber of chicken eyes and its potential to be a model of ocular hypertension and/or glaucoma was also explored.

Acknowledgements

I would first like to express outpouring gratitude and admiration to Dr. Stacey Choi and Dr. Radouil Tzekov for their time, expertise, continued support, encouragement, and guidance, for which this thesis would not have been possible without. Furthermore, I dedicate this thesis to them.

I have a multitude of gratitude for those directly involved with technical assistance of my research projects. I would like to thank all my committee members for their time (Dr. Koevary, Dr. Thorn, Dr. Tzekov), and especially Dr. Tzekov and Dr. Koevary for their aid with injections and developing protocols. I would also like to thank Dr. Nickla, Dr. Koevery, and Dr. Coletta for their generosity in sharing lab equipment. I am deeply appreciative of Dr. Nickla and Kristin Totonelly, as they were invaluable to proper training with equipment, handling of the animals, and developing protocols. I would like to thank Rebecca Kivlin for aiding with data collection. I would also like to thank Dr. Doble and Dr. Choi for their expertise in optics, which they generously shared. In addition, I would like to thank Dr. James Morgan for his visit and demonstration of microbead injections in rats.

I would also like to thank the New England College of Optometry for the opportunity to not only advance as an optometric clinician but as a vision scientist. I would especially like to thank Dr. Fisch and Barbara McGinley for their continued emotional support and guidance. In addition, I am appreciative of those who had involvement with administration, teaching, execution, and/or funding of the dual Doctorate of Optometry and Master of Science in Vision Science (OD/MS) program. As funding is essential to keeping research

projects running, I am appreciative of aid from the New England College of Optometry as well as the National Institutes of Health (NIH) grant EY007149.

Table of Contents

ABSTRACTS BASED ON MATERIAL PRESENTED IN THE PRESENT THESIS 12

LIST OF FIGURES 13

LIST OF TABLES 14

ABBREVIATIONS 15

CHAPTER 1: GENERAL INTRODUCTION 17

CHAPTER 2: AGE-RELATED CHANGES OF OCULAR DIMENSIONS IN THE WHITE LEGHORN CHICKEN 19

2.1 INTRODUCTION 19

2.2 MATERIALS AND METHODS 21

2.2.1 Animals 21

2.2.2 Ultrasound Biometry 23

2.2.2.1 Ultrasound Biometry Method of Measurement 25

2.2.3 Refractive Error Measurement 25

2.2.3.1 Refractometry 25

2.2.3.2 Streak Retinoscopy 26

2.2.4 Optical Coherence Tomography (OCT) 26

2.2.5 Estimation of Ocular Growth Parameters of Published Non-Primate and Primate Studies 29

2.2.6 Statistical Analysis 29

2.3 RESULTS 30

2.3.1 Growth of Ocular Dimensions 30

2.3.2 Corneal Thickness 37

2.3.3 Anterior Chamber Depth 37

2.3.4 Lens Thickness 38

2.3.5 Vitreous Chamber Depth 38

2.3.6 Retinal Thickness 39

2.3.7 Choroidal Thickness 39

2.3.8 Axial Length 39

2.3.9 Refractive Error 40

2.3.10 A Summary of Ocular Parameters with Exponential Growth 41

2.3.11 Gender Comparisons 44

2.3.12 Comparison of Some Ocular Parameter Values with Published Studies 44

2.3.13 Changes in Retinal and Nerve Fiber Layer Thickness with Eccentricity and Age 45

2.3.13.1 Changes with Eccentricity 45

2.3.13.2 Changes with age 45

2.4 DISCUSSION 48

2.4.1 Growth of Ocular Parameters with Age 48

2.4.2 Corneal Thickness 48

2.4.3 Anterior Chamber Depth 50

2.4.4 Lens Thickness 51

2.4.5 Vitreous Chamber Depth 52

2.4.6 Retinal Thickness 52

2.4.7 Choroidal Thickness 53

2.4.8 Axial Length 54

2.4.9 Refractive Error 55

2.4.10 Cross-Sectional vs. Longitudinal Data 57

2.4.11 Gender Differences 58

2.4.12 Changes in RNFL thickness and RT with Eccentricity and Age 59

2.4.13 SD-OCT imaging 60

2.4.14 Comparison of Ocular Parameter Growth Rates 60

2.4.14.1 ACD Growth 60

2.4.14.2 CrT, VCD, and AL growth 62

2.4.14.3 Similarities in Growth of Ocular Parameters to Chickens and Other Species 64

2.4.14.4 Differences in Growth of Ocular Parameters to Chickens and Other Species 66

2.4.14.5 Summary of Ocular Growth 68

2.4.15 Possible Confounding Factors and Limitations of the Present Study 70

2.5 CONCLUSIONS 72

CHAPTER 3: OCULAR HYPERTENSION MODELS IN CHICKEN: FEASIBILITY AND FUTURE DIRECTIONS 73

3.1 INTRODUCTION 73

3.2 MATERIALS AND METHODS 78

3.2.1 Animals 78

3.2.2 Intraocular Pressure 81

3.2.3 Microbead Injected Eyes 82

3.2.3.1 Purification of Microbeads (magnetic and non-magnetic) 82

3.2.3.2 Anterior Chamber Injections of Magnetic Microbeads 83

3.2.3.3 Spectral Domain Optical Coherence Tomography (SD-OCT) of one Ocular Hypertensive animal 85

3.2.4 Saline Control Eyes 85

3.2.4.1 Injection of Saline Control Eyes 86

3.2.4.2 Ultrasound Biometry of a Saline control animal 86

3.2.5 Statistical Analysis 87

3.3 RESULTS 87

3.3.1 Control Eyes 87

3.3.1.1 IOP of non-injected Control Animals 88

3.3.1.2 IOP of non-injected and saline-injected Control Eyes 92

3.3.1.3 Ultrasound Biometry of a Saline Control Animal 94

3.3.2 Microbead-injected Eyes 95

3.3.2.1 IOP of all Microbead-injected Eyes 96

3.3.2.2 SD-OCT Imaging of one Ocular Hypertensive Animal 99

3.4 DISCUSSION 100

3.4.1 IOP of Control Animals and Eye(s) 100

3.4.1.1 IOP of non-injected Control Animals and Eye(s) 100

3.4.1.2 IOP of saline-injected Control Animals and Eye(s) 102

3.4.2 Elevation in IOP via Anterior Chamber Injections of Microbeads in the Present Study 102

3.4.2.1 Elevation in IOP with Microbead Injections of Chicken in the Present Study vs. Primates and Rodents 103

3.4.2.2 The Protocol for Microbead Injections of Elevated IOP may be Age-Dependent 106

3.4.2.3 Magnetic Microbead Elevation in IOP in the Present Study Differs from Constant Light Induced Elevation in IOP 107

3.4.3 Comparison of Elevation of IOP in the Present Study to Past Studies 108

3.4.4 Questionable Gender Differences in Elevation of IOP 109

3.4.5 Could the Elevation in IOP be a Result of the Material Composition itself? 109

3.4.6 SD-OCT Imaging of an Animal with Elevated IOP 110

3.4.7 The Effect of Saline Injections on Lens Thickness (LT) 111

3.4.8 Possible Confounding Factors and Limitations of the Present Study 112

3.4.9 Future Directions on the use of the Chicken for in-vivo Experimental Chicken Models of Elevated IOP 113

3.5 CONCLUSIONS 114

CHAPTER 4: GENERAL DISCUSSION AND CONCLUSION 115

BIBLIOGRAPHY 117

ABSTRACTS BASED ON MATERIAL PRESENTED IN THE PRESENT THESIS:

Abstracts

Choi, J.L., Tzekov, R.T., Choi, S.S. (2012). Age-related changes in ocular parameters in White Leghorn chickens. *Invest Ophthalmol Vis Sci. 53*, ARVO (the association for research in vision and ophthalmology) E-Abstract 141

Choi, J.L., Tzekov, R.T., Choi, S.S. (2013). Future insights on an ocular hypertension model in the White Leghorn chicken. *Invest Ophthalmol Vis Sci. 54*, ARVO E-Abstract 6054

Journal Publications

Age-Related Changes of Ocular Dimensions in White Leghorn Chicken. In preparation.

Ocular Hypertension Models in Chicken: Feasibility and Future Directions. In preparation.

LIST OF FIGURES

Figure 2-1: Representative ultrasound A-scan tracings……..24

Figure 2-2: Positioning of the SD-OCT B-scan……..27

Figure 2-3: Representative SD-OCT B-scan……..28

Figure 2-4: Cross-sectionally measured ocular parameters vs. age……31

Figure 2-5: Comparison of growth of ocular parameters……32

Figure 2-6: Asymptotic growth of ocular parameters with age…….…….42

Figure 2-7: Calculated percent contribution of ACD, LT, and VCD towards AL with time.43

Figure 2-8: Total RT and RNFL thickness as a function of eccentricity and age……..47

Figure 2-9: RNFL thickness, RT, and RNFL thickness vs. RT as a function of age and eccentricity……...…48

Figure 3-1: Representative image of the distribution of magnetic microbeads in an animal that developed IOP and the fellow eye of the same animal……..…84

Figure 3-2: Fluctuation of IOP during daylight hours……...…….89

Figure 3-3: IOP vs. age for non-injected control animals……...90

Figure 3-4: IOP vs. age for non-injected and saline injected control eyes…….93

Figure 3-5: Ultrasound biometry of a saline control animal……...…94

Figure 3-6: IOP vs. age for microbead injected eyes with no resultant elevation in IOP…..97

Figure 3-7: IOP vs. age for two animals with elevated IOP……..… 98

Figure 3-8: Total RT, RNFL thickness, and ratio of RNFL thickness to RT in an animal with elevated IOP…….……99

LIST OF TABLES

Table 2-1: Demographics of the animals used in the study……23

Table 2-2: Comparison of ultrasound biometry fits of selected studies……..…35

Table 2-3: Comparison of ocular parameters with exponential growth……..…36

Table 2-4: Species comparisons of relative % contribution of ACD, LT, and VCD to AL of selected studies…….43

Table 2-5: Comparison of cross-sectional data between selected studies……...44

Table 2-6: Growth equations for RNFL thickness, RT, and ratio of RNFL thickness to RT……..……..46

Table 3-1: Demographics of non-injected and injected birds……..80

Table 3-2: Physiological IOP and method of IOP measurement (past studies vs. the present study)……..……..91

Table 3-3: Elevated IOP via different methods (past studies vs. the present study).……..92

ABBREVIATIONS

ACD	anterior chamber depth
ANOVA	analysis of variance
AO	adaptive optics
ARVO	the association for research in vision and ophthalmology
CrT	corneal thickness
ChT	choroidal thickness
F	female
FOV	field of view
GCL	ganglion cell layer
ILM	inner limiting membrane
IOP	intraocular pressure
IR	infrared
LASEK	laser supepithelial keratomileusis
LT	lens thickness
LONGITUD	longitudinal
M	male
mm	millimeter
ms	millisecond
MHz	megahertz
NIH	national institutes of health

OCT	optical coherence tomography
OD	right eye
OD/MS	doctor of optometry/ master in vision science
OS	left eye
OU	both eyes
RE	refractive error
RNFL	retinal nerve fiber layer
RPE	retinal pigment epithelium
RT	total retinal thickness
SD-OCT	spectral-domain optical coherence tomographer/tomography
VCD	vitreous chamber depth
μm	micrometer

CHAPTER 1: GENERAL INTRODUCTION

A large proportion of ocular research is devoted to animal models of both normal and abnormal ocular development to better understand these processes in humans. Animal models are commonly employed as they are more cost-effective, easily obtainable, and grow faster in comparison to humans. In particular, the chicken is commonly used for these reasons and also because of its relatively large eyes, ocular anatomical and functional similarities (Glasser, Murphy, Troilo & Howland (1995); Renard, Hirsch, Savoldelli & Pouliquen (1980), Tripathi & Tripathi (1973)), and because it's cone-dominated retina (Kram, Mantey, & Corbo (2010); Meyer & May (1973) and optical properties allow for in - vivo imaging (Headington et al. (2011); Kisilak et al. (2012)). An abundance of the ocular literature utilizing the chicken has been for further understanding of ocular conditions such as myopia, form deprivation, or emmetropization (Avila & McFadden (2010); Schaeffel & Howland (1988); Nickla, Wildsoet & Wallman (1998), Zhu, Lin, Stone & Laties (1995); Wallman & Adams (1987); Weiss & Schaeffel (1993); and many more). Thus, better understanding of the etiology and mechanism of these processes in chickens has the potential to provide additional insights into prevention and treatment of these refractive conditions in humans. Other investigators and specifically those at the New England College of Optometry have extensively and successfully used chicken as animal models of these particular ocular conditions. As sight threatening conditions such as myopia and form deprivation could possibly be due to emmetropization gone awry, one popular topic of investigation has been the understanding of the normal emmetropization process. Thus,

studying emmetropization might shed new insights into the pathogenesis of such pathological conditions. The majority of ocular studies in chickens, utilized chickens less than 4 weeks of age, some used chickens over one year post-hatching, but very few have studied the chicken between 4 weeks and 1 year of age. Out of the few studies in chickens that investigated normal growth of ocular structures within this range, a limited number of ocular structures were studied and some of the results were not consistent between studies. Thus, little is known about normal ocular development or about ocular disease processes such as glaucoma during this interval. Furthermore, we sought to better understand the normal emmetropization process and its relationship to the growth of many of the ocular components of the eye in the juvenile chicken with an additional emphasis on the feasibility of the use of chicken as an animal model of elevated intraocular pressure (IOP) and glaucoma.

CHAPTER 2: AGE-RELATED CHANGES OF OCULAR DIMENSIONS IN THE WHITE LEGHORN CHICKEN

2.1 INTRODUCTION

Avians are frequently used to study ocular parameters. In particular, chickens have been used extensively to investigate physiological properties of the eye such as emmetropization and ocular diurnal rhythms, refractive abnormalities such as myopia and form deprivation, or reparative processes such as healing following laser supepithelial keratomileusis (LASEK) surgery. They are commonly used in these studies because they are cost effective, easily accessible, fast growing, and have relatively large eyes.

In particular, an important area of study among both animals and humans has been the "critical period" of emmetropization as it provides insight into effectively treating and preventing myopia and other ocular conditions such as amblyopia. Thus, many studies have commonly employed chickens as models of experimentally-induced ametropias (i.e. form deprivation, lens defocus, constant light) (Weiss & Schaeffel (1993); Bartmann, Schaeffel, Hagel & Zrennen (1994); Cohen, Belkin, Yehezkel, Avni & Polat (2008); Schmid & Wildsoet (1996); Wallman & Adams (1987); Zhu et al. (1995)). Most refractive experimental manipulations are done prior to four weeks of age and studies have reported a rapid phase in emmetropization to ~ +1D by 28 days of age (Avila & McFadden (2010):11 days; Pickett-Seltner, Sivak & Pasternak (1988):14 days, Wallman, Adams, & Trachtman (1981): 28 days). Thus, most of these studies are confined to an age range of less than 28 days post-hatching, some studies focus on age more than 1 year, and very few studies investigated the period between 28 days and 1 year post-hatching.

Due to the belief that there is a large axial component to refractive status (Cegarra, Izquierdo, Alsonso, Hernandez Gil de Tejada, et al. (2001)) there have been many studies that looked at normal and abnormal growth of ocular axial length. In various species, a peak in rapid axial ocular growth in infancy was found to be followed by a period of slower growth where a species transitions into a juvenile growth stage (mice: Schmucker & Schaeffel (2004); monkeys: Graham & Judge (1999), humans: Larsen (1971d)). It is possible that a juvenile growth period exists where ocular parameters such as anterior chamber depth (ACD), lens thickness (LT), and vitreous chamber depth (VCD) may need to stabilize or slow their growth rate. Groshke, Anderson, & Briggs (1948) provided evidence that before the age of 50 days chicken eye development might be most susceptible to factors such as diet. They found a correlation between a highly purified diet of 8% glycine and enlargement of the eyes severe enough to interfere with the nictitating membrane and normal vision in the growing chick up to 49 days of age but not in the older adult hen. Thus, a "critical period of juvenile ocular growth" in the chicken may exist from ~ 2 weeks onwards to a certain age.

The following studies focused on quantifying the growth of the developing chicken eye. Schaeffel & Howland (1988) produced the first schematic eye based on data for 30-day-old Cornell K White Leghorn chickens. In this work (using additional data from Troilo, Gottlieb & Wallman (1987) and Gottlieb, Fugate-Wentzek, & Walllman (1987)), growth curves for many of the major ocular components (corneal curvature, ACD, LT, lens radius, axial length (AL)) were reported. Similarly, Irving, Sivak, Curry & Callendar (1996) used primarily cross-sectional data from the fellow eye of broiler chicks of 0-16 days of age that had

unilateral treatment with defocusing and/or translucent goggles to create growth curves. They created schematic eyes for age 0, 7 and 14 days from ocular parameters measured using A-scan biometry with a 10 MHz (megahertz) probe immediately after animals were sacrificed or with images of frozen sections and a millimeter ruler. Avila & Mc Fadden (2010) produced schematic eyes in untreated White Leghorn chicks in the early post hatching period of 0-15 days and compared changes in ocular dimensions in a cross-sectional and longitudinal manner. Montiani-Ferreira, Cardoso & Peterson Jones, et al. (2004) focused on measuring one ocular parameter (central corneal thickness (CrT)) with ultrasonic pachymetry for the age range 0 to 450 days post-hatching. All studies listed above differed in age range, measurement techniques, as well as scope of ocular parameters measured.

In summary, complete ultrasound biometry and SD-OCT growth data are lacking for the age range of 21-107 days old, a period of potentially important eye development in chicken. The aim of our study was to investigate changes in ocular dimensions (CrT, ACD, LT, VCD, total retinal thickness (RT) at the visual axis, choroidal thickness (ChT), AL, refractive error (RE), RT, retinal nerve fiber layer (RNFL) thickness, ratio of RNFL thickness and RT) during this time period.

2.2 MATERIALS AND METHODS

2.2.1 Animals

Twenty White Leghorn chickens (G*allus gallus domesticus*, Cornell K) were obtained upon hatching (day 0) in the lab and raised under a 12 hours on - 12 hours off light cycle. Ceiling room illumination (Full Spectrum Fluorescent Light: Vita-Lite F40T12) provided

illumination in the cages ranging from 400 to 850 lux. Food and water was provided ad libitim. Demographics are included in Table 2-1. Seventeen out of the 20 chickens were also part of a different study and had experimental manipulation with injected microbeads and/or saline in one or both eyes at some point in the course of the measurements but only values prior to any injections or the non-injected fellow eye data were included in this study. All longitudinal data were measured between 3 and 6 hours after the lights went on. Cross-sectional data were measured over a larger 8 hour time period (3 to 11 hours after the beginning of the light cycle) during light hours.

Care and use of the animals were approved by the New England College of Optometry's Institutional Animal Care and Use Committee and adhered to the ARVO statement for the Use of Animals in Ophthalmic and Vision Research.

Table 2-1 displays the demographics of the birds included in our study. Demographics included gender, eye(s) utilized, the time frame of data collection for each bird, as well as the differentiation of birds used in the cross-sectional vs. the longitudinal part of the study. Cross-sectional animals had injections of microbeads and/or saline into one or both eyes for another project but only the data prior to any experimental manipulation or the data from the untreated fellow eye were included. Three out of the four animals who were followed over a longer time span (longitudinally) did not have any experimental manipulation in either eye. The fourth animal (# 2268*) had one injection of saline into the anterior chamber of the right eye only at the age of 29 days. As its ocular parameters did not show any deviations in the

saline-injected eye from the non-injected fellow eye, the data from the right eye of animal #2268 was included in the longitudinal part of the analysis.

Table 2-1 Demographics of the animals used in the study. Bolded bird numbers indicate animals used in the longitudinal part of the study. An asterisk (*****) next to bird 2268 indicates the only longitudinal bird that had an anterior chamber injection of saline at day 29 in the OD. OU = both eyes, OD = right eye, OS = left eye.

	Bird #	**Gender**	**Eye(s) Used**	**Age Range Used (days)**		**Bird #**	**Gender**	**Eye(s) Used**	**Age Range Used (days)**
1	**2268***	FEMALE	OU	21-107	**11**	**2356**	MALE	OU	21-87
2	**2363**	FEMALE	OU	21-87	**12**	**2273**	MALE	OU	21-107
3	2123	FEMALE	OU	30-39	13	2184	MALE	OU	OD (12-25) OS (12-56)
4	1972	FEMALE	OU	OD (20-25) OS (20-54)	14	2162	MALE	OU	OD (22-24) OS (22-66)
5	1971	FEMALE	OU	20-38	15	2122	MALE	OU	30-39
6	1968	FEMALE	OU	OD (30-33) OS (30-46)	16	1975	MALE	OU	89
7	1948	FEMALE	OS	33-98	17	1950	MALE	OS	33-70
8	1939	FEMALE	OU	36-50	18	1943	MALE	OU	36-50
9	1921	FEMALE	OS	33-70	19	1910	MALE	OU	22-25
10	1913	FEMALE	OU	22-25	20	1901	FEMALE	OU	22-25

2.2.2 Ultrasound Biometry

Ultrasound biometry was performed using an A-scan ultrasound instrument operating at 35MHz (Model 5072PR, Panametrics, Waltham, MA). The ocular parameters estimated directly from the ultrasound tracings were CrT, ACD, LT, VCD, RT, and ChT. The accuracy of these measurements depends on the consistency of the various waveforms and the ability to accurately assign appropriate peaks. In addition, the axial length of each eye was

estimated by adding the values for CT, ACD, LT, VCD, RT and ChT. The estimated resolution of the A-scan measurements in this study was generally comparable to another study (Nickla, Wildsoet & Wallman (1998): 19.6 µm for ACD, 18.2 for LT, 18.2 for VCD, 3.5 for RT, and 8.3 for ChT). All animals were deprived of food and water for 30 minutes prior to isofluorane anesthesia (1.5 % halothane in oxygen, Halocarbon Laboratories). The animals were placed in an adjustable holder with their heads in an upright position and a lid retractor was used to keep one eye open at a time. The probe was directed perpendicular to the central cornea. A representative ultrasound tracing with various ocular parameters is shown in Figure 2-1.

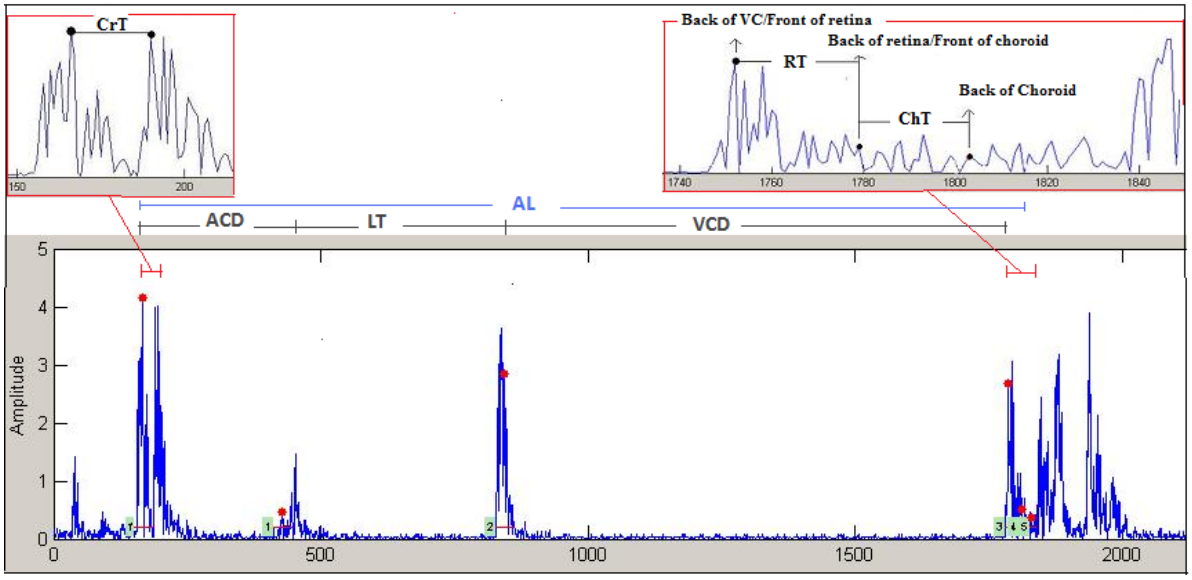


Fig. 2-1 Representative ultrasound A-scan tracings. Enlarged ultrasound A-scan tracings with peaks identified. The main bottom panel presents the original A-scan amplitude vs. time (blue color). The horizontal axis represents time (ms) and the vertical axis represents amplitude. The time markings used to determine the size of ACD, LT, and VCD are indicated in black above the main panel. Two areas of the signal with numerous peaks occurring closely one after another are enlarged horizontally (not to scale, for illustrative purposes only) in two red boxes above the main panel. The left upper panel shows an enlarged view of the region containing CrT peaks, while the right upper panel shows an enlarged view of signal containing RT and ChT peaks.

2.2.2.1 Ultrasound Biometry Method of Measurement

Corneal thickness was determined by subtracting the second peak of the doublet of the back of the cornea from the highest intensity peak of the front of the cornea. ACD was the measured distance from the back of the cornea to the front of the lens. LT was defined as the distance from the front of the lens to the back of the lens, while VCD was the distance from the back of the lens to the front of the retina, and RT from front of the retina to the front of the choroid. ChT was defined as the front of the choroid to the front of the scleral interface. AL was calculated as the sum of ACD, LT, VCD, RT, and ChT.

2.2.3 Refractive Error Measurement

Refractive error (RE) was measured using a refractometer up to 70 days of age and streak retinoscopy thereafter. Food and water was withheld 30 minutes prior to any RE measurements. For both refractometry via Hartinger and streak retinoscopy, isofluorane anesthesia was applied in the same manner as described above for ultrasonography. A lid retractor was also used to hold the eyelids open. All refractive error measurements were performed without any paralytic or mydriatic ophthalmic drops although it should be noted that isofluorane anesthesia has a mild mydriatic effect.

2.2.3.1 Refractometry

Refractive errors of the two principal meridians were measured along the pupillary axis with a Hartinger's coincidence refractometer (Jena Coincidence Refractometer: Carl Zeiss Meditec, GmbH, Jena, Germany). A set of five consecutive readings were recorded in each

eye. These values were converted in Diopters according to the formula (Wallman & Adams (1987)): $\text{Diopters (D)} = 2.09 \times (\text{Horizontal or Vertical Reading}) + 20$ and the average of the vertical and horizontal meridians were recorded. The five readings were then averaged and this averaged reading was used for analysis.

2.2.3.2 Streak Retinoscopy

Streak retinoscopy (Heine Beta 200 retinoscope with xenon halogen light source, HEINE Optotechnik, Herrshing, Germany) was used to measure the refractive error along both the horizontal and vertical meridians at a working distance of 50 cm. A set of three readings were taken. The spherical equivalent of the three readings were averaged and used for analysis.

2.2.4 Optical Coherence Tomography (OCT)

A spectral-domain optical coherence tomography instrument (SD-OCT) (Model RT100, Optovue Inc., Fremont, CA) was used in awake and dilated chickens to measure the total RT and RNFL thickness near the optic nerve head (ONH). The measurement procedure started with the application of an anesthetic 0.5% proparacaine hydrochloride ophthalmic solution (Alcon Laboratories Inc, Forth Worth, Texas) followed by paralytic and pupil dilating drops, 1% vercuronium bromide. These drops were administered 5 minutes apart for 30 minutes until maximum dilation was achieved for that particular age of the bird (pupil size ranged from ~ 3.0 to 4.0 mm). Prior to the SD-OCT measurements, one drop of proparacaine was instilled in the eye prior to the insertion of a lid retractor. The same person held the animals' head in front of the SD-OCT to ensure that the same retinal location was scanned when

imaging all the animals. At least 10 line scans centered at the tip of the pecten were acquired (6mm scan length) and averaged.

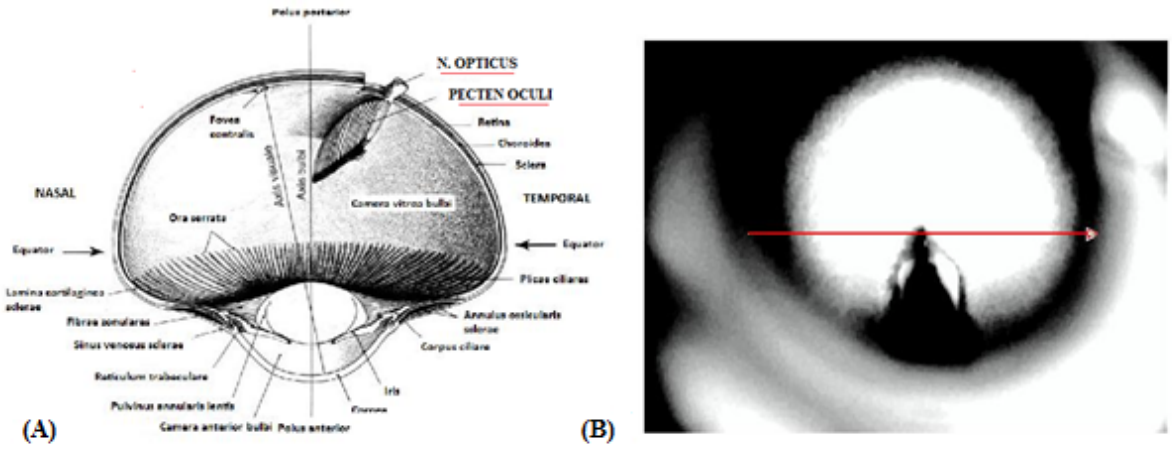


Fig. 2-2 Positioning of the SD-OCT B-scan. (A) Drawing of the chicken eye showing the pecten interfering with the view of the ONH (N. Opticus). (Evans 1996) (B) Representative OCT enface IR (infrared) image of the right eye of an 88 day old chicken: position of the B-scan is indicated with a horizontal red arrow. The dark inverted tear drop shaped structure below the center of the arrow represents a front view of the tip of the pecten.

Figure 2-2A shows an illustration by Evans 1996 of the pecten vasculature and the chicken optic nerve (N. Opticus) posterior to the pecten. Figure 2-2B is an IR enface image of the SD-OCT with a red arrow indicating the position of the B-scan. All the animals were held in such a way that all B-scans went through the same portion of the fundus and optic nerve head by using the appearance of the pecten as a guide landmark (see Fig 2-2B).

The magnification factor for one degree field of view was calculated for each scan by measuring the axial length of the individual eye and taking into account the optical power of the eye. The one degree field of view (FOV) was computed directly from the focal length:

1 degree FOV (μm) = 1000 × focal length (mm) × tan (1 × π /180). Each OCT scan was then scaled accordingly in the horizontal dimension. Manual measurement of RT and RNFL thickness was done in Image J (Rasband 1997).

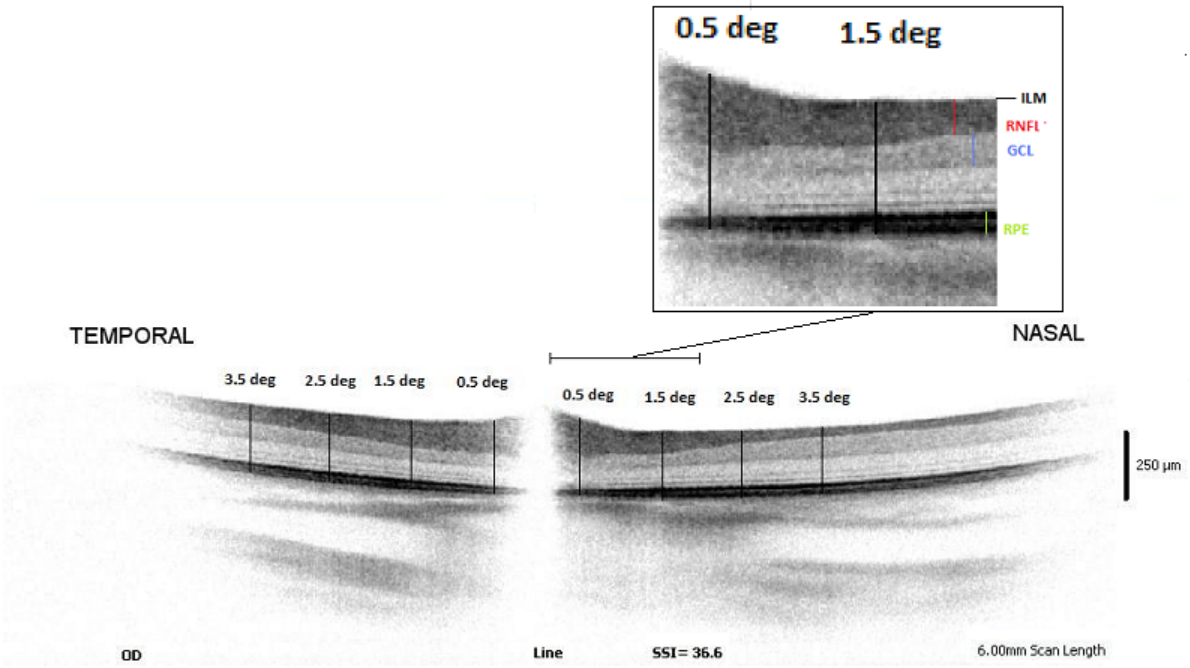


Fig. 2-3 Representative SD-OCT B-scan. Vertical lines (black) indicate points on the retina where RNFL and RT measurements were taken. Eccentricity in degrees relative to the center of the optic nerve is indicated above each point of measurement. ILM = inner limiting membrane, GCL = ganglion cell layer, and RPE = retinal pigment epithelium. The right upper panel is an enlarged view of the nasal area with ILM (horizontal black line), RNFL (red line), GCL (blue line), and RPE (green line) labeled.

Figure 2-3 shows a representative SD-OCT B-scan image used for analysis. The vertical lines represent areas where RNFL and RT measurements were taken at 0.5, 1.5, 2.5 and 3.5 degrees eccentricity relative to the center of the optic nerve. At these eccentricities RNFL is indicated by the vertical length in micrometers of the top uppermost grayish black layer/band. The RPE band is the lowest darkest black line observed. Total retinal thickness

is the length in micrometers from the top of the RNFL layer (ILM) to the bottom of the RPE band. The grayscale shading of dark vs. light areas in our OCT images were inverted compared to typical OCT images to enhance contrast.

2.2.5 Estimation of Ocular Growth Parameters of Published Non-Primate and Primate Studies

From graphs of Qiao-Grider, Hung, Lee, Ramamirtham & Smith (2007), x and y coordinates were estimated of their best fit exponential curves to generate approximately the same curves. These curves were used to determine 90% plateau mean values and corresponding ages for humans (ACD, VCD, AL) and rhesus monkeys (ACD, VCD) for comparison to chickens in the present study. Their best fit curves (humans) were an average of Zadnik, Manny & Yu (2003), Garner, Kinnear, & Frith (1995), and Larsen (1971a-d). Reported 90% plateau (Qiao-Grider, et al. (2007)) was 800 days for AL and 776 days for this same 90% plateau via the estimated AL curve we generated, thus validating this method as a means of approximate comparison. Calculated relative percent contribution of ACD, LT, and VCD towards total axial length was provided for infant humans and rhesus monkeys by Qiao-Grider et al. (2007) and the same ratios were calculated for the present study at age 21 days for chickens via taking the ratio of each ocular parameter to axial length and multiplying by 100.

2.2.6 Statistical Analysis

The original data was tabulated and prepared in Microsoft Excel. Linear and non-linear regression models of the data of each ocular parameter vs. age as well as scatter plots of

paired ocular parameters to test for correlation were generated via GraphPad Prism 5.0 (GraphPad Software, Inc., La Jolla, CA). The statistical analysis package in GraphPad Prism was used to evaluate differences between different data sets via two way analysis of variance (two-way ANOVA), any deviation from a horizontal-slope in linear regression functions, as well as significance of Pearson r correlation coefficients. Statistical significance was defined as p-value of < 0.05. All data are presented as mean values ± SEM.

2.3 RESULTS

2.3.1 Growth of Ocular Dimensions

Ocular parameter growth curves for both the cross-sectional and longitudinal part of the present study are shown in Figure 2-4. The longitudinal fits from the present study are also compared to past studies that included fits of ocular parameters (see Figure 2-5).

The dynamics of ocular growth based on cross-sectional data were in good agreement with the growth based on longitudinal data with the exception of ChT. From Figure 2-4F it is evident that there was a large variability in ChT in the cross-sectional data, which was not seen among the longitudinal data. The reported ChT values in the present study of animals measured longitudinally were lower than those measured cross-sectionally (Fig. 2-4F).

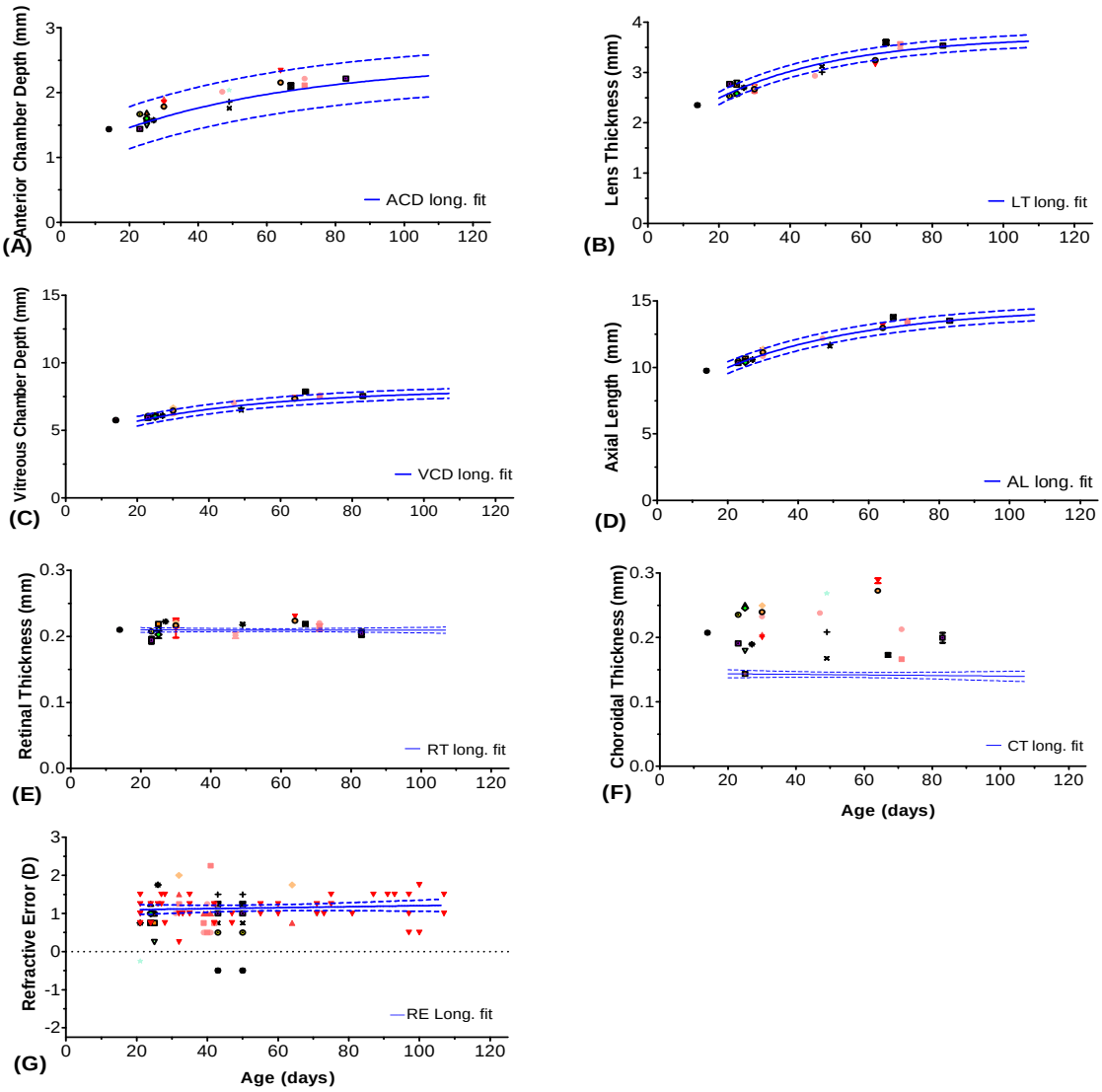


Fig. 2-4 Cross-sectionally measured ocular parameters vs. age. Change in ocular parameters based on cross-sectional data from the present study. Exponential association equations were fit for (A) - (D) and linear growth equations were best fit for (E) - (G). (D) Axial length is the sum of ACD, LT, VCD, and RT. (F) Choroidal thickness showed more variability in cross-sectional animals while animals used in the longitudinal part of the study showed lower levels of variability in choroidal thickness.[1]

[1] Note: Choroidal thickness measurements were taken over an 8 hour time period during light hours in the cross-sectional part of the study while animals followed longitudinally had choroidal thickness measured between 3 and 6 hours after the lights turned on.

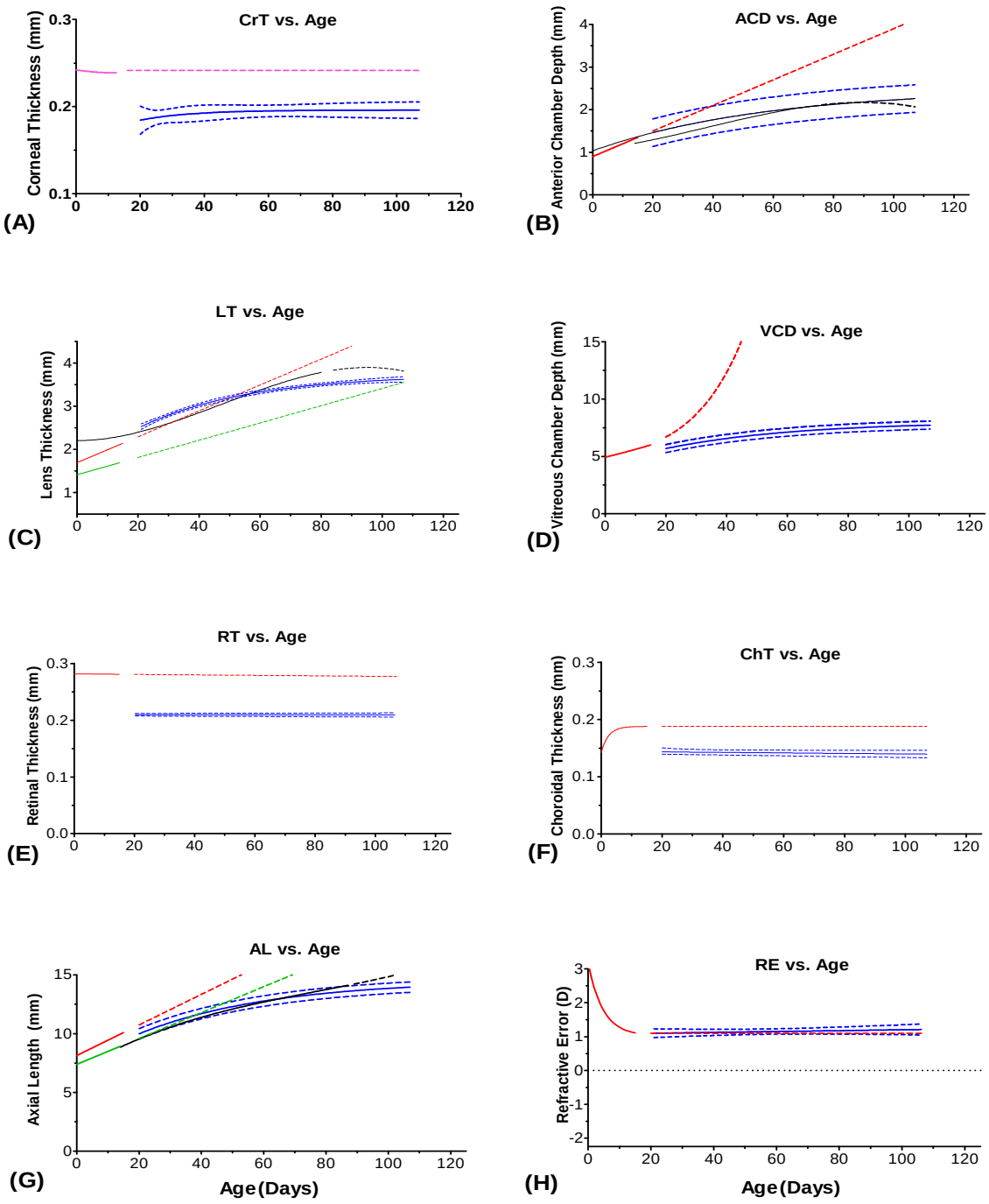


Fig. 2-5 Comparison of growth of ocular parameters. Change in ocular parameters in the chicken from different longitudinal studies. The blue solid line represents the mean fit of the present study, while the blue dotted lines represent the 95% confidence interval around this mean. Exponential association functions were used to fit (A) - (D) and (G) whereas linear functions were used to fit (E), (F) and (H). (A) The purple solid line is a fit derived from the

data by Montiani-Fereirra et al. (2004) (age range 0 - 12.5 days) and the purple dotted line the same fit extrapolated beyond 12.5 days. (B)-(H): The red solid line represents a fit based on data from Avila & Mcfadden (2010), while red dotted indicates the growth function extended beyond 14 days. (B),(C),(G): The solid black line represents a fit based on Schaeffel & Howland (1988) and the dotted black line is the fit extended beyond the age range used in their study. The solid green line is a fit based on data from Irving et al. (1996) and the dotted green line is the fit extended beyond the age range used in their study.[2]

As ChT is believed to be thinnest in the morning and thickens throughout the day (Nickla, Wildsoet & Wallman (1998)), difference in time of measurement could explain the discrepancy between cross-sectional vs. longitudinally followed animals. The animals participating in the longitudinal part of the study had measurements taken during a three hour time period at the same time each day, whereas animals participating in the cross-sectional part of the study were measured during an eight hour time period throughout the day. Similarly, RE among the cross-sectional group had a larger variability in refractive errors when compared to the more narrow range of RE values seen in the longitudinal group (Fig. 2-4G).

RT, ChT, and RE with age were best described as linear functions (Table 2-2), as non-linear fits did not improve the quality of the fits. The growth of corneal thickness appears to plateau at a younger age of 68 days when compared to the other parameters (~ 279 - 637 days). Although it appears as if ACD, LT, VCD, and AL are reaching a plateau towards the

[2] The fits based on the data by Montiani Ferreira et al. (2004), Avila & McFadden (2010), Schaeffel & Howland (1988), and Irving et al. (1996) were plotted based on the equations in their publications with the exception of Avila et al. (2010) for RT and ChT. As both a cross-sectional and longitudinal fit of RT and ChT vs. age was shown in their Figure 3 and only the cross-sectional fit equation was expressed in their Table 1, we estimated the points on their graph for their longitudinal fit of these parameters and included them in the current graph.

end of our measurement period of 107 days, our growth equations extended would predict very slow growth and a plateau at 637, 279, 388, and 338 days of age; respectively (Table 2-3). Future studies measuring the same parameters over an extended age period (107-637 days) would be helpful in verifying this projection. It is interesting to note that VCD and AL follow the same growth pattern with a similar predicted maturation time with VCD reaching adult levels only one month after AL. Out of all of the measured parameters, corneal thickness matures the quickest, followed by LT, VCD and AL, while the anterior chamber is last to reach maximum levels. Thus, if the growth equations determined by the present data are found to be applicable to an age range of 107-637 days, this would indicate a full development of ocular components (CrT, LT and, AL) by approximately one year of age, full maturation of VCD one month after these parameters, and maximal adult levels of ACD by 2 years of age. While complete maturation is expected by two years of age for all parameters measured, the estimated time it takes to reach 95% maturation for most of the parameters (CrT, LT, VCD, AL) would occur during the observation period of the current study (by 100 days) and ACD would reach 95% maturation soon after (Table 2-3). Of note, CrT was first to reach 95% maturation at age 22 days, about the time measurements were first taken (21 days) and thus the minimal growth during the observation period resulted in a poor goodness-of-fit ($R^2 = 0.04$) compared to the other ocular parameters who showed asymptotic growth and excellent goodness-of-fit (0.95 to 0.99).

A summary of available data on ultrasound biometry of the growing chicken eye in past studies compared to the present study is presented in Table 2-2 and a comparison of ocular parameters with asymptotic growth is shown in Table 2-3.

Table 2-2 Comparison of ultrasound biometry fits of selected studies. Growth equations derived from analysis of the ultrasound biometry data and refractive error data from the present study compared to other published studies. In the present study ACD, LT, VCD and AL were the only parameters to deviate significantly from a zero slope ($p < 0.05$). Fits of Avila & McFadden (2010) was provided as cross-sectional data only. Of note: As described previously we estimated their longitudinal fit of RT and ChT to include in Figure 2-5 and thus the fits provided in this table for cross-sectional data do not apply to their estimated RT and ChT functions in Figure 2-5.

Ocular Parameter (mm)	Current study 21-107 days	Schaeffel & Howland (1988) (Gottlieb et al. (1987)/ Troilo et al. (1987)) 14-78 days	Avila & McFadden (2010) 0-15 days	Montiani-Ferreira et al. (2004) 0-450 days	Irving et al. (1996) 0-16 days
Corneal Thickness (CrT)	y = 0.156 + 0.0397(1-e^(-0.06143x)) R^2=0.04207	N/A	N/A	y = 0.2421-0.00053x +0.000021x²* y = 0.2417/(1+((0.2417-0.2388/0.2388))*e^(-0.00691(x-12.5))**	N/A
Anterior Chamber Depth (ACD)	y = 1.034 +1.447(1-e^(-0.01752x)) R^2=0.9582	y = 1.0617+0.0079x-2.384e-4x^2-2.08e-6x^3 R^2=N/A	y = 0.03x + 0.90 R^2=0.997	N/A	N/A
Lens Thickness (LT)	y = 1.529 +2.198(1-e^(-0.02859x)) R^2=0.9825	y = 2.2607+3.388e-6x+5.616e-4x^2-3.935e-6x^3 R^2=N/A	y = 0.03x + 1.69 R^2=0.9995	N/A	y = 1.41 +0.22x† R^2=0.93 y = 1.65+0.04x‡ R^2=0.85
Vitreous Chamber Depth (VCD)	y = 4.264 +3.763(1-e^(-0.02364x)) R^2=0.9773	N/A	y = 4.26 + 0.78e0.06x R^2=0.993	N/A	N/A
Retinal Thickness (RT)	y = 0.2090-0.000003202x R^2=0.00019	N/A	y = 0.32 – 0.0004x R^2=0.9985	NA	N/A
Choroidal Thickness (ChT)	y = 0.1448-0.00005125x R^2=0.01379	N/A	y = 0.22 + 0.07(1 - e-0.39x) R^2=0.9835	N/A	N/A
Axial Length (AL)	y = 7.226 + 7.304[(1-e^(-0.0237x))] R^2=0.9902	y=6.86+0.1596x-0.0014x^2+6.061e-6x^3 R^2=N/A	y = 0.12x + 8.56 R^2=0.9997	N/A	y = 7.39 +0.11x† R^2=N/A
Refractive Error (RE)	y = 0.00101x +1.054 R^2=0.01674	N/A	N/A	N/A	N/A

Table 2-3 Comparison of ocular parameters with exponential growth. Estimated parameters related to ocular growth for CrT, ACD, LT, VCD, and AL. Mean values are presented as mean ± 95% CI.

Ocular Parameter	CrT	ACD	LT	VCD	AL
Expected mean value at plateau (mm)	0.196 ± 0.010	2.481 ± 0.323	3.727 ± 0.124	8.027 ± 0.352	14.530 ± 0.445
Estimated age at plateau (days)	68	637	279	388	338
Expected mean value at 90% plateau	0.176 ± 0.010	2.233 ± 0.323	3.354 ± 0.124	7.722 ± 0.352	13.077 ± 0.445
Estimated age at 90% plateau (days)	N/A	99	62	74	68
Expected mean value at 95% plateau	0.186 ± 0.010	2.357 ± 0.323	3.541 ± 0.124	7.626 ± 0.352	13.803 ± 0.445
Estimated age at 95% plateau (days)	22	140	86	94	97
Mean value at age 21 days (mm)	0.185 ± 0.010	1.472 ± 0.323	2.504 ± 0.124	6.066 ± 0.352	10.047 ± 0.455
Mean value at age 107 days (mm)	0.196 ± 0.010	2.269 ± 0.323	3.623 ± 0.124	7.727± 0.352	13.950 ± 0.445
Absolute growth age 21 to 107 days (mm)	0.011	0.797	1.119	1.661	3.903
% growth age 21 to 107 days	6	54	45	27	31

2.3.2 Corneal Thickness

In the present study central corneal thickness from 21 to 107 days was found to show an asymptotic growth pattern with mean CrT at age 21 days of ~ 185 μm and a plateau at the age of 68 days to ~ 196 ± 10 μm (Fig. 2-5A, Table 2-3). Although complete maturation was predicted to occur about midway through the observation period, most of the growth (95 %) was predicted to occur shortly after hatching by 22 days of age (Table 2-3), only one day after the measurements were first taken. Montiani-Ferreira et al. (2004) reported a decrease in central corneal thickness from birth to 12.5 days of age followed by a slower growth in thickness with a plateau also at ~ 70 days of age. Thus, both the present study and Montiani-Ferreira et al. (2004) are in agreement with the maturation of central corneal thickness by 70 days post-hatching.

2.3.3 Anterior Chamber Depth

As observed in Figure 2-5B, the dynamic of the ACD growth was in good agreement with the measurements obtained by Schaeffel & Howland (1998) over their entire time period. Of note, the extended fit for ACD growth based on early (0-15 days) measurements by Avila & McFadden (2010) has a higher growth rate when compared to the data fits based on empirical observation by Schaeffel & Howland (1998) and the present study, indicating a change in ACD growth from a linear to a shallow exponential function around the age of 20 days. The ACD fit in the present study appears to grow at a very small rate reaching 2.269 ± 0.323 mm towards the end of the 107 day period with 95 % maturation estimated to occur about one month later (140 days), and an actual plateau predicted to occur at a much later age of 637 days (Fig. 2-5B, Table 2-3).

2.3.4 Lens Thickness

Lens thickness (Fig. 2-5C) growth was in good agreement with the exponential fit based on data from Schaeffel & Howland (1988) and the extended linear fit of Avila & McFadden (2010) between ~ 50 to 60 days post-hatching. LT in the present study was similar in value to the fit of Schaeffel & Howland (1988) and with Avila & McFadden (2010) extended at values below this time period, with a greater deviation in LT measurements from 60-107 days of age. The extended fit of LT (Irving et al. (1996): 0-16 days) underestimated the LT in the present study throughout the entire observation period. The LT measurements in the present study appear to be reaching a plateau near the end of our measurement period to ~ 3.727 ± 0.124 mm with a predicted time of reaching a plateau at 279 days post-hatching (Fig. 2-5C, Table 2-3). While full maturation is predicted to occur by 1 year of age, the growth is very slow beyond the measurement period in the present study and 1 year of age as 95% maturation was predicted to occur much sooner at 86 days post-hatching.

2.3.5 Vitreous Chamber Depth

The growth curve of the vitreous chamber derived from the data in the present study (Fig. 2-4C, Fig. 2-5D) indicates a slow increase in VCD depth with a decline in the rate of growth towards the end of the measurement period to a maximum depth of ~ 7.722 ± 0.352 mm at 107 days (Table 2-3). The current fit would predict complete adult values in vitreous chamber length at the age ~ 388 days with 95 % of the growth expected to occur by 94 days post-hatching (Table 2-3). As with lens thickness, extrapolating growth rate based on the early post-hatching period (0-15 days, Avila & McFadden (2010)) would have overestimated

the rate of growth, an indication of change in growth pattern around the period 15 -20 days of age.

2.3.6 Retinal thickness

There was no observable change in retinal thickness for the period studied (Fig. 2-4E, Fig. 2-5E). Projected RT change based on data by Avila & McFadden (2010) beyond their measurement period also demonstrates very little change with time. As measurements began at 21 days post-hatching, complete maturation in RT to ~ 209 μm was presumed to occur before this age.

2.3.7 Choroidal thickness

The pattern of ChT growth with age was similar to that of RT with stability over the observed time period (Fig. 2-4F, Fig. 2-5F). ChT was stable at an average thickness of ~ 145 μm. The invariability in ChT with age is in accordance with the extrapolated data from Avila & McFadden (2010). The data collection in the present study began at day 21 and was thus past the plateau (9 days post-hatching) that was reported by Avila & McFadden (2010), thus ChT was expected to be stable over the 21 – 107 day period.

2.3.8 Axial Length

Axial length was found to have an asymptotic growth pattern over the observed time period similar to the growth trend of the major ocular components comprising it (CrT, ACD, LT, VCD) (Fig. 2-4D, Fig. 2-5G, Fig. 2-6). Comparable to ACD, LT, and VCD, the growth rate of AL appears to decrease with age reaching a very slow rate of growth towards the end of the 107 day measurement period. From the fit of AL with age, time to reach maximum adult

values in AL was predicted to occur ~ one month earlier (338 days of age) than the vitreous chamber (388 days) (Table 2-3). Although complete maturation was predicted to occur at ~ one year of age, most of the growth (95%) was completed by 97 days of age (Table 2-3). The data obtained in the present study for the growth of AL was in good agreement with the data by Schaeffel & Howland (1988) for the period 20-84 days. The projection of the growth curves based on early post-hatching periods (Avila & McFadden (2010); Irving et al. (1996)) would overestimate the growth in axial length compared to the observed rate in the present study, indicating a change in growth dynamic of AL around 14-20 days post-hatching.

2.3.9 Refractive Error

Refractive error in the present study showed stability with age, similar to that of RT and ChT. Refractive error measurements in the early post-hatching period by Avila & McFadden (2010) found RE to be ~ + 3D immediately after birth with a gradual reduction taking place to ~ + 1D by 15 days of age. When they applied a correction for inherent hyperopia observed with performing retinoscopy on small eyes ("small eye artifact": Glickstein & Millodot (1970)) this reduced the observed hyperopia by ~ + 1.2D at 15 days of age thus placing the estimated value for RE to plano (~ 0D) by 15 days of age. In the present study, the measured RE was stable at about + 1D ± 0.75D throughout the entire observational period between 21 and 107 days (Fig. 2-4G, Fig. 2-5H) in good correspondence with the projection based on extrapolation of the formula used by Avila & McFadden (2010) for the period 0 to 15 days. As measurements began at 21 days post-hatching, it was presumed that most of the reduction in hyperopia after birth occurred prior to the initial measurement period in the present study.

2.3.10 A Summary of Ocular Parameters with Exponential Growth

As observed in Figure 2-6, the estimated values for CrT, ACD, LT, VCD, and AL all follow an asymptotic growth pattern over the 21-107 day time frame. The predicted time of reaching a plateau and reaching 95% of the plateau for each ocular parameter is shown in Table 2-3. In addition, the mean values of each ocular parameter at the start of the measurement period in the present study at 21 days post-hatching as well as the final mean value of these parameters at 107 days of age with corresponding absolute and percent growth are shown in Table 2-3. ACD showed the largest deepening during the 86 day observational period and CrT grew the slowest and had the smallest increase in thickness (Table 2-3). Of note, VCD and AL have similar growth rates of ~ 30% over the observational period. Based on estimated curves of Qiao-Grider et al. (2007), 90% plateau in humans for ACD, VCD, AL was predicted to be ~ 3.227 mm (704 days), ~ 14.364 mm (1304 days), and ~ 20.916 mm (776 days), respectively. Based on the 90% plateau rates, ACD (humans) was found to mature ~ 2x more rapidly than VCD while the opposite trend in time of maturation was observed in chickens from the present study (VCD < ACD) and in rhesus monkeys (estimated 90% plateau: ACD: ~ 476 days; VCD: ~ 419 days), thus pointing towards possible species differences. The chicken to human ratio of 90% plateau was approximately 1:7.0, 1:17.5, and 1:11.8 for ACD, VCD, and AL respectively.

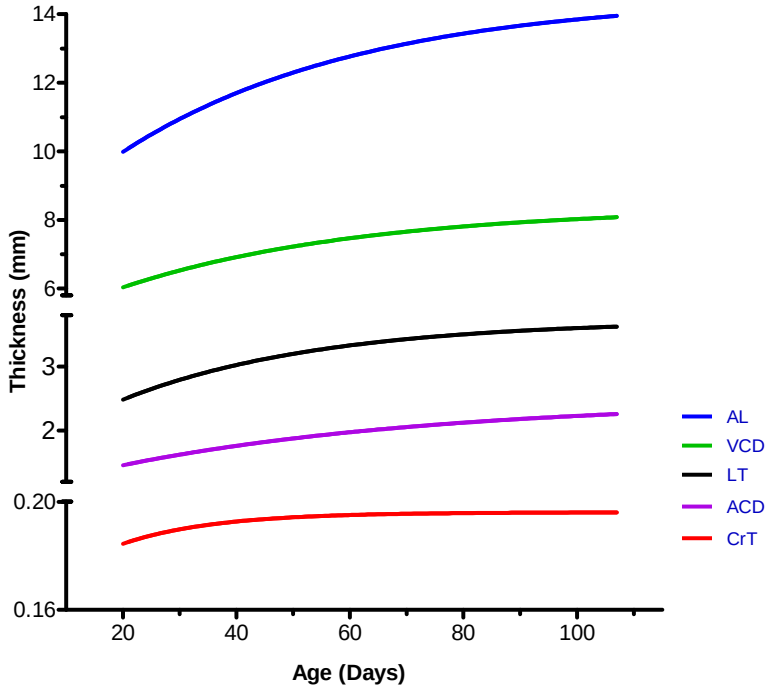


Fig 2-6 Asymptotic growth of ocular parameters with age. Ocular parameters in the present study with asymptotic growth are shown over the 21-107 day measurement period. Legend: AL (blue), VCD (green), LT (black), ACD (purple), CrT (red)

The contribution of ACD, LT, and VCD towards AL over time is shown in Figure 2-7. Relative contributions of these ocular components towards axial length (Table 2-4) during infancy were similar among the 3 species: chickens vs. humans vs. rhesus monkeys; ACD: 14.9% vs. 15% vs. 16.3%; LT: 24.3% vs. 21.4% vs. 24.2%; VCD: 57.3% vs. 63.6% vs. 59.4%. A similar high positive correlation was found for chickens (21-107 days) in the present study between ACD vs. AL, LT vs. AL, and VCD vs. AL ($r = 0.9756$, 0.9658, 0.9753, respectively).

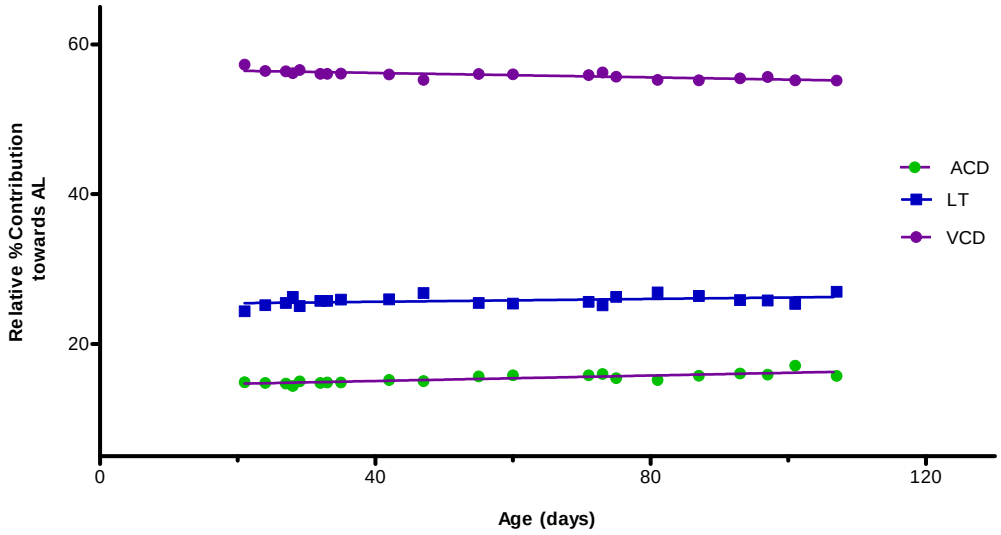


Fig 2-7 Calculated percent contribution of ACD, LT, and VCD towards AL with time. Calculated percent contribution of the major axial ocular components (ACD, LT, VCD) towards AL with time.

Table 2-4 Species comparisons of relative % contribution of ACD, LT, and VCD to AL of selected studies. Comparisons in chickens, non-human primates, and humans: calculated relative percent contribution of major axial ocular components (ACD, LT, VCD) towards AL.

Species	Relative % Contribution of ACD to AL	Relative % Contribution of LT to AL	Relative % Contribution of VCD to AL
Chickens (Present study)	14.9	24.3	57.3
Humans (Qiao-Grinder et al. 2007)	15	21.4	63.6
Rhesus Monkeys (Qiao-Grinder et al. Table 2 of data from Lotmar 1976)	16.3	24.2	59.4

2.3.11 Gender Comparisons

We did not observe any statistically significant differences (Student *t* test: $p > 0.05$) for any ocular parameters in the present study between male and female animals.

2.3.12 Comparison of Some Ocular Parameters Values with Published Studies

Comparison of the estimate of the mean values of the ocular parameters based on the cross-sectional part of the present study to other published studies is shown in Table 2-5. The values in this table from Li, Glasser, & Howland (1995) were an approximation of the true value as these values were extrapolated based on their graphs of ACD, LT, VCD, and AL vs. age. Additionally, a comparison with data provided by Zhu et al. (1995) and Rymer, Cho, Bharadway, Padmanabhan et al. (2007) are presented. As evident from Table 2-5, most of the ocular parameters in the present study were in fairly good agreement with the other studies.

Table 2-5 Comparison of cross-sectional data between selected studies. Comparison of some cross-sectional measurements of ocular parameters with Li et al. (1995) and Zhu et al. (1995), and Rymer et al. (2007). All measurements are expressed in mm. Mean values of ACD, LT, VCD, and LT were estimated graphically from growth curves from Li et al. (1995) as growth equations were not reported.

Ocular parameter and age (days)	Present study	Li et al. (1995) estimated (mm)	
ACD (21)	1.48 ± 0.32	1.45	
ACD (76)	2.10 ± 0.32	2.16	
LT (21)	2.52 ± 0.12	2.45	
LT (76)	3.48 ± 0.12	3.35	
VCD (21)	5.73 ± 0.35	5.50	
VCD (76)	7.40 ± 0.35	7.50	
AL (21)	10.09 ± 0.45	9.50	
AL (76)	13.23 ± 0.45	13.0	
		Zhu et al. (1995) (mm)	
		Males	Females
ACD (28)	1.60 ± 0.32	1.72 ± 0.07	1.72 ± 0.09
LT (28)	2.74 ± 0.12	2.65 ± 0.09	2.54 ± 0.11
VCD (28)	6.09 ± 0.35	6.25 ± 0.26	6.08 ± 0.15
AL (28)	10.77 ± 0.45	10.61 ± 0.32	10.34 ± 0.17
		Rymer et al. (2007) (mm)	
ACD (27)	1.58 ± 0.32	1.73 ± 0.05	
LT (27)	2.71 ± 0.12	2.55 ± 0.04	
VCD (27)	6.04 ± 0.35	6.20 ± 0.14	

2.3.13 Changes in Retinal and Nerve Fiber Layer thickness with Eccentricity and Age

2.3.13.1 Changes with Eccentricity

According to Figure 2-8A, RT appears to decrease between 0.5 and 1.5 degrees eccentricity from the center of the optic nerve head reaching a plateau at ~ 1.5 degrees eccentricity to an average value of ~ 250 μm. However, even the most peripheral retinal thickness measurement by SD-OCT at 3.5 degrees eccentricity is still within relative proximity to the borders of the optic nerve head. Therefore, it would be located at a considerable distance from the projection of the visual axis on the retina where the ultrasound A-scan measurements were taken in the present study and in Avila & McFadden (2010) at an earlier age range. Total retinal thickness values were more variable closer to the center of the optic disk between 0.5 and 1.5 degrees eccentricity compared to values outside that range. In contrast to RT, RNFL thickness demonstrated a continuous gradual decrease nasally and temporally from 0.5 to 3.5 degrees eccentricity from the center of the optic nerve (Fig 2-8B).

2.3.13.2 Changes with Age

RNFL thickness, total RT, and ratio of RNFL thickness vs. total RT at different eccentricities and as a function of age are presented in Figure 2-9 with accompanying linear growth equations in Table 2-6. Fits based on exponential or logarithmic equations did not improve the quality of the estimated linear functions. RNFL thickness was stable over the 21-107 days measurement period at all measured retinal eccentricities with less variability than RT near the optic disc with age. Similar to RNFL thickness change with age, RT was stable with age at 0.5, 1.5, and 2.5 degrees eccentricity (Fig. 2-9A,B). The stability in RT with age is in

agreement with the stability in RT with age when measured at the visual axis via ultrasonography (Fig. 2-4E, Fig. 2-5E, Fig 2-9B). Of note, RT decreased with age in a statistically significant manner ($p < 0.05$) at 3.5 degrees (Fig. 2-9B). Interestingly, although total RT at 3.5 degrees declined with age, the ratio of RNFL thickness to RT was stable over that time period at that eccentricity.

Table 2-6 Growth equations for RNFL thickness, RT, and ratio of RNFL thickness to RT. Growth equations and goodness-of-fit estimates for RNFL thickness, RT, and ratio of RNFL/RT from 21-107 days of age at all eccentricities measured in the present study. The goodness-of-fit (R^2) is shown for all parameters. All growth equations (with the exception of RT at 3.5 degrees) did not show statistically significant changes with age. The slopes for RNFL thickness, RT, and RNFL/RT were not significantly different between the four animals ($p > 0.05$) but the y intercepts were ($p < 0.0001$).

Ocular parameter	0.5 deg	1.5 deg	2.5 deg	3.5 deg
RNFL thickness	Y=111+0.3101x R^2=0.1539	Y=85.32+0.008893x R^2=0.0004	Y=59.20+0.02050x R^2=0.0046	Y=49.32+0.03635x R^2=0.02677
Total retinal thickness (RT)	Y=275.1+0.03708x R^2=0.0011	Y=265.1+0.3191x R^2=0.1678	Y=265.6-0.2475x R^2=0.2117	Y=287.1-0.8621x R^2=0.9300
RNFL/RT	Y=0.497+0.003963x R^2=0.03377	Y=0.3162+0.000599x R^2=0.1381	Y=0.2138+0.0004808x R^2=0.1498	Y=0.1808+0.0002554x R^2=0.07011

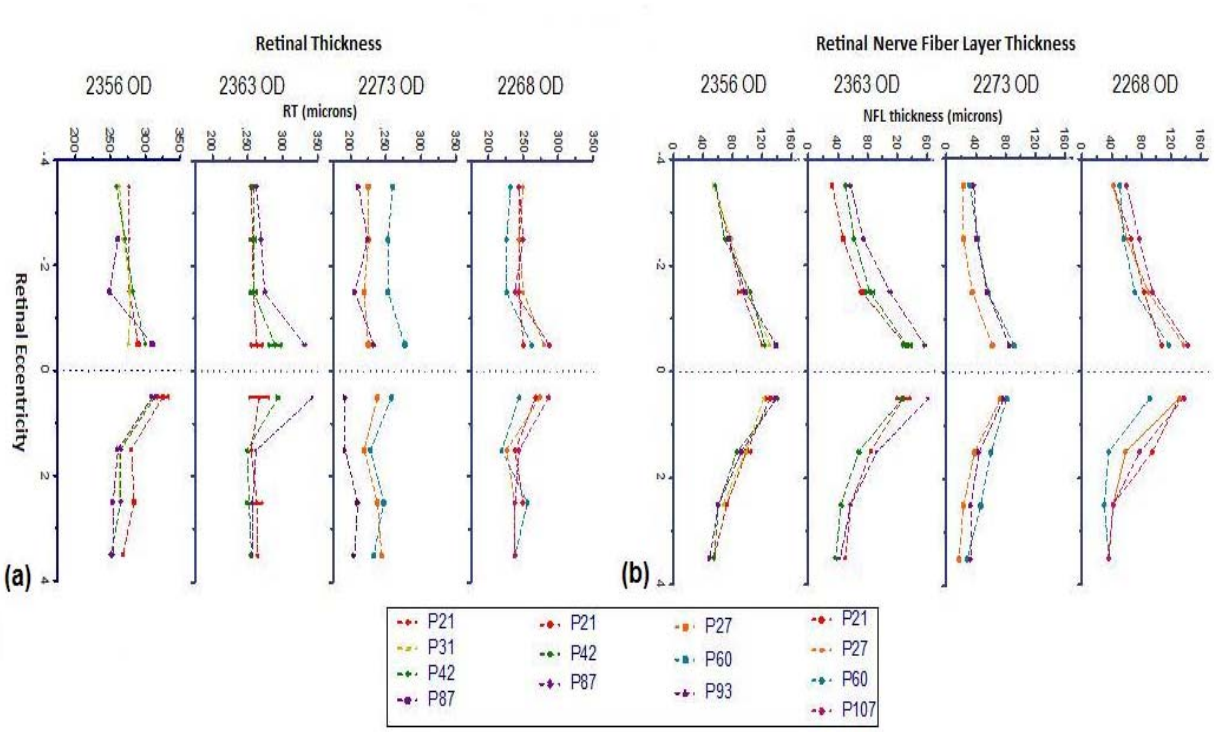


Fig 2-8 Total RT and RNFL as a function of eccentricity and age. (A) Total RT and (B) RNFL thickness as a function of eccentricity (0.5 to 3.5 deg) and age (P21-P107) for the right eye of 4 longitudinal birds. The dotted horizontal line at 0 degrees eccentricity indicates the estimated center of the optic nerve head. Positive numbers on the vertical axis indicate nasal eccentricity, while negative numbers indicate temporal eccentricity. [3]

[3] Data included for the four birds were at different time points. Animal #2356 included RT and RNFL values at day 21, 31, 42 and 87. Measurements for animal #2363 included days 21, 42, and 87 and days 27, 60, and 93 for animal #2273. Four time points at day 21, 27, 60, 107 were included for animal #2268.

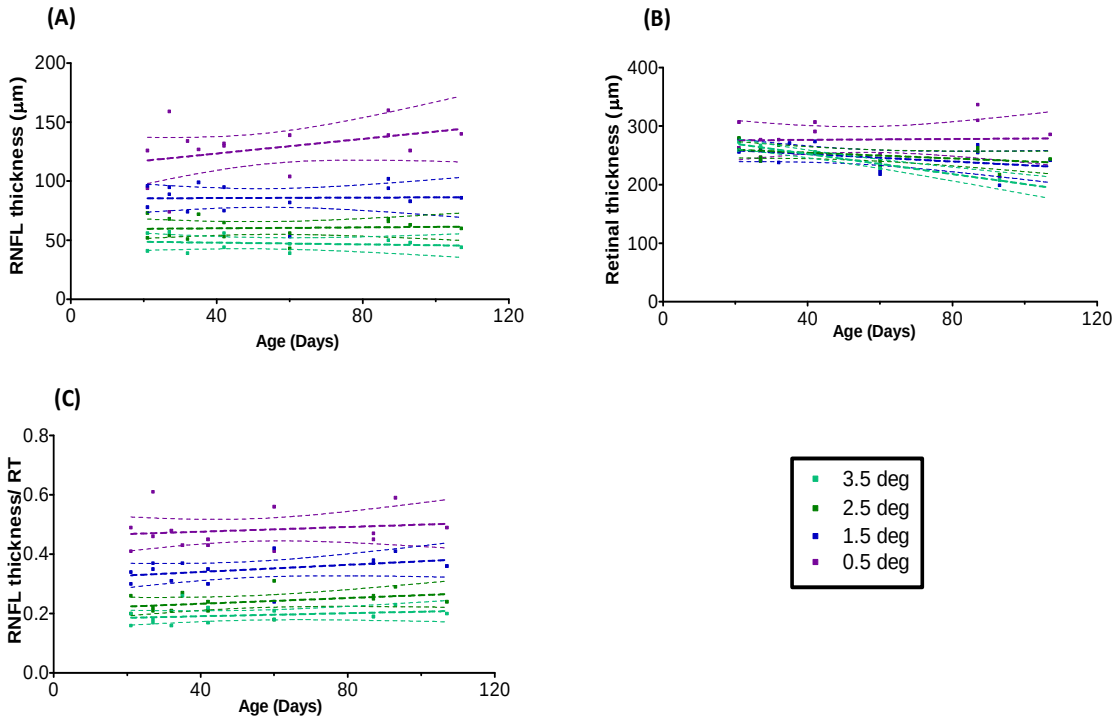


Fig. 2-9 RNFL thickness, RT, and RNFL thickness vs. RT as a function of age and eccentricity. (A) RNFL thickness vs. degree eccentricity from the center of the ONH (B) RT vs. degree eccentricity from the center of the ONH (C) The ratio of RNFL thickness/RT as a function of eccentricity from the center of the ONH. (A-C): all data was from animals who participated in the longitudinal part of the study

2.4 Discussion

2.4.1 Growth of Ocular Parameters with Age

We have shown growth rate of various ocular parameters in chicken (White Leghorn) for the age range of 21 to 107 days old. Here, we discuss each parameter in turn:

2.4.2 Corneal Thickness:

The structure and composition of the chicken cornea is very similar to the human cornea and thus contributes to the popularity of its use in various experimental studies and underscores

the importance of understanding its growth throughout the life of the animal (Lee, Javier, Change, Kato & Azar (2002); Tappeiner, Goldblum, Katsoulis, Sarra & Fruch (2011)). Despite the common use of chickens to study corneal refractive surgery, to the best of our knowledge only one study has explored central corneal thickness measurements over time via ultrasonic pachymetry in chickens (Montiani-Ferreira et al. (2004)).

Montiani-Ferreira et al. (2004) reported thinning (4 μm) of the central corneal thickness from 1 to 12.5 days which then gradually increased to reach a plateau to the initial thickness observed at birth at 70 days of age. We confirmed the same approximate 70 days of age for complete central corneal maturation utilizing a different method- a high-resolution ultrasound. Both ultrasonic pachymetry and ultrasound biometry use the property of sound wave interference to determine CrT but ultrasonic pachymetry is typically done in the awake chicken while biometry is typically performed under light isofluorane anesthesia. Both studies thus provide evidence towards maturation of the central corneal thickness by 70 days of age (equivalent to 2 human years). Similarly, maturation of central CrT was also observed in humans but at a later age of 5-11 years (Hikoya, Sata, Tsuzuki, Koide, et al. (2009); Pediatric Eye Disease Investigation Group (2011)). The mean central CrT measured in the present study was thinner in comparison to other reports: Avila & Mc Fadden (2010): ~ 230 μm; Montiani-Ferreira et al. (2004): ~ 240 μm; Irving et al. (1996): ~ 220 μm; Hayes, Fitzke, Hodos & Holden (1986): ~ 260 μm at age 22-55 days.

There is a possibility like with other known ocular parameters with daily growth rhythms (ACD, VCD, ChT, AL) that there might be a daily corneal rhythm of elongation that would

thus cause CrT to be dependent on measurement time. To date, we are not aware of any studies that reported possible diurnal growth rhythm in CrT in chickens. Of note, in humans central CrT is thickest right after awakening for approximately one hour, which then thins slightly by the same rate each hour after for the next 11 hours (Kiely, Carney & Smith (1982)).

2.4.3 Anterior Chamber Depth

We found that ACD had exponential growth with a mean value of ~ 1.472 mm at age 21 days deepening to ~ 2.269 mm at ~ 107 days. Although ACD appears graphically to be nearing a plateau in value at 107 days, the ACD fit would predict a maximum ACD of a little less than 2 years of age (14 human years). Schaeffel & Howland (1988) also showed asymptotic growth in ACD that is in agreement with the data from the present study throughout the entire time period. This trend for deepening of the anterior chamber with age has also been shown in humans (Weale (1982, 1983); Larsen (1971a)). Weale (1982, 1983) reported that ACD at 9 months was ~ 2.25 mm which reached a plateau of ~ 3.25 mm at the age of 5 years to ~ mid twenties which then declined from thereafter. Larsen (1971a) reported a period of exponential growth of the ACD for the first 1.5 years after birth which then slowed to about 1/3rd the initial growth rate; furthermore appearing to have reached a plateau at ~ 14 years of age. The data in the present study shows a similar trend of ACD development comparable to humans.

2.4.4 Lens Thickness

In the present study LT increased exponentially from 2.504 mm at age 21 days to 3.623 mm at age 107 days. Although LT growth rate appears to be approaching a plateau at 107 days, the growth equation based on the data in the present study indicates an estimated time of reaching a plateau in LT around 279 days post-hatching. Schaeffel & Howland (1998) found a similar exponential growth in LT. Avila & McFadden (2010) extended showed linear instead of exponential growth as their measurements were an extension of early post-hatching growth. The LT at ~ 4 weeks was in general agreement with that reported by Zhu et al. (1995) and Rymer et al. (2007). Lens thickness reported by Irving et al. (1996) was thinner than reported by both Avila & McFadden (2010) and the present study. This might be attributed to measurement technique when compared to Irving et al. (1996); ultrasound was performed immediately after their experimental animals were sacrificed while the present study and Avila & McFadden (2010) performed ultrasound biometry in the living chicken which may subject the lens to different tensile forces. Irving et al. (1996) and Avila & McFadden (2010) found that the process of freezing caused expansion of the lens thus overestimating true LT over their measurement period: first 14 days post-hatching. Of note, Schaeffel & Howland (1988) did not find an increase in LT in their frozen lenses. Schaeffel & Howland (1988) as well as Irving et al. (1996) both used excised eyes for their studies and it is currently unknown if ocular parameters are affected after enucleation of the eyes but it is possible LT might change.

The thickening of the crystalline lens with age in humans follows a different initial pattern of growth than that observed in chicken, with human lenses actually thinning initially (Larsen

(1971b)). They found LT to have an initial period of thinning from birth to ~ 8-10 years of age, followed by continual growth in the adult human lens (Cook, Koretz, Pfahnl, Hyun & Kaufman (1994)). Although the fit for LT in the present study predicted a plateau at 279 days of age in the chicken (equivalent to 6 human years), it is possible that growth continues beyond that age.

2.4.5 Vitreous Chamber Depth

In the present study VCD was found to follow a similar exponential growth pattern as that described for ACD and LT. Although the rate of growth slows towards the end of the observational period, it appears as if the vitreous chamber will continue to deepen after that, albeit at a much lower rate of growth. The predicted growth equation for VCD estimates a plateau in the growth of the vitreous chamber to be reached at ~ 388 days post-hatching (equivalent to 9 human years). Mean VCD at ~ 4 weeks of age was thinner than predicted by Rymer et al. (2007) and Zhu et al. (1995). Differences in reported VCD might be due to measurement technique. In humans, the growth curve pattern of VCD elongation as well as AL follow the same trend graphically as observed in the present study (Larsen (1971c)).

2.4.6 Retinal Thickness

Total retinal thickness at the center of the eye was invariable at ~ 209 μm during the entire measurement interval. Two studies also found RT to be stable at an earlier age (Avila & McFadden (2010): 0-15 days; Rymer et al. (2007): 4-27 days). The mean RT of 209 μm in the present study was identical to mean RT via histological sections reported by Schmid, Papastergiou, Nickla, Riva, Lin, Stone, & Laties (1998). Retinal thickness from 0-16 days of

age via frozen sections (Hayes et al. (1986): ~ 200 µm) was in close agreement with the present study. At 21 days post-hatching Rymer et al. (2007) reported a similar RT of 230 ± 15 µm (30 Mhz ultrasound). When RT was measured via Doppler interferometry, Schmid et al. (1996) found RT to be ~ 30 µm thicker at 3 weeks of age compared to the results from the present study. Similarly, Nickla, Wildsoet & Wallman (1998) and Papastergiou et al. (1998) ~ 30 µm bigger total retinal thickness compared to the present study. Hayes et al. (1986) reported RT values in excised untreated eyes: 0.26 ± 0.02 mm from 20 – 55 days of age. While Avila & McFadden (2010) reported average RT to be 0.278 ± 0.060 mm thick and in agreement with the values reported from frozen sections used by Schaeffel & Howland (1988) and Irving et al. (1996), they reported that their measurements with ultrasound were higher because of the inclusion of the RPE rather than strain differences. Thus, thinner total RT values in the present study must be attributed to some other factor such as resolution of the different measuring techniques used in each study and possible strain differences.

2.4.7 Choroidal Thickness

The choroidal thickness determined in the present study averaged ~145 µm and was stable throughout the observation period of 21-107 days post-hatching. While the present study reports stability, Avila & Mc Fadden (2010) and Rymer et al. (2007) report ChT thickening during their earlier observation periods. Avila & McFadden (2010) reported a mean ChT of ~ 140 µm at birth to a plateau of ~ 180 µm (0-15 days). Rymer et al. (2007) reported similar results to Avila & McFadden (2010) with an increase in ChT from a mean of 162 ± 26 µm at 4 - 5 days after hatching to ~ 213 ± 24 µm at day 21.

Differences between longitudinal and cross-sectional data were noted in both the present study and Avila & McFadden (2010). Avila & McFadden (2010) reported ~ 60 μm thicker ChT in comparison to the present study. These differences were most likely attributed to the normal diurnal rhythm in ChT growth as well as the increased difficulty of distinguishing echoes from the choroid. ChT is believed to be thinnest in the morning and thickens throughout the day to a maximum thickness at night (Nickla, Wildsoet & Wallman (1998)). Measurements in the present study were taken between 3 and 6 hours after the beginning of the light cycle while Avila & McFadden (2010) took measures at a later time in the day between 3 and 5PM, thus it was expected that Avila & McFadden (2010) would report thicker values. Mean ChT determined from macrophotographs in excised eyes for ages 20-55 days as reported by Hayes et al. (1986) was 210 ± 70 μm. Schmid et al. (1996) reported a mean choroidal thickness at 3 weeks of age of ~ 218 μm via laser Doppler interferometry and in close approximation to the present study when measured via histology (~ 138 μm). Measurement time was not available for Hayes et al. (1986) or for Schmid et al. (1996) and thus it is possible that circadian rhythm in ChT as well as measurement technique caused discrepancies between the studies.

2.4.8 Axial Length

Axial length was computed as the sum of the major axial components: ACD, LT, VCD, RT and ChT. The growth of AL is thus primarily a factor of the largest axial component, namely the VCD. Axial length followed a similar growth pattern as ACD, LT, and VCD all appear to reach a plateau towards the end of 107 days of age. The projected time of reaching a plateau based on the fit for AL was similar but not exact to the time projected for VCD to

reach a plateau ~ 339 days. Based on the growth equation for axial length the mean value of AL at the end of the observational period (107 days) was estimated at 13.95 mm. The projected fit of AL in the present study would predict a value in AL of 14.53mm at the age of 339 days which is very close in agreement to the value reported by Papastergiou et al. (1998) at 360 days of age when measured via laser Doppler interferometry (14.41 ± 0.09 mm).

Differences in AL may also be a factor of how it is defined. Avila & McFadden (2010) defined AL as anterior cornea to posterior retina and did not include ChT but yet their values were thicker than reported by Irving et al. (1996). Rymer et al. (2007) and Papastergiou et al. (1998) reported optical axial length (anterior cornea to posterior vitreous) rather than axial length.

Humans have a similar pattern in growth of axial length with age compared to the one observed in the present study. In humans AL increases from birth to 1.5 years followed by a period of slower growth (Larsen (1971d)). They defined AL similar to how optical axial length was defined in chicken studies. The AL growth vs. age growth curve in the present study was similar in appearance to the same growth curve in humans (Larsen (1971d).

2.4.9 Refractive Error

Most of the past studies in different species of chickens show that most of the emmetropization process occurs by 11-16 days of age. Pickett-Seltner et al. (1988) reported a rapid drop in hyperopia the first day post-hatching with continual decrease in hyperopia at a slower rate for the next 13 days. Avila & McFadden (2010) showed that most of the emmetropization occurred within the first 11 days of age with ~ 2D reduction of hyperopia to

~ +1.0D at 11 days post-hatching. We found mean refractive error to be stable around ± 1D of hyperopia throughout the observational period, which is in good agreement with the projection by Avila & McFadden (2010) as well as the reported RE of Rymer et al. (2007): + 0.5 ± 0.7D and Wallman et al. (1981): ~ +1.0 D at age 28 days post-hatching. Pickett-Seltner (1988) also reported a similar time frame of emmetropization by two weeks of age with ~ + 2.7D of hyperopia at birth and + 0.1 ± 0.05D at 14 days of age. Irving et al. (1996) also reported a substantial reduction in hyperopia between birth and 16 days of age. A reduction of hyperopia shortly after birth was also evident among human studies that reported decreasing hypermetropia with age (Mohindra & Held (1980); Larsen (1971a)).

Both Irving et al. (1996) and Avila & McFadden (2010) reported ~ 65% reduction in refractive status the first 2 weeks post-hatching; 16, and 11 days, respectively. Although, they reported a similar reduction in RE the first 14 days of age, it is difficult to know if the first two weeks after birth represent full emmetropization. During this two week time frame, Avila & McFadden (2010) reported a decrease in the artifact of retinoscopy with age. We did not perform retinoscopy until 70 days of age and with the constant growth in axial elongation with age and the belief that the artifact of retinoscopy decreases with larger eyes, we assume that at 70 days of age, this artifact will be less than at earlier ages.

There is a possibility that the gender difference in refractive error shown in Zhu et al. (1995) at 4 weeks of age may have been influenced by the act of deprivation of the contralateral eye. In the present study, the possibility of an influence on the non-injected fellow eye of animals injected with microbeads and/or saline in the other eye should not be ruled out. Assuming

refractive status is mainly axial in nature and that the circadian rhythm of axial length influences refractive error, this could explain the large variability among RE among the cross-sectional compared to the longitudinal animals. It was presumed that since the present study began at 21 days, most of the emmetropization had already occurred, as RE was stable at ~ + 1D throughout the entire observation period.

2.4.10 Cross-sectional vs. Longitudinal Data

In the present study there was good agreement between cross-sectional and longitudinal ocular parameters (ACD, LT, VCD, RT, AL) with the exception of ChT and RE. As described earlier ChT and RE had a high variability when measured in a cross-sectional manner because of the larger sampling during the day which was affected by their daily growth rhythms. Of note, RE is primarily axial in nature and although a RE growth rhythm does not exist per se, it is affected by the daily growth rhythm of axial elongation.

Some evidence for influences of experimental manipulation of the fellow eye on the untreated eye has been described above. More evidence towards eye(s) not acting independently was reported by other authors. Wildsoet & Wallman (1995) and Papastergiou et al. (1998) also found that form deprivation had an influence on the fellow eye. We are not entirely confident that anterior chamber injections of microbeads of fellow eyes influenced the non-injected eye(s) but it is possible and thus we found it important to include animals in the present study without any experimental manipulation.

Past studies have shown deviations between cross-sectional and longitudinal ocular parameters. Avila & McFadden (2010) reported differences in growth rates among ACD and

VCD between those measured in a cross sectional vs. longitudinal manner. Cross-sectional data for both RT and ChT showed the same trend in growth but cross-sectional data were on average about 10 μm thicker. This provides evidence for differences in cross-sectional and longitudinal measurements which Avila & McFadden (2010) believed may be due to more frequent sampling with longitudinal animals.

2.4.11 Gender Differences

A statistically significant gender difference among all ocular parameters in the present study was not found. While Montiani-Ferreira et al. (2004) and most human newborn studies (Portellinha & Belfort (1991); Price, Koller & Price (1999), Remon et al. (1992)) did not report a gender difference in CrT, Rushood et al. (2012) found a difference in newborns. Zhu et al. (1995) (chickens: 4 weeks of age) did not report sex differences in ACD but males have been shown to have a deeper, albeit small difference in ACD compared to females in humans (Larsen (1971a); Weale (1982)). Qiao-Grider et al. (2007) found no gender disparities in ACD in the rhesus monkey. While mean LT, VCD and AL at 28 days of males were thicker than females (Zhu et al. (1995)), their values were comparable to the present study. In humans, Larsen (1971c) also reported a deeper VCD in males when compared to females. Zhu et al. (1995) found a small gender difference in RE at 4 weeks of age with values comparable to the present study. No gender difference in emmetropization time was found in humans (Larsen (1971a)) or in the rhesus monkey (Qiao-Grider et al. (2007)). Reasons for the minor gender discrepancies between the studies may be precision of instruments, experimental manipulation of the fellow eye having differential influences on genders, and measurement time.

2.4.12 Changes in RNFL thickness and RT with Eccentricity and Age

Both RNFL and total RT increased with increasing proximity to the optic nerve head. Mean RT between 0.5 and 3.5 degrees eccentricity from the center of the optic nerve head was ~ 50 μm thicker than reported when measured through the visual axis via ultrasound but in better agreement to reported RT values measured on axis by past chicken studies. These findings suggest considerable variations in total RT across the retina in birds. We found that both RNFL thickness and RT were stable with age at 0.5, 1.5, and 2.5 degrees eccentricity. One exception was thinning of RT at 3.5 degrees during the observation period. This may be an important factor when utilizing the chicken for experimental induction of ocular hypertension. Despite the thinning of RT at 3.5 degrees eccentricity, we found the ratio of RNFL thickness to RT to be stable, as was RNFL/RT ratio at 0.5, 1.5, and 2.5 degrees eccentricity. Glickstein & Millodot (1970) reported that RT was similar among different species of mammals despite the absolute eye size. Several studies (including the present study) have reported chickens with mean RT values comparable to those found in mammals. We reported mean RT near the ONH to range from ~ 200 to 250 μm. Despite a smaller eye size in rodents, Schmucker & Schaeffel (2004) reported a similar RT in mice near the optic nerve head in C57BL/6 mice grew from 177 μm at age 22 days to 223 μm at 100 days of age.

2.4.13 SD-OCT Imaging

To the best of our knowledge, no other reports on the use of SD-OCT to measure retinal parameters in the chicken are available. Use of the pecten as a geographical marker was helpful to ensure reproducibility of the location of SD-OCT imaging with time. The optic nerve is immediately posterior to the pecten and thus imaging location is superior in the

ONH. Precise measurement of the RNFL and total RT by SD-OCT may be helpful when studying the effects of various pharmacological agents on the layers of the retina or in establishing ocular hypertensive models in birds.

2.4.14 Comparison of Ocular Parameter Growth Rates

2.4.14.1 ACD Growth

The ACD growth pattern in the present study was in full agreement with results obtained by Schaeffel & Howland (1988), and in the present study data was reported slightly beyond the age range used in their study. Thus, it is likely that ACD grows during this period and beyond. The exact reason for continual ACD growth is unknown but correlation coefficients between ACD and AL in chicken probably increase with age (Irving et al. (1996): $r = \sim 0$ at 7 days; present study: $r = 0.9756$ at 21-107 days). It is likely that the continued growth of the ACD is a compensatory mechanism for the continuous (although relatively much smaller) growth of VCD and LT. As RE has been shown to be dependent on corneal power, lens power and axial length in human studies (Sorsby, Benjamin & Sheridan (1961)), corneal power and lens power might have increasing responsibility for maintenance of RE as AL stabilizes. As lens power is believed to decrease with age in humans (Sorsby et al. (1961)), ACD must increase to compensate for the decreased lens power with age (Brown (1974)) to maintain stability in refractive error with age. The enlargement of the anterior chamber to match the demands of emmetropization (decreasing lens optical effectivity) was coined the "inflatable anterior segment" mechanism of emmetropization in humans (Koretz, Rogot, & Kaufman (1995); Brown et al. (1999)). If applicable to chickens as suggested by the present

study, this concept could explain why ACD has the largest percent growth out of all other ocular parameters during the observation period of the present study. This could explain also why ACD was the only parameter predicted to deepen between 1 and 2 years post-hatching while the other ocular parameters (including LT) essentially are predicted to stop growing around 1 year of age. Thus, the "inflatable anterior segment" mechanism provides fine tuning and maintenance of refractive error by decreasing the lens effectivity (by increasing ACD) while the lens power continues to decrease with age. The anterior segment is not the only component that influences refractive status as Koretz et al. (1995) also reported that both anterior segment length (ACD, LT) and posterior segment length (VCD, RT, and ChT) are independent of age in humans suggesting that the anterior segment and vitreous cavity must increase proportionally to maintain emmetropia. Disruptions in this proportionality would result in ametropia. This may be applicable to the chicken also and support the notion that emmetropization was functioning normally in the present study as the combined absolute growth of ACD + LT was approximately equal to the absolute growth in VCD in the present study over the 21-107 day time period. Similar to the lens, the cornea flattens with age and axial length in humans (Koretz et al. (1995), Brown et al. (1999)). Thus, to maintain emmetropia as axial length increases, the anterior corneal radius of curvature increases (flattens) thus lowering the Dioptric power of the eye to compensate for the increase in total power of the eye associated with increasing axial length in humans (Sorsby et al. (1961); Koretz et al. (1995): "inflatable globe"). Although the present study did not measure corneal curvature, Schaeffel & Howland (1988) and Troilo (1990) reported an increase in corneal curvature with age (~ 14 to 78 and 56 days, respectively) in chicken and thus a decrease in

corneal power with age. In humans, a positive correlation exists between both anterior segment length and vitreous cavity length to axial length in emmetropes (Koretz et al. (1995)). The present study also found positive correlations in anterior and poster segment length in chickens. Furthermore, these correlation coefficients were remarkably similar between ACD, LT, and VCD on AL ($r \sim 0.97$). In summary, taking into account Schaeffel & Howland (1988) findings of changes of corneal curvature with emmetropization and the findings of good correlations of the major axial ocular components with axial length in the present study, the mechanism of the " inflatable globe" and "inflatable anterior segment" are likely present in chicken as emmetropization was present throughout the entire observed period.

2.4.14.2 CrT, VCD and AL Growth

CrT showed cessation of growth significantly earlier (68 days) compared to the other ocular components in full agreement with Montiani-Ferreira et al. (2004) for the observed age range. The exact reason why the maturation of the corneal thickness happens more quickly is unclear, but it might be related to the early maturation of the corneal power as seen in monkeys (Qiao-Grider et al. (2007)). During the observed time period in the present study VCD had the greatest contribution towards total axial length followed by LT then ACD (Fig. 2-7, Table 2-4). VCD and AL both demonstrate similar exponential growth time courses in the present study with similar maturation time in between that of LT and ACD at ~ 1 year of age. As commented earlier, the similarity between the predicted times to reach a plateau for VCD and AL as well as a comparable ~ 30 percent growth from 21 and 107 days (Table 2-3) could imply interdependence in growth rates and may help explain why studies in chicken

have found increased axial growth via form deprivation and constant light to be primarily the result of posterior elongation (form deprivation: Wallman & Adams (1987); Stone, Lin, Desai, & Capehart (1995); Troilo (1990); constant light: Hayes et al. (1986); Pickett-Seltner et al. (1988)). While Wallman & Adams (1987), Stone et al. (1995), and Troilo (1990) attributed the resultant myopia in experimental form deprivation studies to be largely due to deepening of the vitreous chamber, constant light rearing produced eye enlargement also primarily as a result of elongation of the vitreous chamber, conversely without any inherent myopia up to a certain age (Hayes et al. (1986); Pickett-Seltner et al. (1988)). The different mechanisms of axial elongation via form deprivation and constant light provide evidence towards the dependence of axial length on VCD. As previously described in humans, there is a positive correlation between vitreous cavity length and axial length with a decrease in ACD and lens thickness as the vitreous deepens (Koretz et al. 1995). Similar predicted time to reach a plateau in growth of the VCD and AL as well as similar increase in value (~ 30%) over the observational period in the present study point towards a relationship between the two parameters. In contrast, Avila & McFadden (2010) reported a decline of the influence of VCD on refractive status during the first two weeks post-hatching despite a large decrease in hyperopia. As the majority of the emmetropization process in chickens is believed to occur by ~ two weeks of age and refractive error was stable over the observed time period in the present study, the influence of VCD on refractive error could possibly be for maintenance rather than a change in refractive error.

2.4.14.3 Similarities in Growth of Ocular Parameters to Chickens and Other Species:
In the present study, while some ocular parameters such as RT, RNFL thickness, ChT, and particularly RE demonstrated stability with age over the range of 21-107 days, other parameters showed continual growth. Thus CrT, ACD, LT, VCD, and AL all show a period of exponential growth followed by a slower phase. This pattern of stability in RE despite a slowed continual growth of the major components of the eye is in general agreement with findings in chickens (Irving et al. (1996); Avila & McFadden (2010); Wallman et al. (1981); rhesus monkeys (Qiao-Grider et al. (2007); and humans (Larsen (1971a; Mutti, Lynn Mitchell, Jones, Friedman, et al. (2004,2005); Giordano et al. (2009)). In chickens, a large reduction in refractive error was reported by Avila & McFadden (2010), Irving et al. (1998), and Wallman et al. (1981) during the first two weeks of life. In the present study, with measurements beginning at 21 days post-hatching, after the presumed rapid phase in emmetropization, refractive error was expected to vary minimally and this was indeed the case.

In humans, two stages (rapid and slow) of reduction in hyperopia were noted by several authors (Larsen (1971a); Mutti et al. (2004, 2005); Giordano et al. (2009)). Larsen (1971a) was the first study to report a two phase decline in RE consisting of a reduction in hyperopia from 1 year of age to ~ 6 years of age to a mean RE value of ~ + 0.7D (females) to + 1.0D (males) followed by a slower decline to plano refractive error around 12 to 13 years in both genders. Giordano et al. (2009) reported no significant change in spherical equivalent refractive error between 6 and 71 months thus providing additional evidence that emmetropization occurs mostly during early infancy and stabilizes on average to ~ +1D of

hyperopia (Caucasians: ~ +1.49D, African Americans: ~ +0.71D). These findings are in good agreement with earlier work by Mutti et al. (2004, 2005) who reported most emmetropization occurring between 3 and 9 months and stabilizing at around +1D during adolescent years. Of note, this same trend in reduction of moderate hyperopia at birth to stabilization at ~ +1D has also been shown in a small mammal (Zhou, Qu, Xie & Wang, et al. (2006): guinea pig).

The distinct pattern of a rapid phase of emmetropization followed by a more subtle slower period of emmetropization was also in agreement with findings in rhesus monkeys as Qiao Grider et al. (2007) reported a rapid decline in refractive error from birth (~ + 3.2D) to ~ + 1.5D at ~ 450 days (15 months) and a slower reduction in refractive status to ~ + 1.0 D during adolescence (50 months) despite continued ocular growth.

Therefore; it appears as if the time course of emmetropization in humans, non-human primates and chickens follow a similar time course and pattern of a rapid decline in hyperopia during infancy with stabilization to ~ + 1D followed by or a very small decline in hyperopia at a later age despite continued ocular growth. These two phases of emmetropization might possibly follow a neuronal growth pattern. Cummings et al. (2012) reported a correlation between gestational length and eye diameter in primates thus providing evidence that the eyes might follow a neural pattern of growth. Evidence of ocular development following a neuronal pattern of growth might also be true in chickens as an asymptotic growth pattern after birth has been shown in the present study for the major axial components of the eye and Atkinson (2007) also reported a similar growth pattern in brain

development. Of note, the two stages of emmetropization might be related to brain synapse development as there was a similar time course between the rapid stage of emmetropization and formation of brain synapses and the slower stage of emmetropization and maturation of brain synapses. The formation of synapses was completed by 14 days in the chicken (Rostas & Dunkley (1991); Atkinson(2007)) and between the third trimester until ~ 2 years in humans (Levitt (2003)) with the synaptic maturation period until 70 days of age in chickens (Rostas & Dunkley (1991); Atkinson (2007) and from ~ 0.75 years until 21 years in humans (Atkinson (2007)). The similarity in RE change between the chickens, non-human primates, and primates extends also to relative scaling of some ocular parameters. Thus, as shown in Table 2-4 the present study found that the infant chicken eye has similar scaling of the major axial components of the eye (ACD ~ 15 %, LT ~ 24 %, VCD ~ 60 %) to axial length when compared to both rhesus monkeys (Qiao-Grider et al. (2007)) and humans (Lotmar (1976)).

2.4.14.4 Differences in Growth Between Chickens and Other Species

Some ocular growth trends were found to differ among chickens vs. rhesus monkeys or humans. Lens thickness in humans (Larsen (1971b); Koretz et al. (1987), Brown et al. (1999)) and non-human primates (Qiao-Grider et al. (2007)) decreased during early life whereas chickens exhibited an asymptotic growth pattern (the present study). Application of the Gullstrand optical effective power formula to the lens: for lens power to decrease with age the radius of curvature and/or lens thickness must increase and/or the refractive index of the lens must decrease. Furthermore, as the lens curvature increases with age (Brown et al. (1999)), decreases in lens power with age are most likely attributed to changes in lens radius of curvature and/or the influence of lens cortex changes with age on the refractive index of

the lens. As Qiao-Grider et al. (2007) reported an increase in anterior lens radius of curvature with age in monkeys and reported a small insignificant increase in the lens index with age, as well as lens thinning with age, the major contributor to the decrease in lens power with age in monkeys is most likely the increase in radius of curvature of the lens. In agreement with monkeys, the reported data for chickens showed a slight increase in lens index (Schaeffel & Howland (1988): first 40 days post-hatching) as well as an increase in the anterior radius of lens curvature with age (Schaeffel & Howland (1988): ~ 5- 78 days post-hatching, Troilo (1990): 14 to 56 days post-hatching). Species differences among chickens, monkeys, and humans may account for all of these differences in the contribution of parameters that affect lens power and total power of the eye.

Based on the results in the present study of varying chicken to human ratios of 90% plateau for ACD, VCD and AL in days, the maturation of some ocular components during infancy in the chicken eye (ACD, VCD, and AL) might actually occur faster when compared to humans (~ 7 - 18 x the expected growth rate in humans based on absolute values in days). Thus, maturation of ocular components in the chicken might not have a simple scaling of 8 times faster maturation when compared to humans and thus using this conversion factor might not produce equivocal age equivalents. Similarly, Qiao-Grider et al. (2007) reported quicker maturation time of these ocular components in the rhesus monkey with maturation time during infancy of ACD, VCD, and AL to be about 3 times more rapid than the expected growth rate of these parameters in humans when based off absolute values (days) of 50% plateau values. Of note, while the present study and Qiao-Grider et al. (2007) estimated this conversion factor for life spans between different species during infancy, in actuality the

estimated growth of the eye may vary depending on the length of the time period studied as conversion factors between ages of different species are usually based on a time period from birth to death. Thus, relative contributions of ACD, LT, and VCD might vary between chickens and rhesus monkeys because the present study evaluated chickens during a human equivalent infancy period and Qiao-Grider et al. (2007) followed rhesus monkeys from a human equivalency of birth to adolescence. In agreement with rhesus monkeys and humans, each individual ocular parameter had varying growth rates indicating that the individual ocular structures did not mature in a proportional manner and was not a simple scaling of the ocular components of the eye. Species differences and the observed time period could be a contributor to this discrepancy although age equivalent comparisons might also be problematic.

2.4.14.5 Summary of Ocular Growth

Chickens follow a similar pattern of growth of the major ocular components comparable to both non-human primates and humans with the notable exception of the pattern of LT growth. Similarly, chickens show the same trend as humans and non-human primates in emmetropization: moderate levels of hyperopia at birth reaching ~ + 1D spherical equivalent and maintaining this refractive power throughout infancy which might possibly parallel the two phases of synaptic brain maturation. Like primates, they also seem to show both an active “inflatable anterior segment” and a passive “inflatable globe” component of the normal ocular growth process. Additional evidence for an active component of emmetropization in chickens, non-human primates, and primates has thoroughly been described in Wildsoet (1997). In addition, the relative contributions of ACD, LT, and VCD

towards axial length are comparable to humans and non-human primates. Similar to rhesus monkeys, chickens were found to have maturation of VCD preceding ACD, while the opposite was true for humans. Although full maturation for all ocular parameters in the present study are predicted to occur by 2 years post-hatching based on the predicted exponential growth fits, all of the ocular parameters in the present study meet 95% maturation by the end of the observation period of 107 days with the exception of ACD. ACD is likely to continue growth beyond that period probably due to the increasing growth of the VCD + LT with age ("inflatable anterior segment" hypothesis). Rhesus monkeys were found to have about a proportional infancy maturation rate of ACD, VCD, and AL compared to humans (1:3) in agreement with life span calculations (Torczynski (1979)). Similarly, chickens were found to have a proportional infancy ocular maturation 7 to 18 times that of humans, a range slightly larger than the expected life span conversion factor of 8. The growth pattern of ocular components in all three species (chicken, non-human primates, humans) suggests that the growth of the eye is likely driven by active emmetropization and maintenance of emmetropization by disproportional growth of the major ocular components of the eye.

2.4.15 Possible Confounding Factors and Limitations of the Current Study

Illumination and measurement time was a variable that differed between the present and other studies and may be a contributing factor for slight discrepancies between observed growth of ocular structures and refractive error. Studies have reported that light intensity has an impact on the normal growth and development of ocular parameters in the chick (Cohen et

al. (2008); Stone et al. (1995); Lauber & Oishi (1987); Li et al. (1995); Jenson & Matson (1957); Chiu, Lauber & Kinnear (1975); Bartmann et al. (1994); Morgan & Boelen (1996)). Comparing exact illumination and sources of illumination between studies is difficult as some studies report illumination at eye level and some provided a range of luminance levels. In humans, light exposure also plays a role in the development of refractive errors (Hoyt et al. (1981); O'Leary and Millodot (1979)). As both ChT and AL in chickens have a circadian rhythm of elongation (~ opposite to one another) (Nickla, Wildsoet & Wallman (1998), Weiss & Schaeffel (1993)), time of measurements was also a factor. Thus, it is important to take measurements at the same time point each day.

As described earlier, gender differences as well as the process of experimental manipulation of the fellow eye may also cause discrepancies between the present study and other studies. While we did not report any gender differences in the ocular parameters in the present study Zhu et al. (1995) found small, sometimes statistically significant or insignificant gender differences among the ocular parameters they studied. Although experimental visual deprivation was not performed in the present study, evidence for gender differences and influences of experimental manipulation was shown by Schmid & Wildsoet (1996) and Zhu et al. (1995) who reported that males are more affected (higher myopia and longer axial lengths) by the procedure than females. These studies provide evidence that some types of experimental manipulation of one eye may in fact affect the other eye and thus potentially disturb normal eye growth of ocular components and refractive error. In the present study, as few chicks did have experimental anterior chamber injections in the fellow eye and cross-sectional vs. longitudinal data was in good agreement, it is unlikely that experimental

manipulation of the fellow eye had significant effects on the normal growth of ocular parameters.

Measurement errors via the instruments and techniques utilized may also be possible. Although both Hartinger and streak retinoscopy are known to be accurate methods of determination of refractive status slight differences in precision of refractive error might exist. Also, the varying precision of ultrasound instrumentation may be a factor to differences found when compared to other studies. Differences in reported ocular parameter values between studies could be due to a difference in accuracy of the instruments used (Avila & McFadden (2010): 18.8 MHz ultrasound; Current study: 35 MHz ultrasound; Hayes et al. (1986): macrophotographs; Irving et al. (1996): 10 MHz ultrasound; Montiani-Ferreira et al. (2004): ultrasonic pachymeter). Another possible reason for reported differences in values might be attributed to in vivo (Montiani-Ferreira et al. (2004), Avila & McFadden (2010), the present study) vs. ex vivo (Irving et al. (1996), Hayes et al. (1986) techniques. The use of light anesthesia for both retinoscopy and ultrasonography most likely did not have a significant effect on true values as isofluorane has a slight mydriatic effect helping to prevent accommodation and anesthesia time was limited to less than 5 minutes per eye to perform both ultrasonography and retinoscopy.

2.5 CONCLUSIONS

Better understanding of the development of the chicken eye would be beneficial for several aspects of vision science, including eye growth in different species and better planning and interpretation of studies using the chicken eye as a model. We studied the growth of ocular parameters by collecting cross-sectional and longitudinal data in White Leghorn Cornell K chicks over a defined age range. Results from the current study demonstrated development of ocular parameters in the adolescent chicken, which for the most part correlated well with similar measurements reported by other studies. In general, the growth pattern observed in the chicken also showed similarity with the growth rate of human and non-human primate ocular parameters. Future studies investigating both corneal curvature and lens curvature for the age range in the present study may be combined with the data from the present study to construct a schematic eye in the chicken for the age range 21-107 days of age. Future studies might also extend the observation period of ocular parameters beyond 107 days to confirm the prediction that LT, VCD, and AL would reach maximum maturation by ~ 1 year of age, while ACD growth would reach a plateau at about twice this time period at ~ 2 years post-hatching.

CHAPTER 3: OCULAR HYPERTENSION MODELS IN CHICKEN: FEASIBILITY AND FUTURE DIRECTONS

3.1 INTRODUCTION

Glaucoma is a term for a heterogeneous group of optic neuropathies of varying etiologies (Casson, Chidlow, Wood, Crowston & Goldberg (2012)). It is also the second leading cause of blindness after cataracts worldwide (Quigley & Broman (2005); Ray & Mookherjee (2009)). The world estimated number of individuals with open angle glaucoma (OAG) and angle closure glaucoma (ACG) was estimated to rise from a combined number of 60.5 million people in 2010 (74% OAG, 26% ACG) to 79.6 million in 2020 with bilateral blindness affecting ~ 4-6 million of them (Quigley & Broman (2005). Glaucoma is divided into subcategories and may be characterized as primary or secondary depending on the cause of the insult, by the extent to which the anterior chamber angle is open, and/or by the amount of ocular hypertension. Common clinical features include vertical elongation and deepening of the optic disc cup, degeneration of retinal ganglion cells and their corresponding axons, as well as visual field defects. In humans, visual field loss can be correlated with the extent of retinal ganglion cells (RGCs) and retinal nerve fiber layer (RNFL) loss (Quigley & Green (1979)) and also with changes in the outer retina (Choi, Zawadzki, Lim, Brandt, et al. (2011); Fazio, Heckenlively, Martin, & Christenson (1986); Nork et al. (2000); Vaegan, Goldberg, Buckland, & Hollows (1995), Werner et al. (2011)).

Ocular hypertension is considered a risk factor for glaucomatous progression (Gordon (2002); Rivera, Beld, & Feldman (2008)). Elevated IOP has been shown to degenerate

RGCs by apoptosis in animal models (Garcia-Valenzuela et al. (1995); Quigley, Nickells, Zack, & Kerrigan (1994); WoldeMussie, Ruiz, Wijona, & Wheeler (2001)). RGC functional damage has been studied by measuring electroretinogram (ERG) amplitude and/or visual field loss (Banitt, Ventura, Feuer, Savatovsky, et al. (2013); Frankfort, Khang, Tse, Chung, et al. (2013); Sommer, Kat, Quigley, Miller, et al. (1991); Ventura, De Los Santos, Feuer, & Prociatti (2006), Ventura & Prociatti (2006)). Various aspects of the disease, including both inner and outer retinal changes and their function, have been investigated, but the exact disease mechanism of glaucoma is yet to be understood (Argarwal, Gupta, Argarwal, Saxena (2008), Berninger & Arden (1988); Burdon (2012); Freddo & Gong (2009); Georgiou, Francesca Cordeiro & Salt (2013); Kendell, Quigley, Kerrigan, Pease, & Quigley (1995); Mehaffey, Hologigian & Seiple (1993); Ray & Mookherjee (2009); Rieck (2013); Vaegen et al. (1995); Wygnanski, Desarnik, Quigley, & Glovinsky (1995)). Animal models of OHTN and/or glaucoma have been studied extensively to enhance our understanding of the mechanism of elevated IOP insult to the optic nerve head and retina as a whole.

Although non – human primates have the closest anatomical and functional similarities to human disease processes, rodents are used with most prevalence due to their low cost, availability, and faster disease progression. Many investigators were able to produce elevation of IOP via different techniques (i.e. episcleral vein injection of hypertonic saline, cauterization of limbal vessels, microbead injections into the anterior chamber, injection of ghost red blood cells, etc.) to study the effects of IOP on inner and outer retinal function and /or the optic nerve utilizing rodents (Chauhan, Pan, Archibald, LeVatte, et al. (2002); Chen, Wei, Cho, & Chen (2011); Frankfort et al. (2013); Georgiou, Francesca Cordeiro, & Salt

(2013); Feng, Chen, Suyeoka, & Liu (2013); Garcia-Valenzuela et al. (1995); Mittag et al. (2000); Kwong, Vo, Quan, Nam, et al. (2013); Moorison, Johnson, Cepurta, & Jia (2005); Joos, Li, & Sappington (2010); Moorison, Cepurna, & Johnson (2010); Moorison, Moore, Deppmeier, Gold, et al. (1997); Samsel, Kisiswa, Erichsen, Cross, & Morgan (2011); Sappington, Carlson, Crish, & Calkins (2010); WoldeMussie et al. (2001)) and non-human primates (Gaasterland & Kupfer (1974); Gaasterland, Tanishima & Kuwabara (1978); Gardiner, Fortune, Wang, Downs & Burgoyne (2012); Hayreh, Jonas & Zimmerman (1998); Kalvin, Hamaski, & Gass (1966); Lessell & Kuwabara (1969); Nork et al. (2000); Quigley & Addicks (1980); Quigley & Hohman (1983); Shimazawa, Nakamura, Miwa, Tsunama, et al. (2013); Weber & Zelenak (2001); Wygnanski et al. (1995)).

Methods of IOP elevation common to both non-human primates and rodents include: 1) Photocoagulation of the trabecular meshwork via argon laser (primates: Gaasterland & Kupfer (1974); Gaasterland, Tanishima & Kuwabara (1978); Hayreh, Jonas, & Zimmerman (1998); Nork et al. (2000); Quigley & Hohman (1983); Schuman, Pedut-Kloizman, Pakter, Wong, et al. (2007); rodents: Ebneter, Casson, Wood & Chidlow (2012); Kwong et al. (2013)) and 2) Injection of microbeads into the anterior chamber (non-human primates: Weber & Zelenak (2001); rodents: Chen et al. (2011); Samsel et al. (2011); Sappington et al. (2010)). Photocoagulation of the trabecular meshwork has been shown to produce IOP elevation sustainable for weeks with corresponding axonal and RGC death (Kwong et al. (2013)). Trabecular meshwork photocoagulation could cause inflammation with a possible blockage of the visual axis, making this technique less suitable for in-vivo imaging. Furthermore, additional complications such as irreversible ocular and thermal damage to the

sclera have been reported. Thus, a more recent innovation has been obstruction of the aqueous humor outflow pathway by the injection of microbeads into the anterior chamber angle in rodents and non-human primates. Advantages to the microbead injected method of ocular elevation include: glaucomatous damage with minimal to no ocular inflammation, simplicity, and cost-effectiveness (Chen et al. (2011)). In mice this method produced a mild and chronic elevation in IOP with few IOP spikes, and slow mildly progressive RGC loss characteristic of early stages of glaucoma (Frankfort et al. (2013)). The newest adaptation of this method requires the injection of magnetic microspheres into the anterior chamber angle with the ability for better control over the placement of microbeads in the anterior chamber angle with the use of a magnet (Samsel et al. (2011)). A clear visual axis is needed for detailed imaging of the retina by spectral-domain optical coherence tomography (SD-OCT) and, potentially, adaptive optics, this is a promising approach. Additionally, with better direction of the beads into the anterior chamber angle there is less chance for the beads to adhere to the cornea. One of the possible disadvantages is that magnetic microbeads are limited to a maximum 5 micrometer diameter. Furthermore, microbead induced aqueous outflow blockage protocols were adapted for chickens in the present study for future species comparisons on the effects of elevated IOP on the retina.

Although experimental models of ocular hypertension have been developed in primates and rodents, there is a lack of ocular hypertension studies in the chicken, an animal whose large eyes and optics, fast growth rate, availability, and ocular anterior segment anatomical and functional similarities (Glasser et al. (1995); Renard, Hirsch, Savoldeli, & Pouliquen (1980), Tripathi & Tripathi (1973)) to human eyes make it a favorable animal of use. Chickens also

have an advantage as they have a cone-dominated retina (Kram, Mantey, & Corbo (2010); Meyer & May (1973)), whereas cones are underrepresented in mice retinas (Jeon, Strettoi & Masland (1998)). Thus, chickens are good candidates for in-vivo imaging of cone photoreceptors with (Headington, Choi, Nickla, & Doble (2011)) and without Adaptive Optics (AO) (Kisilak, Bunghard, Hunter, Irving, & Campbell (2012)). Our previous work also shows the ability to track longitudinal changes in total retinal thickness (RT) and nerve fiber layer (NFL) thickness with spectral domain optical coherence tomography (SD-OCT) in chicken. While current glaucoma therapies have focused on preventing glaucomatous damage with pharmaceutical and surgical interventions, other investigations in both animal and human glaucoma models have been targeted at stem cell regeneration of functional RGCs to misplace already damaged RGCs (Karl (2013)). Furthermore, the chicken has already been shown to be an appropriate species for retinal regeneration studies (Coulombre & Coulombre (1965); Fischer (2005); Hayes et al. (2007); Karl and Reh (2010)) and may thus provide invaluable information in developing potential therapeutic interventions for glaucoma. For these many reasons, the chicken has been chosen as a species that could possibly be used as an appropriate model of ocular hypertension and/or glaucoma.

As experimental animal models of elevated IOP are dependent on accurate IOP measurements, it is necessary to understand the normal expected IOP with age for accurate correlations of IOP changes in experimentally elevated eyes followed in a longitudinal manner. To date, only two other studies have measured IOP longitudinally over time in chickens (Schmid, Hills, Abbott & Humphries (2003); Lauber, Boyd & Boyd (1972)). While Schmid et al. (2003) measured IOP from 2 days to 42 days post-hatching via Tonopen XL,

Lauber, Boyd & Boyd (1972) measured IOP between 42 and 140 days of age via manometry. As differences between manometric and Tonopen XL have been shown (Nickla, Wildsoet & Wallman (1998); Papastergiou et al. (1998)), the present study determined the normal time course of IOP over the age range of 21-107 days post-hatching with Tonopen XL. In addition to tracking the normal course of IOP development in the older chicken, the use of the chicken for experimental induction of ocular hypertension and/or glaucoma by obstruction of the anterior chamber angle by microbeads has been investigated.

3.2 MATERIALS AND METHODS

3.2.1 Animals

Twenty White Leghorn chickens (G*allus gallus domesticus*, Cornell K) of both genders (12-110 days old) were obtained upon hatching (day 0) in the lab and raised under a 12 hours on - 12 hours off light cycle. Lights came on at 8AM and off at 8PM. Ceiling room illumination (Full Spectrum Fluorescent Light: Vita-Lite F40T12) provided illumination in the cages ranging from 400 to 850 lux. Food and water was provided ad libitim. All data was taken over an 8 hour time period during light hours (3 to 11 hours after the lights turned on), while four non-injected control animals (#2268, 2273, 2356, 2363) had data taken during a narrower sampling interval (3 to 6 hours after the lights turned on). Three of the animals (animal #1901, 1910, 1913) had 3 days of measurements (age 22-24 days) over a 13 hour daily time interval from 30 minutes before lights came on to 30 minutes after lights came off at 6 time points (7:30AM, 9:30AM, 12PM, 4PM, 7:30PM, and 8:30PM). These measurements were used to determine the normal fluctuation in daytime IOP.

Demographics are included in Table 3-1. There were 5 control animals (21-107 days old) total: two animals with saline injected into one eye only (# 2162, 2268) and three animals (#2273, 2356, 2363) with no injections in either eye. An additional 15 chickens (12-110 days old) were subjected to one of 13 different combinations of doses and types of magnetic and/or non-magnetic microbeads injections into the anterior chamber angle. Three of these animals had microbead injections into both eyes (#1901, 1910, 1913), while the rest had one eye injected with microbeads and the other eye used as a control (in 5 Cases, saline solution was injected and in 18 Cases, no injections were given). Animal #1901, 1910, and 1913 were also used to determine the normal fluctuation of IOP during daylight hours at age 22, 23 and 24 days (prior to any injections). Magnetic Microbeads (4.5 μm diameter M 450 Epoxy magnetic polystyrene dynabeads: Invitrogen, Life Technologies, Carlsbad, CA, or 4.5 μm diameter magnetic polystyrene microbeads: Corpuscular, Cold Spring, New York) or non - magnetic microbeads (12 μm diameter plain polystyrene microbeads: Corpuscular, Cold Spring, New York) were used. Injections into the anterior chamber angle were performed with a 25 5/8 G needle under isofluorane anesthesia and intraocular pressure (IOP) was monitored frequently before and after injections with Tonopen under local anesthesia. Ocular and systemic health was regularly checked daily. A Burton lamp with individual fluorescein strips was used to check for leakage of aqueous and integrity of the cornea before and after applanation during the first few days after injections. Ultrasound biometry (35 MHz) was only performed on one saline injected animal (#2162) prior and post three saline injections to determine any causal effects on the axial parameters of the eye after three subsequent saline injections. Spectral-domain optical coherence tomography (SD-OCT) was

used to measure total retinal thickness (RT) and retinal nerve fiber layer (RNFL) thickness in one animal (#1975) who had elevation of IOP for 3 days. The ratio of RNFL thickness to RT was calculated. SD-OCT measurements were taken prior and post IOP elevation at 0.5, 1.5, 2.5, and 3.5 degrees eccentricity nasally and temporally in the x-coordinate plane from the center of the optic disc.

Care and use of the animals were approved by the New England College of Optometry's Institutional Animal Care and Use Committee and adhered to the ARVO statement for the Use of Animals in Ophthalmic and Vision Research.

Table 3-1: **Demographics of the non-injected and injected birds.** The number and type of injections, injection volume, concentration, amount of beads injected as well as which eye(s) had injections of microbeads and/or saline are shown. The age the animal was at for each injection as well as the age range followed and gender are included in the table. Inv. = Invitrogen. Corp. = Corpuscular Mag. = magnetic. M = male. F = female. OD = right eye. OS = left eye. OU = both eyes. Conc. = concentration.

Bird # (eye(s) injected with beads and/or saline)	Sex	Age range followed (days)	# injections of beads (age at injection(s) in days) eye(s)	# injections of saline (age at injection(s) in days) eye(s)	Volume injected (Type of bead/saline) [age at injection(s) in days] eye(s)	Conc. of beads injected	# of beads injected
2356 (none)	M	21-87	0	0	N/A	N/A	N/A
2363 (none)	F	21-87	0	0	N/A	N/A	N/A
2373 (none)	M	21-87	0	0	N/A	N/A	N/A
2268 OD	F	21-107	0	1 (27)OD	70 µL (Saline) [27]OD	N/A	N/A
2162 OD	F	22-66	0	3 (25,36,51)OD	90 µL (Saline) [25]OD 80 µL(Saline)[36,51]OD	N/A	N/A
1901 (OU)	F	22-41	1(28)OU	0	10 µL (Inv. Mag.)[28]OU	$4x10^8$	$4x10^6$
1910 (OU)	M	22-41	1(28)OU	0	10 µL (Inv. Mag.)[28]OU	$4x10^8$	$4x10^6$
1913 (OU)	F	22-41	1(28)OU	0	10 µL (Inv. Mag.)[28]OU	$4x10^8$	$4x10^6$
1950 OD	M	33-70	1(33)OD	0	20 µL (Inv. Mag.)[33]OD	$4x10^8$	$8x10^6$
1921 OD	F	33-70	1(33)OD	0	20 µL (Inv. Mag.)[33]OD	$8x10^8$	$16x10^6$

1939 OU	F	36-69	1(51)OD	1(51)OS	60 µL (Inv. Mag.)[51]OD 60 µL (Saline)[51]OS	$20x10^8$ N/A	$120x10^6$ N/A
2184 OD	M	12-56	2(26,41)OD	0	70 µL (Corp. Mag.) [26]OD 50 µL (Corp. Mag.) [41]OD	$14x10^8$	$98x10^6$ $70x10^6$
2122 OD	M	30-62	2(40,51)OD	0	70 µL (Corp. Mag.) [40]OD 80 µL (Corp. Mag.) [51]OD	$14x10^8$	$98x10^6$ $112x10^6$
2123 OD	M	30-62	2(40,51)OD	0	70 µL (Corp. Mag.) [40]OD 60 µL (Corp. Mag.) [51]OD	$14x10^8$ $16x10^8$	$98x10^6$ $96x10^6$
1943 OD	M	36-81	2(51,65)OD	0	70 µL (Inv. Mag.)[51]OD 70 µL (Corp. Mag.)[65]OD	$20x10^8$	$140x10^6$ $140x10^6$
1972 OD	F	20-54	2(26,40)OD	0	70 µL (Corp. Mag.) [26]OD 70 µL (Corp. Non-Mag.)[40]OD	$14x10^8$ $140x10^6$	$98x10^6$ $875x10^8$
1971 OU	F	20-73	2(40,55)OD	2(40,55)OS	70 µL(Corp. Non-Mag.)[40,55]OD 70 µL (Saline)[40,55]OS	$140x10^6$ N/A	$125x10^8$ N/A
1968 OU	F	30-81	3 (40,48,63)OD	2(48,63)	60 µL (Corp. Mag.) [40] 60 µL (Corp. Non-Mag.) [48] 60 µL (Corp. Non-Mag.) [63] 70 µL (Saline 48,63)	$14x10^8$ $180x10^6$ $250x10^6$ N/A	$84x10^6$ $180x10^8$ $250x10^8$ N/A
1975 OU	M	30-107	3(71,79,90)OD	1(90)OS	70 µL (Corp. Mag.) [71]OD 70 µL (Inv. Mag.)[79]OD 80 µL (Corp. Mag.) [90]OD 80 µL (Saline)[90]OS	$14x10^8$ $20x10^8$ $20x10^8$ N/A	$98x10^6$ $140x10^6$ $160x10^6$ N/A
1948 OU	F	33-110	2(33,99)OD	1(78)OU	60 µL (Inv. Mag.)[33]OD 25 µL (Saline) [78]OD 60 µL (Inv. Mag.) [99]OD 80 µL (Saline) [78]OS	$8x10^8$ N/A $14x10^8$ N/A	$48x10^6$ N/A $84x10^6$ N/A

3.2.2 Intraocular Pressure

Intraocular pressure was measured daily to every few days in all 20 animals. IOP was measured (for details, see Nickla, Wildsoet, & Wallman (1998)) with a hand held applanation tonometer (Tonopen XL, Mentor O & O, Norwell, MA, U.S.A) with topically applied corneal anesthetic 0.5% proparacaine hydrochloride ophthalmic solution (Alcon Laboratories Inc, Forth Worth, Texas) prior to all measurements. Nickla, Wildsoet &Wallman (1998) found manometric vs. Tonopen XL readings over the range of 10mm Hg to 50 mm Hg to be related by the equation: $manometric\ pressure = 1.48 * (tonopen\ reading) - 7.05\ mm\ Hg$, thus a

small difference in IOP was noted between 10mmHg and 20mmHg (≤ 2 mm Hg) and this difference increased between 20 mm Hg to 50 mm Hg. Papastergiou et al. (1998) also determined the relationship between Tonopen XL and manometric IOP via the equation: $IOP\ Tonopen = 0.014 \times IOP\ transducer - 1.523$. To determine if these equations between Nickla, Wildsoet, & Wallman (1998) and Papastergiou et al. (1998) were interchangeable we plugged in numbers to determine manometric pressure and tonopen IOP (i.e. Tonopen reading of 15 mm Hg had a calculated manometric IOP of 15 mm Hg via the Nickla, Wildsoet & Wallman (1998) equation but when this manometric pressure of 15 mm Hg was used in the Papastergiou et al. (1998) equation to determine tonopen IOP, predicted IOP was lower: 10.7 mm Hg). Furthermore, as there were deviations between these two formulas, in the present study Tonopen readings were used as is and are not adjusted to manometric pressures.

3.2.3 Microbead Injected Eyes

15 chickens were subjected to one of 13 different combinations of doses and types of magnetic and/or non-magnetic microbeads injections into the anterior chamber angle (Table 3-1). Only one animal (#1975) with elevated IOP had SD-OCT imaging prior and post a 3 day elevation in IOP.

3.2.3.1 Purification of Microbeads (magnetic and non-magnetic)

The purification of microbeads (Corpuscular magnetic and non-magnetic and Invitrogen magnetic) included vortexing the beads and washing them with 10x Tris buffered saline (Boston BioProducts, Ashland, MA) and 1M NaOH followed by placement on a platform

rocker and removal of supernatant with gravity being the primary force of separation for non-magnetic beads and the use of a 0.45 Tesla magnet for ease of separating the magnetic microbeads from the solution. In this same manner, the beads were then washed with sterile distilled water and sterile Balanced Salt Solution (BSS, Alcon Corp.) for three instances in a period of three days with a final resuspension in sterile BSS (the volume of BSS added varied and was dependent on the concentration of beads sought) under sterile protocols. Under sterile procedures this suspension was then vortexed and aliquots into sterile centrifuge test tubes were prepared for future use. The final concentrations, volumes, and amount of microbeads prepared are shown in Table 3-1.

3.2.3.2 Anterior Chamber Injections of Magnetic Microbeads

Procedure for anterior chamber injections of magnetic microbeads was adapted from a rodent model (Samsel et al. (2011)). The Samsel et al. (2011) protocol was followed in terms of actual injection procedure with a slight variation in exact needle and syringe model and topical anesthetic used (present study: 0.5% proparacaine hydrochloride ophthalmic solution: Alcon Laboratories Inc, Forth Worth, Texas). All animals were deprived of food and water for 30 minutes prior to isofluorane anesthesia (2.5 % halothane in oxygen, Halocarbon Laboratories). A BD Precisionglide 25 G 5/8 needle with 1 mL syringe was used to produce a self healing wound through the cornea with injection of appropriate volumes and varying concentrations of microbeads with minimal to no leakage upon withdrawal of the needle (Table 3-1). During the procedure care was taken to not touch the lens or posterior surface of the cornea with the needle. Minimal leakage of aqueous humor during the process was noted. Vetropolycin antibiotic drops (Dechra, Overland Park, Kansas) as well as Refresh

Celluvisc lubricating drops (Allergan, Irvine, California) were administered post injection and as needed thereafter. Mental and ocular health (with special attention to the clarity and signs of inflammation of the cornea, conjunctiva, anterior chamber, and lens) were followed prior injections and especially during recovery. Additional injections were performed as needed with a maximum of 3 injections per eye. Monitoring of IOP occurred prior to injections and daily or every few days in all animals after injections. A representative image of the distribution of magnetic microbeads in an animal at the 7th day of elevated IOP in the right eye only (Fig. 3-1A) with fellow control eye (Fig. 3-1B) is shown.

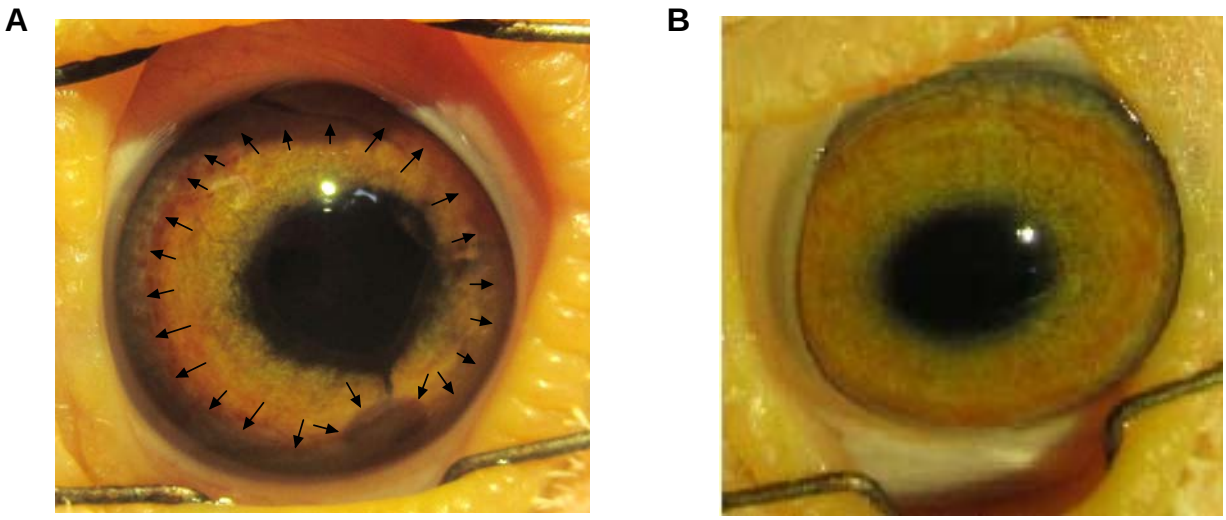


Fig. 3-1 Representative image of the distribution of magnetic microbeads in an eye of a bird that developed elevation of IOP and the fellow eye of the same animal. (A) Animal # 1943 right eye. Representative image of the distribution of magnetic microbeads in an eye of a bird that developed elevation of IOP after injections with magnetic microbeads only. (B) Animal # 1943 left eye. Representative image of the fellow eye of the bird depicted in A. Note: The eyes were dilated with vercuronium bromide prior to capturing these photographs (images taken at age 72 days).

3.2.3.3 Spectral domain optical coherence tomography (SD-OCT) of one ocular hypertensive animal

A spectral-domain optical coherence tomographer (SD-OCT) (Model RT100, Optovue Inc., Fremont, CA) was used on an awake animal with pupil dilation to measure total retinal thickness (RT) and retinal nerve fiber layer (RNFL) thickness near the optic nerve head (ONH) in one of the animals (Animal #1975) whom developed elevated IOP prior and post all injections. The measurement procedure started with the application of an anesthetic 0.5% proparacaine hydrochloride ophthalmic solution (Alcon Laboratories Inc, Forth Worth, Texas) followed by paralytic and pupil dilating drops, 1% vercuronium bromide. These drops were administered 5 minutes apart for 30 minutes until maximum dilation was achieved for that particular age of the bird (pupil size ranged from ~ 3.0 to 4.0 mm). Prior to the SD-OCT measurements, one drop of proparacaine was instilled in the eye prior to the insertion of a lid retractor. The same person held all the animals' head in front of the SD-OCT to ensure that the same retinal location is positioned for imaging for all the animals. At least 10 line scans centered at the tip of the pecten were acquired (6mm scan length) and averaged.

3.2.4 Saline control eyes

Two animals (2 eyes) were used solely as saline controls with one to three saline injection(s) into one eye only while six other animals had cases where microbeads were injected into one eye and saline in the other (Table 3-1). One control animal (#2162) had ultrasound biometry performed prior and post all three saline injections in both eyes for comparison between the saline and non-injected eye.

3.2.4.1 Injection of saline control eyes

Injection of saline was performed in the same manner as described for microspheres with the only exception that a magnet was not necessary for redirection. Exact volumes injected for each animal are shown in Table 3-1. A maximum of 3 saline anterior chamber injections per eye was performed in all animals. Control animal #2162 (Table 3-1) had three 80-95 μL sterile saline injections into the right eye while the left eye was not injected at age 25, 36, and 51 days post-hatching.

3.2.4.2 Ultrasound Biometry of a Saline control animal

In one of the control birds (# 2162) injected with repeated saline injections into the anterior chamber of the right eye only, under isofluorane anesthesia, A-scan biometry was used to measure ocular axial distances prior and post all injections in both eyes. Topical application of an anesthetic (0.5% proparacaine hydrochloride ophthalmic solution: Alcon Laboratories Inc, Forth Worth, Texas) was applied prior to measurements. Ultrasound biometry was performed using an A-scan ultrasound instrument operating at 35MHz (Model 5072PR, Panametrics, Waltham, MA) and ACD, LT, VCD, RT, and ChT were estimated directly from the ultrasound tracings while AL was estimated as the sum of these components. The accuracy of these measurements depends on the consistency of the various waveforms and the ability to accurately assign appropriate peaks. Animal #2162 was deprived of food and water for 30 minutes prior to isofluorane anesthesia (1.5% halothane in oxygen, Halocarbon Laboratories). Animal #2162 was placed in an adjustable holder with the head in an upright

position and a lid retractor was used to keep one eye open at a time. The probe was oriented perpendicular to the central cornea.

3.2.5. Statistical Analysis

The original data were tabulated and prepared in Microsoft Excel. Linear regression models of the data of each ocular parameter vs. age were generated via GraphPad Prism 5.0 (GraphPad Software, Inc., La Jolla, CA). The statistical analysis package in GraphPad Prism was used to evaluate differences between different data sets via two way analysis of variance (two-way ANOVA), any deviation from a horizontal-slope in linear regression functions, as well as significance of Pearson r correlation coefficients. Statistical significance was defined as p-value of < 0.05. All data are presented as mean values ± SEM.

3.3 RESULTS

3.3.1 Control Eyes

Control eyes included animals that did not have injections into either eye, the fellow non-injected eyes of microbead or saline-injected animals, and IOP measurements of animal # 1901, 1910 and 1913 prior to any microbead injections (Table 3-1).

3.3.1.1 IOP of non-injected Control Animals

The change in IOP during a 13 hour time span which started 30 minutes before the beginning of the light cycle and 30 minutes after the end of the light cycle was determined from 3 animals (# 1901, 1910 and 1913) for ages 22, 23, and 24 days. Figure 3-2 shows IOP as a function of time of day in military time (7:30, 9:30, 12, 4, 19:30 and 20:30) for 22, 23, and 24 days post-hatching. The 12 hour light and dark cycle is shown with the beginning of the light cycle starting at 8AM and the end of the light cycle at 8PM. There were no statistically significant differences ($p > 0.05$) at 7:30, 9:30, 12, 4, 19:30, and 20:30 (military time) between the right and left eyes of the 3 animals or between each animal at ages 22, 23, and 24 days. Thus, the mean IOP of both eyes was taken and then the mean of this value for each of the 3 animals at each of the 6 time points for the 3 day span were included in Figure 3.2. As evident from Figure 3-2, there was inter-day variability between mean IOP amplitudes (during light hours) of the 3 animals, with ~ 3, 1.5, and 1 mm Hg variation in IOP during light hours at 22, 23, and 24 days, respectively. There was also inter-hour variability in IOP measurements, which made it difficult to determine when exactly IOP was the highest or lowest during the daylight hours but for the most part IOP fluctuated minimally around ~ 14 mm Hg.

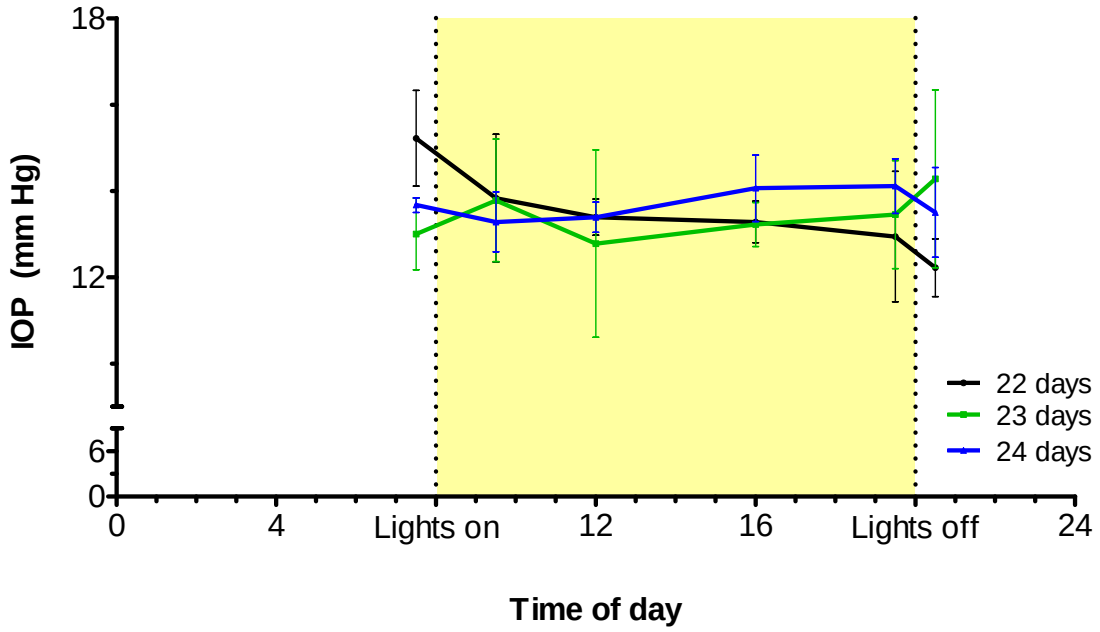


Fig 3.2 Fluctuation of IOP during daylight hours. The mean IOP of both eyes (6 eyes total) for animal # 1901, 1910, and 1913 at 7:30AM, 9:30AM, 12PM, 4PM, 7:30PM, and 8:30PM is shown over a 3 day time span (age 22-24 days). The x-axis is time of day represented in military time. The 12 hour light period is indicated with yellow shading.

A growth curve for IOP as a function of age for 4 control animals (#2268, 2273, 2356, 2363) over the time period of 21-107 days is shown in Figure 3-3. IOP over this observed time frame is related to age by the equation: mean IOP: $y = 0.02445x + 12.44$ ($R^2 = 0.8905$). Although a small increase in mean IOP was found (~ 2mmHg) between 21 and 107 days post-hatching in the present study, this was found to deviate significantly from zero ($p < 0.05$) (Fig. 3-3). Mean IOP (21 to 107 days) was 14 ± 0.6 mm Hg.

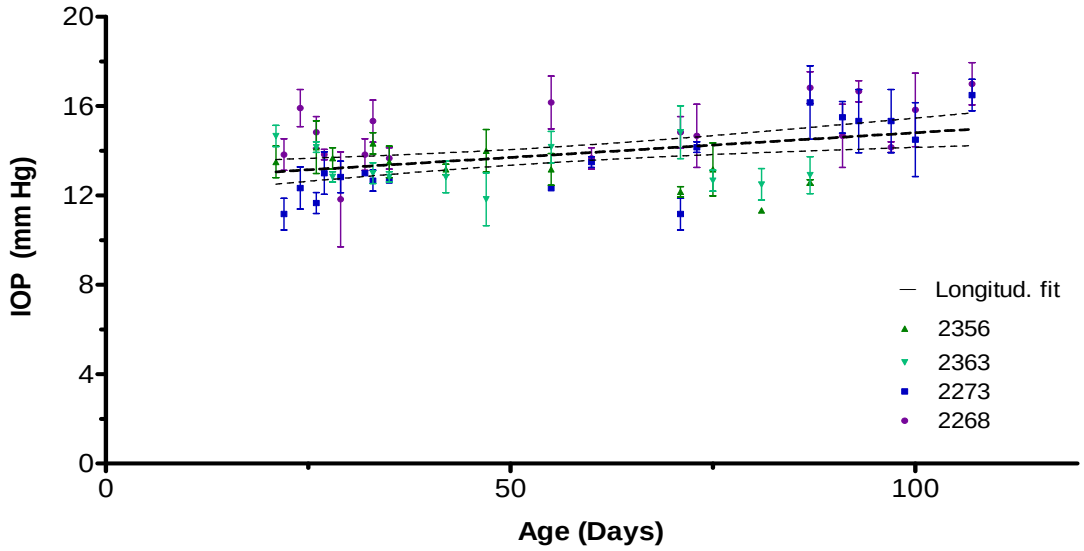


Fig. 3-3 IOP vs. age for non-injected control animals. Change in IOP with age of four non-injected control animals (#2268, 2273, 2356, 2363). Note: #2268 did have one saline injection but because there were no statistical differences in ocular parameters between the right and left eyes, #2268 was used as a non-injected control. The fit of the mean IOP from these four control animals with the upper and lower limit of the 95% CI is shown.

In comparison to the present study, past studies that have reported IOP in diurnally raised animals without any experimental manipulation in one or both eyes are shown in Table 3-2. Manometry was the predominate method of measuring IOP for decades, the Shiotz and Draeger tonometer are rarely used, and the most recent studies (including the present study) use Tonopen XL (Table 3-2). Of note, the past studies prior to 1998 in Table 3-2 did not specify time of IOP measurement or measurement time interval.

Table 3-2 Physiological IOP and method of IOP measurement (past studies vs. the present study). Comparisons of normal physiological IOP in animals raised under a diurnal light cycle are shown between past studies and the present study. The different methods of measuring IOP in each study are shown.

Study	IOP of normal diurnal reared chickens (age) [mm Hg]	Method of IOP measurement
Present study	Mean (12-107 days): 14 ± 0.6 Animal #1943 mean 70-77 days: 12.8 ± 0.6 Animal # 1975 mean 114-117 days: 13.7 ± 1	Tonopen XL
Schmid et al. 2003	Mean (day 2):12.7 ± 5.3 Mean (day 9): 18.0 ± 5.1 Mean (week 6): 13.4 ± 1.9	Tonopen XL
Nickla, Wildsoet, & Wallman 1998	Mean daytime (2 weeks): 19.8 Mean nighttime (2 weeks):13.1	Tonopen XL
Papastergiou et al. 1998	13 ± 2 (21 days) Mean IOP(start of light cycle at 7 days):16.8 ± 0.7 Mean IOP (end of light cycle at 7 days): 20.8 ± 1.2	Manometry (21 days) Tonopen XL calibrated to manometric IOP (7 days)
Lauber & Kinnear 1979	12.3 ± 0.98 (21 weeks)	Manometry
Bercovitz, Harrison & Leary 1972	14.28 ± 0.57 (1 day) 20.44 ± 0.75 (35 days) 19.27 (70 days)	Manometry
Lauber, Boyd, & Boyd 1972	10.6 ± 0.3 (6 weeks) 10.8 ± 0.5 (8 weeks) 12.03 ± 0.6 (10 weeks) 10.8 ± 0.4 (12 weeks) 11.1 ± 0.4 (20 weeks)	Manometry
Lauber, Boyd & Boyd 1970	12.2 ± 1 (week 16, 20)	Manometry
Smith, Becker & Podos 1969 (Fig. 7)	~ 22 (21, 40 days) 23 (by 5th week)	Draeger handheld applanation tonometer
Frankelson, Lauber & Boyd 1969	10.9 ± 0.9 (right eye 98 days) 11.4 ± 0.7 (left eye 98 days)	Manometry
Harrison, Bercovitz & Leary 1968 (Fig. 2)	IOP range (35 to 45 weeks):18.5 to 23.5	Manometry
Seaman & Himelfare 1951	Mean IOP (~ 1 year): 18.6	Shiotz tonometer

To date, the only other study to use Tonopen XL to investigate possible age-related changes in IOP of diurnal animals without any type of ocular manipulation was Schmid et al. (2003). Although graphically they showed IOP as a function of age at an earlier age range (2 to 42 days) than the present study, regression equations were not provided. In contrast to Schmid et al. (2003) where a negative slope of IOP is shown between 3 and 6 weeks, the present study found an opposite trend (positive slope) during this time interval (Fig. 3-3). In the present study mean IOP was in agreement with Schmid et al. (2003) and Papastergiou et al. (1998) at 42 and 21 days, respectively (Table 3-2). The present study overestimated IOP reported by Lauber, Boyd & Boyd (1972) at 6, 8, 10, and 12 weeks by ~ 1- 3 mm Hg (Table 3-2). In the present study mean IOP in diurnal un-injected animals

was below 17 mm Hg (Fig. 3-2) and ~ 3- 5 mm Hg lower than reported by other studies at the same ages (Table 3-2: Bercovitz, Harrison & Leary (1972); Smith, Becker & Podos (1969)). At 98 days of age, expected IOP (14.8 ± 0.6 mm Hg) via Tonopen XL in the present study was ~ 2 mm Hg higher than the reported manometry measured IOP of Frankelson, Lauber & Boyd (1969).

Table 3-3 Elevated IOP via different methods (past studies vs. the present study). Comparisons of studies that have reported an increase in IOP in chicken. Different methods of elevating IOP in chicken in the past and present are shown.

Study	IOP of normal diurnal reared chickens (age) [mm Hg]	Elevation of IOP [mm Hg]	Method of IOP elevation
Present study	Mean (12-107 days): 14 ± 0.6 Animal #1943 mean 70-77 days: 12.8 ± 0.6 Animal # 1975 mean 114-117 days: 13.7 ± 1	Animal #1943 mean 70-77days: 17.5 ± 0.6 Animal #1975 mean 114-117 days: 22.5 ± 6.5	Magnetic microbeads
Schmid et al. 2003	Mean (day 2):12.7 ± 5.3 Mean (day 9): 18.0 ± 5.1 Mean (week 6): 13.4 ± 1.9	~16 (at ~53 days of lens wear) while +15 lens was ~ 13 at this same age	-15D lens
Nickla, Wildsoet, & Wallman 1998	Mean daytime (2 weeks): 19.8 Mean nighttime (2 weeks):13.1	Mean nighttime (2 weeks):18.7	Form deprivation
Papastergiou et al. 1998	13 ± 2 (21 days) Mean IOP(start of light cycle at 7 days):16.8 ± 0.7 Mean IOP (end of light cycle at 7 days): 20.8 ± 1.2	N/A	N/A
Lauber & Kinnear 1979	12.3 ± 0.98 (21 weeks)	16.1 ± 1.71 (21 weeks)	Constant illumination
Bercovitz, Harrison & Leary 1972	14.28 ± 0.57 (1 day) 20.44 ± 0.75 (35 days) 19.27 (70 days)	N/A	N/A
Lauber, Boyd, & Boyd 1972	10.6 ± 0.3 (6 weeks) 10.8 ± 0.5 (8 weeks) 12.03 ± 0.6 (10 weeks) 10.8 ± 0.4 (12 weeks) 11.1 ± 0.4 (20 weeks)	21.1 ± 1.9 (20 weeks)	Constant illumination
Lauber, Boyd & Boyd 1970	12.2 ± 1 (week 16, 20)	≥ 25 (16-20 weeks)	Constant illumination
Smith, Becker & Podos 1969 (Fig. 7)	~ 22 (21, 40 days) 23 (by 5th week)	33 (by 5th week)	Constant illumination
Frankelson, Lauber & Boyd 1969	10.9 ± 0.9 (right eye 98 days) 11.4 ± 0.7 (left eye 98 days)	19.1 ± 0.5 (right eye 98 days) 18.4 ± 0.5 (left eye 98 days)	Constant illumination
Harrison, Bercovitz & Leary 1968 (Fig. 2)	IOP range (35 to 45 weeks):18.5 to 23.5	N/A	N/A
Seaman & Himelfare 1951	Mean IOP (~ 1 year): 18.6	N/A	N/A

3.3.1.2 IOP of non-injected and saline-injected Control Eyes

Growth curves of IOP over time for fellow non-injected eyes of animals with experimental manipulation, as well as eyes subjected to anterior chamber injections of saline are displayed

in Figure 3-4. As shown in Figure 3-4 both non-injected eyes and saline injected eyes have comparable IOP. These eyes also had similar IOP to the non-injected control animals in Figure 3-2. Thus, saline-injected eyes could also be used as baseline control eyes when compared to microbead injected eyes.

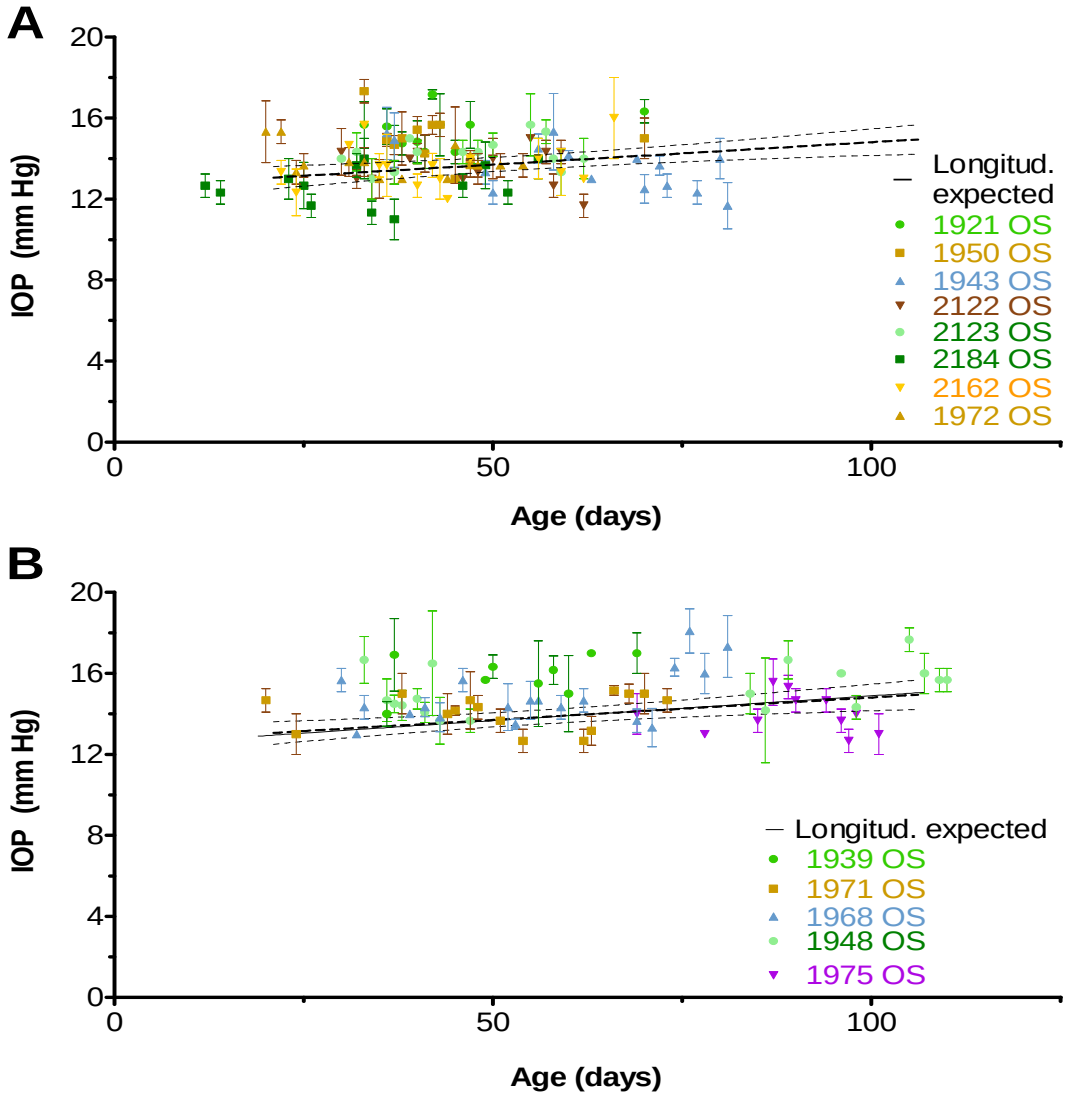


Fig. 3-4 IOP vs. age for non-injected and saline injected control eyes. Intraocular pressure as a function of age for (A) all 8 non-injected control eyes (B) all 5 saline injected control eyes. The fit of the mean IOP from the four longitudinal animals is displayed as the

bolded dashed line with the upper and lower limit of the 95% CI depicted as the thin dashed lines. Longitud. = longitudinal. OS = left eye.

3.3.1.3 Ultrasound Biometry of a Saline Control Animal

Only one animal (#2162) had ultrasound biometry performed before and after three injections of saline to look at any potential effects on the axial components of the eye. Figure 3-5 displays the ultrasound biometry parameters before any of the three saline injections in the right eye of animal #2162 at 23 days and after all injections at 83 days. ACD, VCD, RT, ChT, and were not affected by 3 saline injections (Fig. 3-5). At age 83 days, LT was the only parameter to show inhibited growth after the 3 injections of saline (Fig. 3-5).

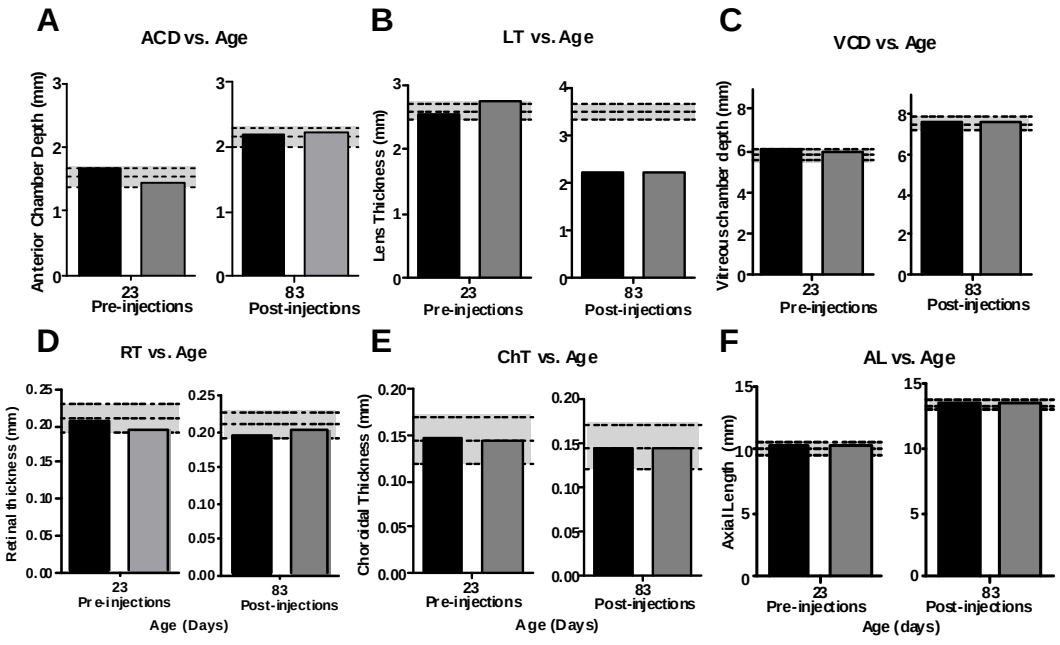


Fig. 3-5 Ultrasound biometry of a saline control animal. Ultrasound A – scan measurements for the right eye (black) and left eye (dark grey) of animal #2162 before and after saline injections. The mean predicted values and the 95% prediction intervals (dashed lines) were determined from longitudinal fit equations as presented in our previous study. Note: The left eye was not injected.

3.3.2 Microbead-injected Eyes

A representative image of a magnetic microbead injected eye (Fig. 3-1A) and the fellow non-injected eye (Fig. 3-1B) are shown. Magnetic microbeads are brown in color and are distributed around the anterior chamber angle (Fig. 3-1A). As millions of beads were injected into the anterior chamber angle, some microbeads were found to coalesce and pool in the inferior anterior chamber with some adherence of microbeads to the iris (Fig. 3-1A). Non-magnetic microbeads were white in color and after injection the anterior chamber had a hazy appearance from these beads. Within 24 hours after an injection of non-magnetic beads the visual axis was clear. The visual axis remained clear in 15 out of the 17 eyes magnetic microbead injected eyes. The clearing of the non-magnetic injected eyes and the maintenance of a clear visual axis in magnetic microbead injected eyes is possibly due to the low mass of the microbeads ($\sim 8 \times 10^{-11}$ g/microbead) enabling the microbeads to follow in the natural convection of aqueous humor flow into the anterior chamber angle. Occasional air bubbles during the injection procedure also helped to keep the central visual axis devoid of microbeads. In the two eyes (animal # 2122 and 2123) that did not result in a clear visual axis after injections, the amount of magnetic microbeads injected (96 to 112 million microbeads) was determined to be an over abundant amount for that particular age and thus size of the anterior chamber. Air bubbles did not negatively interfere with the outcome as they were absorbed within 12 hours post-operatively. Upon injection of microbeads and saline, an immediate white colored opacification of the lens of unknown etiology, which we termed a “transient instantaneous cataract” was noted in all eyes and resolved within 12 hours after the procedure. Three out of the 17 animals had other signs of inflammation such

as cells in the peripheral anterior chamber which cleared within a few days and one animal was sacrificed after the second injection of microbeads due to possible ocular infection. No inflammation post-operatively was noted in any of the saline injected eyes. While all microbead injected eyes had frequent IOP monitoring, only animal #1975 had SD-OCT imaging near the optic disc performed before and post a 3 day elevation in IOP.

3.3.2.1 IOP of all Microsphere-injected Eyes

Figure 3-6 displays the IOP time profile of eyes that received microsphere injections into the anterior chamber without subsequent IOP elevation. One to two injections of 4 to 120 million magnetic microbeads or 18-87.5 billion non-magnetic microbeads did not result in IOP elevation (Table 3-1). As displayed in Figure 3-6, there was greater variability in IOP ranging from about 7 mm Hg to 18 mm Hg in those injected with microbeads. Of note, although the IOP of injected eyes (Fig. 3-6) were measured over an 8 hour daytime interval, the circadian rhythm of IOP likely did not result in the observed increased variability and was more likely due to a result of the experimental manipulation with microbeads as non-injected fellow eyes and saline-injected eyes in Figure 3-4 did not exhibit as large of a variance in IOP. In the right eye of animal #2122 and #2123 an injection of $98x10^6$ magnetic beads at age 40 days and again at age 51 caused blockage of the visual axis. This did not lead to an elevation in IOP. Single or repeated injections ($125x10^8$ to $875x10^8$ beads) of non-magnetic microbeads (n = 1) and the combination of magnetic and non-magnetic microbeads (n = 2) between the age of 40 and 63 days did not result in IOP elevation.

Elevation of IOP with maintenance of a clear visual axis was successful in two (#1943 and #1975) out of 15 microbead-injected animals after two 70µL injections of magnetic microbeads (concentration $20x10^8$ beads/mL). Figure 3-7 depicts the changes in intraocular pressure with time for the two animals (#1943 and #1975) that had an elevation in IOP. Animal #1943 received an injection of $140x10^6$ beads at age 51 days and 65 days; 5 days after the second injection IOP in the injected eye was 5 mm Hg (17 to 18.3 mm Hg) greater than IOP of the fellow eye for a period of 7 days. Animal #1975 received an injection of $140x10^6$ beads at age 99 days and $160x10^6$ beads at age 110 days with a resultant 8 mm Hg elevation in IOP compared to the fellow eye from day 4 to day 7 post second injection. This eye had an elevation in IOP ranging between 18.3 mm Hg and 30 mm Hg and it is possible IOP may have been elevated between age 111 days and 114 days but IOP was not taken during that interval.

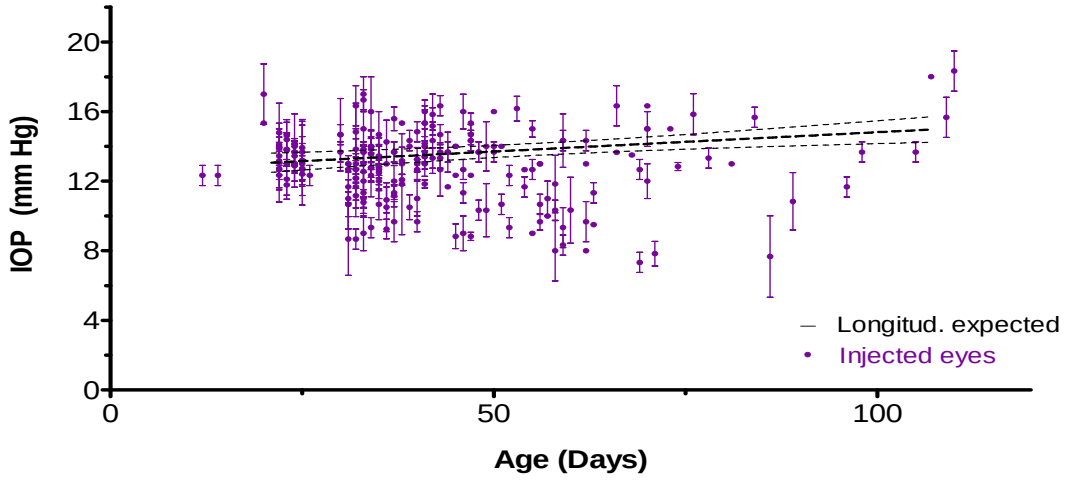


Fig. 3-6 IOP vs. age for microbead injected eyes with no resultant elevation in IOP. Intraocular pressure as a function of age for all eyes injected with microbeads that did not exhibit IOP elevation (16 eyes out of the 18 microbead injected eyes).

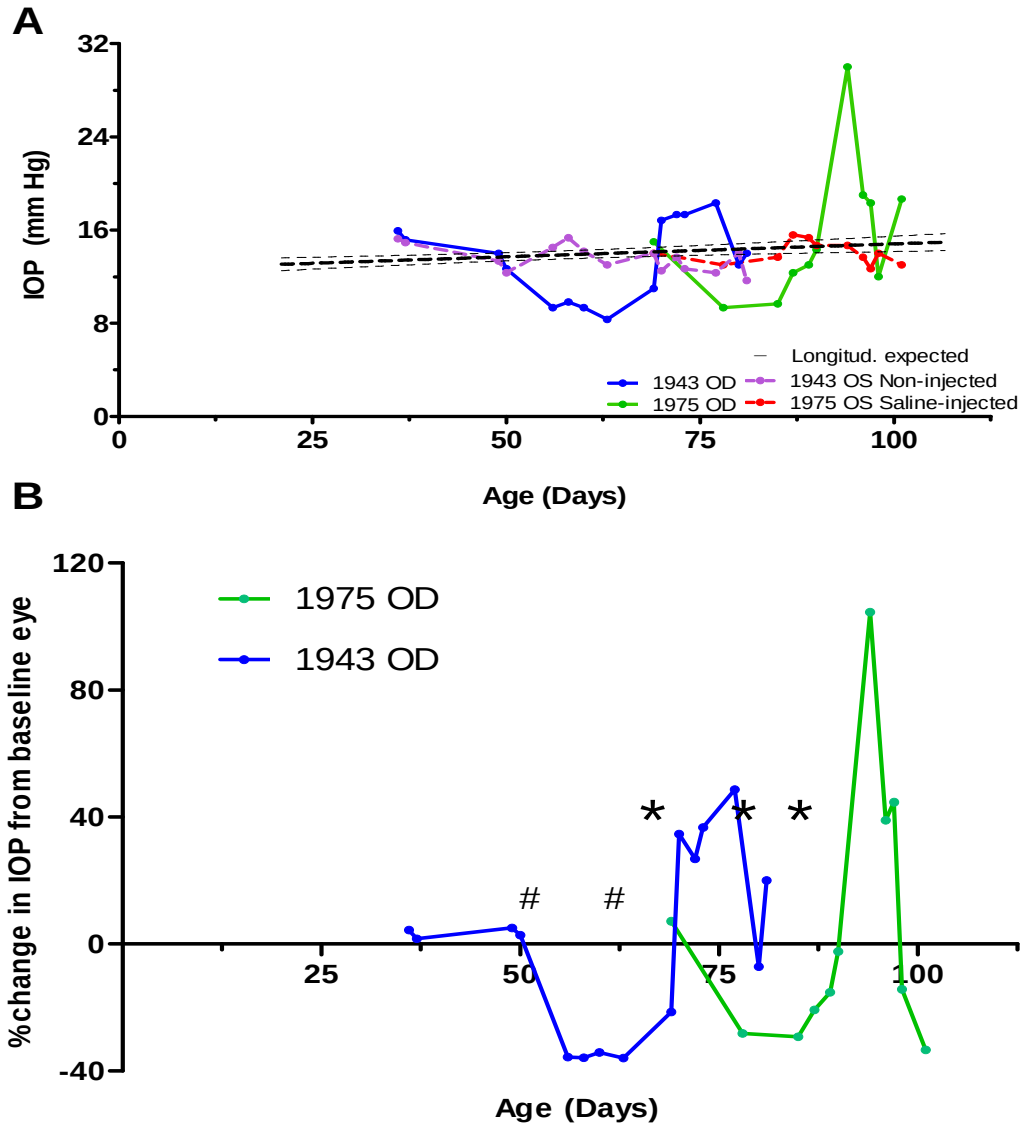


Fig. 3-7 IOP vs. age for two animals with elevated IOP. (A) Intraocular pressure as a function of age for the two animals that had an elevation in IOP (B) Percent change in intraocular pressure of the right eye compared to the baseline control eye of animal # 1943 and #1975. The symbols (#) and (*) represents time of injection of microspheres into the right eyes for animal #1943 and #1975, respectively.

3.2.2 SD-OCT imaging of ocular hypertensive animal #1975

3.3.2.2 SD-OCT Imaging of one Ocular Hypertensive Animal

Figure 3-8 displays an SD-OCT image of the region near the optic nerve head in an animal that had elevation of IOP of 8mm Hg for 3 days (animal #1975). Measurements were taken prior and post elevations. Total retinal thickness, RNFL thickness, and ratio of NFL thickness/RT at 0.5, 1.5, 2.5 and 3.5 degree eccentricity, all appear to be stable and not affected by a 3 day elevation in IOP.

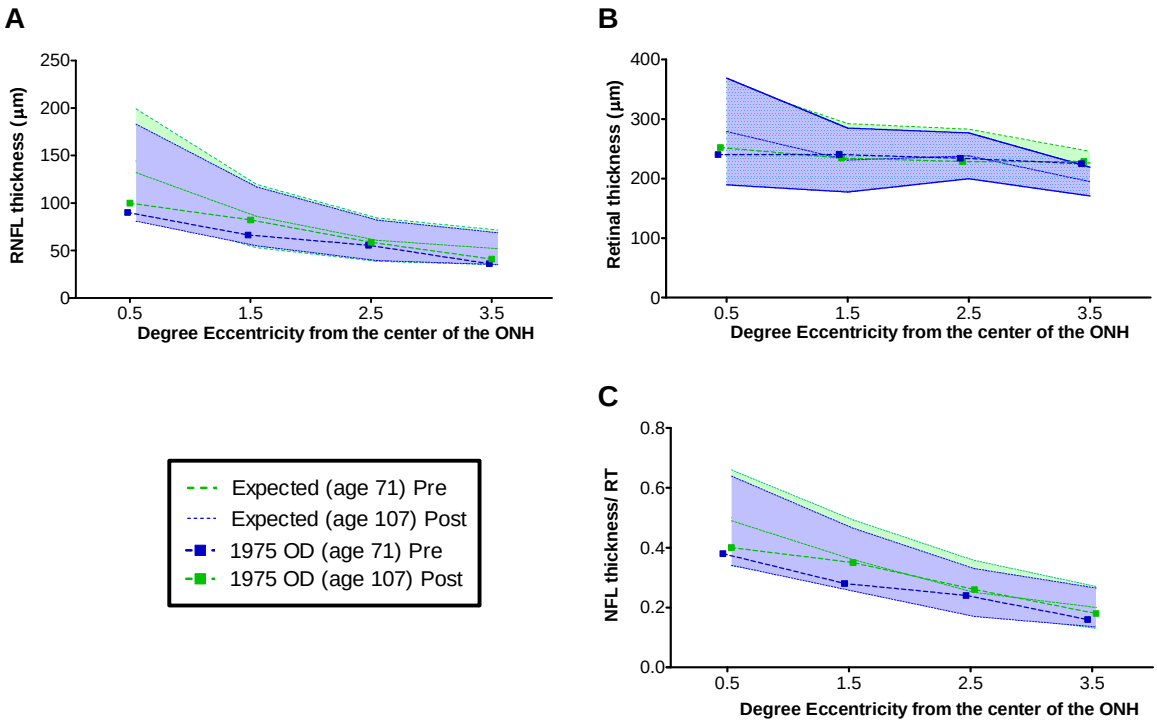


Fig. 3-8 Total RT, RNFL thickness, and ratio of RT/RNFL in an animal with elevated IOP. RNFL thickness (A), RT (B) and ratio of RNFL thickness/RT (C) as a function of eccentricity (0.5 to 3.5 deg) in animal #1975 pre and post all injections. The mean predicted values and confidence intervals [green (age 71 days) and blue (age 107 days)] were determined via longitudinal fit equations as calculated in our previous work. Note: The right eye had 3 microbead injections and the left eye was injected once with saline.

3.4 DISCUSSION

3.4.1 IOP of Control Animals and Eye(s)

3.4.1.1 IOP of non-injected Control Animals and Eye(s)

The normal time course of intraocular pressure for the age range 21-107 days when measurements were taken 3 to 6 hours after the beginning of the light cycle was investigated. The daily rhythm in IOP during the 12 hours of light ranged from 1- 3 mm Hg (age 22-24 days) and was less than reported by Nickla, Wildsoet & Wallman (1998) at an earlier age of ~ 2 weeks post-hatching. Differences between the studies may be due to sample size and age, as Nickla, Wildsoet & Wallman (1998) used a sample size double that of the present study and also used animals ~ 1 week younger than the present study. They also used a 14 light and 10 hour dark cycle instead of a 12 hour on/off cycle. There is a possibility that daily IOP fluctuation may be age-dependent. Over the observation period in the present study (3 to ~ 15 week), IOP was found to increase by about 2 mm Hg. It is unclear exactly why this occurs or the mechanism of this small 2 mm Hg increase but it is possible there might be a relationship between IOP and the normal growth of the axial components of the eye over this age range. As other studies have reported an increase in axial elongation of the chicken eye as IOP was experimentally elevated with intraocular cannulation of fluid (Genest, Chandrashekar & Irving (2012); Nickla, Wildsoet & Wallman (1998); Phillips & McBrien (2004)), it is possible that a converse relationship may exist where IOP increases as eye length increases. If such a relationship exists this may explain why there was a small increase in IOP that parallels the normal developmental increase in axial length over this

same age range. While the present study found an increase in IOP over 21-107 days, Schmid et al. (2003) found a decrease in IOP from 21 to 42 days. This discrepancy was unlikely due to method of measurement, as Tonopen XL was used in both studies. Although a normal diurnal rhythm in IOP exists (Nickla, Wildsoet & Wallman (1998): highest mid-day and lowest at mid-night), the discrepancies between the studies are probably not a result of measurement time or interval as both studies measured IOP during the first half of the light cycle.

As severe myopia has been shown to be risk factor for glaucoma (Loyo-Berrios & Blustein (2007)), understanding the effects of IOP on axial elongation related eye diseases such as myopia might provide further insights into the pathogenesis of glaucoma. Both axial length and refractive error in the two animals with elevated IOP in the present study were not followed in a longitudinal manner, thus the effects of elevated IOP on refractive error and axial length could not determined. Although normal IOP at cross – sectional time points in the present study were comparable with some past studies, there were deviations from other studies. Differences among results might be attributed to measurement time and interval of IOP, as none of the constant light reared studies reported this information. Type of measurement procedure of IOP might also be a confounding factor due to the intraocular invasiveness of manometry in comparison to Tonopen XL, Draeger applanation, and Shiotz applanation. Although IOP in the present study was in agreement between both non-injected control eyes of animals with or without injections of saline or microbeads in the other eye, there is still a possibility that experimental manipulation of one eye might affect the non-injected eye. As discrepancies exist between IOP in the present study and other studies

utilizing the same or different measurement technique, future studies on normal IOP growth are indicated.

3.4.1.2 IOP of saline-injected Control Animals and Eye(s)

In agreement with Sappington et al. (2010) who reported no effect on IOP in mice eye(s) injected with saline into the anterior chamber, saline injections in the present study were also found to have no effect on IOP, albeit in chickens rather than rodents. In contrast, Frankfort et al. (2013) found that saline injections in mice resulted in a 1.6 mm Hg elevation in IOP across all time points. It is unclear why these differences were found, but it might be possible that the increase in IOP observed in Frankfort et al. (2013) might be due to their modified protocol of injecting 3 uL of sodium hyaluronate following the injection of saline. Volume differences in injections likely did not account for the difference as both Sappington et al. (2010) and Frankfort et al. (2013) used a total injected volume 5 µL of fluids. As IOP in saline injected eyes in the present study are comparable to eye(s) without any injections, saline injections were determined to be a reliable control in chickens.

3.4.2 Elevation in IOP via Anterior Chamber Injections of Microbeads in the Present Study

Deducing the appropriate amount of beads as well as the number of injections to elevate IOP with maintenance of a clear visual axis was somewhat difficult as it was based on trial and error of different combinations of microbeads, number of microbeads, and volume of microbeads. The lack of elevation of IOP after one injection of magnetic microbeads was likely due to an insufficient amount of beads blocking the outflow of aqueous humor. There is a possibility that the microbead size used (4.5 to 12 micrometer) was small enough to

easily fit through the pores of the trabecular meshwork and Schlemm's canal and thus easily flushed out with the aqueous humor. Of note, actual pore sizes of these structures in chickens have not been reported in any other studies. This may be the reason why non-magnetic 12 μm polystyrene beads were unsuccessful at elevating the intraocular pressure despite the shear volume of microbeads injected (~ 10^{10} microbeads). Age was also a factor. Animal # 2122 and 2123 had blockage of the visual axis after the second injection of magnetic microbeads at 51 days post-hatching (first injection at 40 days), but yet when an even higher number of microbeads was injected in animal # 1943 and # 1975 at a later age of first injection (51, 71 days respectively) elevation of IOP with no blockage of the visual axis was noted. Thus, two injections of 140 to 160 million magnetic microbeads at a minimum injection age of 50 days seems to be an appropriate starting off dosage to get an initial rise in IOP.

3.4.2.1 Elevation in IOP with Microbead Injections of chicken in the Present Study vs. Primates and Rodents

While we were successful at elevating IOP in two animals, the success was short lived (3-7 days) in comparison to rodents who had an elevation of IOP for weeks at a time from a single injection of non-magnetic microbeads (Chen et al. (2011): 4 weeks (10 μm size) and 2 weeks (15 μm size); Frankfort et al. (2013):12 weeks; Sappington et al. (2010): 2 weeks). These rodent studies differed from Samsel et al. (2010) and the present study because they used non-magnetic (Chen et al. (2011): 10 and 15μm; Frankfort et al. (2013) mix of 6 and 1 μm; Sappington et al. (2010): 15 μm) rather than ~ 5 μm magnetic polystyrene microbeads. Of note, Frankfort et al. (2013) also had a modification in microbead injection technique as they

injected 3 µL of sodium hyaluronate following the mixed size beads to help "push" the beads into the angle, thus possibly contributing to the long duration of IOP from a single injection. Future studies that choose to establish the chicken as a model of elevated IOP might benefit from investigating the use of different size beads with sodium hyaluronate following the injection of microbeads as Frankfort et al. (2013) did with mice. Samsel et al. (2010) reported an increase in IOP for one week in duration from a single injection of magnetic microbeads in rats which is similar to that reported in the present study, albeit the present study required two injections rather than one to achieve an elevation in IOP. Non-human primates on the other hand, required significantly more injections (Weber & Zelenak (2001) ~ 8 – 12 injections) to get an initial rise in IOP. Of note, they injected a lower dose of non-magnetic 10 µm microbeads (~ 2 - 4 $x10^5$) while the present study injected ~ 1 - 2 $x10^8$ (~ 5 µm) magnetic microbeads. Re-injections of non-magnetic microbeads were sometimes bi-weekly for maintenance of elevated IOP in non-human primates (Weber & Zelenak (2001)). In the present study as IOP was elevated for 3 to 7 days, the need for re-injections weekly to bi-weekly was also evident for chickens. The need for more frequent injections may have a correlation with the larger size of the non-human primate and chicken eye in comparison to rodents.

Weber & Zelenak (2001) reported elevation of IOP in primates via 10 µm non-magnetic microbeads which they believed was due to blockage of aqueous outflow at the level of the inner pores of the trabecular meshwork (pore size about $1/5^{th}$ to $1/50^{th}$ the size of the microbeads), as well as the tendency of the microbeads to clump into multi-bead complexes. In the present study, it is possible that with the right concentration and volume, the magnetic

force of the magnetic microbeads might cause sufficient coalescing in the anterior chamber angle thus blocking outflow to an extent where IOP was elevated. This aqueous outflow obstruction could possibly occur at the level of the trabecular meshwork or Schlemm's canal but there is also a possibility that elevation in IOP may arise from possible microbead induced inflammation and swelling within the trabecular meshwork. In mice, injecting smaller sized non-magnetic microbeads of 10 micrometers (in comparison to 15 μm) was more effective at elevating the IOP for a longer duration and with overall higher peak IOP values probably due to the fact that more of the smaller sized microbeads entered Schlemm's canal (Chen et al. (2011)). Thus the 10 μm plain microbeads were an optimal size for entry into Schlemm's canal in the mouse. In chickens in the present study, it is possible that the 4.5μm size might not be an optimal size for effective aqueous outflow blockage in Schlemm's canal. Although a vast array of non-magnetic microbead sizes are available, magnetic microbeads were only available in 5 micrometer diameters and smaller. In the present study, we found 12 micrometer non-magnetic microbeads to have no effect on IOP, and successful elevation of IOP was only possible with 5 micrometer magnetic microbeads. As studies in mice and non-human primates with elevated IOP via microbeads report a loss RGCs and axons after several weeks (Chen et al. (2011); Frankfort et al. (2013); Sappington et al. (2010); Weber & Zelenak (2001)), a similar time scale for glaucomatous damage might also be applicable to the chicken, thus future studies will need to be directed at maintaining elevation in IOP for longer than a week.

3.4.2.2 The protocol for microbead injections of elevated IOP may be age-dependent

Although certain ocular conditions such as refractive error are most susceptible to changes during the critical period of development, perhaps other age related human ocular conditions such as glaucoma are more likely to occur past a critical age. Rearing chickens with constant low intensity blue light causes continued ocular axial enlargement even beyond the time when control eyes were found to slow in eye development at 42-49 days (Bercovitz, Harrison, & Leary (1972)). This age range seems to be a vital time period in normal development of ocular structures as Bercovitz, Harrison & Leary (1972) reported eye enlargement from constant illumination partially reversible up to 80 days of age with reversibility greatly diminished after 44 days post-hatching. Groshke et al. (1948) provided evidence that before the age of 50 days the chick ocular growth may be most susceptible to other factors such as diet thus indicating the importance of this ~ 50 day critical age. In the present study, the lack of elevation in IOP of birds under the age of 50 days of age via our method could possibly be attributed to the growing anterior chamber with age. Although Renard et al. (1980) showed full development of the trabecular meshwork 2 days prior to hatching it is possible the pores in Schlemm's canal might also increase in size parallel with the growth of the anterior chamber. Bead size might influence the amount of microbeads needed to elevate IOP at different ages. Our previous work has shown that most axial parameters (CrT, ACD, LT, VCD, RT, ChT) were predicted to reach at least 90% maturation by 99 days of age. Perhaps these ocular components might need to reach a certain percentage of its full adult size before IOP may be elevated. In the present study, out of the two animals with elevated IOP, the animal with the second injection at a later age (~ 90 days)

had a higher peak IOP value even when the approximate same number of beads was injected. At 90 days of age, most of the axial ocular parameters have reached most of their development, thus indicating that perhaps IOP has a potential to be elevated higher when the major ocular components are less "plastic". Furthermore, more studies will be needed of a larger sample size to determine the exact causal relationship between age and time of injections.

3.4.2.3 Magnetic Microbead Elevation in IOP in the Present Study Differs from Constant Light Induced Elevation in IOP

While constant light rearing results in an elevation of IOP, the mechanism is likely different from the method in the present study. The present study blocks aqueous outflow possibly at the level of the trabecular meshwork with microbeads and although both aqueous outflow facility (Lauber, Boyd, & Boyd (1970,1972); Lauber & Kinnear (1979); Frankelson, Lauber, & Boyd (1969)) and aqueous space (Lauber, Boyd, & Boyd (1970); Lauber & Kinnear (1979); Lauber & McGinnis (1966)) were reduced in constant reared animals, the anterior chamber angle remained open. Constant light also produces many unwarranted physiological lesions such as cataracts and damage to the retina and choroid (Lauber & McGinnis (1966); Li, Troilo, Glassser & Howland (1995)). Lauber & McGinnis (1966) further reported side effects (retinal detachment, blindness) similar to end stage glaucoma. Constant light rearing has also been shown to cause eye enlargement without any inherent myopia or deviations from normal thyroid iodine release rates (Harrison, Bercovitz, & Leary (1968)). Constant light rearing causes corneal changes (Lauber & Oishi (1987); Kinnear, Boyd & Boyd (1974); Lauber (1987); Lauber, Oishi & Vriend (1986)). Lauber & McGinnis (1966) investigated

long term effects (up to 28 months) and reported many pathological and/ or inflammatory changes including retinal detachments, synechiae, cataracts, retinal pigmentation changes, pupil asymmetry, engulfment of pecten, iris, and retina via pathological connective tissue, absence of the retinal pigment layer, thinning of the retina, and more. Smith, Becker, & Podos 1969 reported that uveitis, cataracts, and congestion of iris vessels were common when reared with constant light. Thus, while some of these side effects mimic glaucoma, other unwarranted complications do not.

3.4.3 Comparison of Elevation of IOP in the Present Study to Past Studies

Table 3-3 includes past studies that have reported elevation in IOP via different methods in chickens. In past studies elevation in IOP in chickens was primarily induced by constant light with variable results and in one case form deprivation or by lens decompensation with a -15D lens (Table 3-2). With the exception of Smith, Becker & Podos (1969) who noticed an elevation in IOP around five weeks post-hatching, most cases of ocular hypertension resulting from constant illumination rearing usually did not arise until about 14-21 weeks (Table 3-3). On the other hand, the present study was able to produce elevation in IOP about a month earlier around 10 weeks. Constant illumination produced variable results with IOP ranging from ~ 4 to 12 mm Hg above the fellow eye while the present study reported 5-8 mm Hg elevation in IOP compared to the fellow eye (Table 3-3). Elevation in IOP from constant illumination usually had a period of below normal IOP at 8-12 weeks which preceded the elevation in IOP at ~14-20 weeks. In the present study, after each injection of microbeads there was a period of below normal IOP that preceded the elevation in IOP (Fig. 3-7). This might be attributed to aqueous humor leaving the injection site during the injection process or

a prolonged healing of the hole where the needle penetrated the cornea. To date, the present study was the first to elevate IOP via injection of magnetic microbeads into the anterior chamber.

3.4.4 Questionable Gender Differences in Elevation of IOP

The sample size in the present study included roughly equal numbers of males and females overall but the low numbers of males vs. females subjected to one of the 13 different combinations of injections was too low of a sample size to infer any gender differences. Of note, the two birds that did exhibit elevation of IOP were males.

3.4.5 Could the Elevation of IOP be a Result of the Material Composition of the Beads Itself?

Polystyrene microbeads were commonly employed in rodent and non-human primate glaucoma studies with successful elevation of IOP and retinal ganglion cell and axon death (Chen et al. (2011); Frankfort et al. (2013); Samsel et al. (2011); Sappington et al. (2010)). In the present study polystyrene microbeads were also used to elevate IOP in the chicken. Polystyrene (solid) is the polymerized form of multiple styrene (liquid) molecules. A case report of styrene induced ocular hypertension and visual disturbances (elevated IOP, halos, dull pain, red irritated eyes) have been reported in humans (Inglis, Skalicky & Horowitz 2013). In this particular patient, the ocular side effects subsided when the causative agent (styrene) was removed from his environment. In the polystyrene microbead induced rodent models it was shown that the beads entered Schlemm's canal and blocked outflow (Chen et al. (2011)). We believe it is unlikely that the bead material itself played a major role in elevating IOP in both our studies and past rodent studies but it is possible that the material of

the beads might have a contributory role in elevating the IOP. Part of our belief that the styrene material itself did not cause ocular hypertension in both the chick and rodents was because there was a lack of styrene induced systemic and ocular complications as reported in humans (Campagna, Gobba, Mergler, Moreau, et al. (1996); Campagna, Mergler, Huel, Belanger, et al. (1995); Castillo, Baldwin & Sassine (2001), Chia, Jayaratnam, Ong, Nq, Lee, et al. (1994); Cruzan, Cushman, Andrews, Granville et al. (2001); Eguchi, Kishi, Harabuchi, Yussa, et al. (1995); Gong et al. (2002), Gobba (1991); Inglis, Skalicky, & Horowitz (2013); Rueff, Teixeira, Santos & Gaspar (2009)). Although it may be possible that such neurotoxic symptoms that occur in styrene induced humans do not occur or are easily detected in animals, our study and the rodent studies mentioned above did not report any difference in demeanor or health of the animals after subsequent injections of polystyrene beads. It is possible that styrene in the polymerized form may not produce such toxic side effects and that these effects may be limited to the free styrene liquid form. It is currently unknown if polystyrene is directly toxic to the intraocular components of the eye when injected into the anterior chamber, but possible styrene induced toxicity resulting in elevation of IOP in the present study should not be ruled out.

3.4.6 SD-OCT Imaging of an Animal with Elevated IOP

Although cupping of the optic nerve head is a risk factor commonly looked at in human ocular hypertensive eyes, the pecten vasculature interferes with the view of the optic nerve head in chickens. Thus, rather than looking at IOP induced cupping of the optic nerve, in the present study the use of SD-OCT imaging at a location in the superior optic nerve was used to measure retinal nerve fiber layer (RNFL) thickness and total retinal thickness (RT) to

evaluate possible physiological damage from elevated intraocular pressure. An elevation of 8 mm Hg above the fellow eye for 3 days did not result in changes to RNFL thickness, RT, or ratio of RNFL thickness to RT thus implying that elevation in IOP must be sustained for a longer duration before any changes in the retina are noted. It is also possible that elevation in IOP might not cause observable changes to the retina in chickens with only a 3 day insult to IOP as chickens have the ability for partial regeneration of their retina (Coulombre & Coulombre (1965); Fischer (2005); Hayes, Nelson, Buckingham, & Reh (2007); Karl and Reh (2010)). While chickens might have the potential to regenerate their retina, constant light studies have shown retinal thinning and/or RPE changes to be a result of constant light induced elevation in IOP (Lauber (1983); Lauber & McGinnis (1966)). Constant light induced elevation in IOP has also been shown to be responsive to certain IOP lowering pharmaceutical agents such as acetazolamide and timolol, albeit for a short period of time (Lauber (1987; Lauber 1991), thus implying that the chicken could potentially be useful for future glaucoma therapeutic studies.

3.4.7 The Effect of Saline on Lens Thickness (LT)

In one animal that had three saline injections in one eye, lens thickness after all injections at 83 days of age was thinner than expected at that age. It is possible that the acidity (pH ~ 5.5) of 0.9% sodium chloride (saline) influenced the development of the lens. The lens of vertebrates is avascular and directly influenced by the surrounding media (i.e. aqueous humor) (Bassnett (1990)). Epithelial cells of the lens differentiate to form the lens fiber cells, thus increasing the size of the lens with age (Bassnett (1990)). Thus, any disturbances in this process may prevent normal growth of the lens with age. Furthermore, membrane potential has been shown to be affected by pH in the chicken (Bassnett (1990)). As saline is composed

of ions (sodium and chloride) it is possible that this influx in ion when injected into the anterior chamber might disrupt normal electrochemical ion gradients in the lens. The acidity of saline might have caused permanent damage of the lens as soon as the first injection because the lens thickness value pre and post all injections was roughly the same value with no growth in the lens. Thus, pH of any foreign matter injected into the anterior chamber might have an inhibitory effect on lens growth. In the present study, BSS instead of saline was used in microbead prepared solutions. As BSS has a similar pH (~7.4) to the aqueous humors (~ 7.3) (Bassett (1990)), less ionic disturbances to the lens was expected. In the present study the effect of BSS on lens thickness with time was not determined. Of note, all eyes injected with microbead/BSS solutions and/or saline had an "instantaneous cataract". This might be attributed to a transient disturbance in the normal electrochemical gradient of the lens epithelium, as these lenses were clear within 24 hours.

3.4.8 Possible Confounding Factors and Limitations of the Present Study

As the number of chickens used in the present study was small, selection bias cannot be ruled out as a possible confounding factor. IOP might be influenced by the use of a topical anesthetic, although it is unlikely that this affected the IOP between animals, as all animals had the same amount of drops instilled prior to any measurements. Differences in IOP between the present study and past studies might be attributed to IOP method of measurement (Tonopen XL vs. Shiotz vs. Draeger vs. manometry), as well as rearing differences (diurnal vs. constant light), and possible influences of the experimentally manipulated eye on the fellow eye (form deprivation vs. magnetic microbead injections). A

circadian rhythm of IOP exists in chickens, thus IOP measurement time and interval is critical when comparing studies (Nickla, Wildsoet, & Wallman (1998)). Thus, some discrepancies between the current study and past studies are possibly attributed to this.

3.4.9 Future Directions on the use of the Chicken for in-vivo Experimental Chicken Models of IOP

Via histology, Nork (2000) found focal loss of red and green cones as well as rods or swelling of red and green cones in some laser trabecular photocoagulation induced glaucomatous retinas with no swelling of cones evident in normal retinas of rhesus monkeys. Furthermore, this provides evidence for possible photoreceptor changes in glaucoma and a motive to studying photoreceptor changes in experimentally induced animal models of glaucoma alternatively via in vivo methods such as SD-OCT and Adaptive Optics (AO) imaging. When the pupil of rodents dilates in low luminance environments there is a vast increase in longitudinal aberrations and hypermetropia and thus a reduction of image quality (Hughes (1979)), thus making it difficult to image with AO. In contrast, chickens have less chromatic aberrations and larger eyes thus making AO imaging feasible in the chicken (Headington et al. (2011)). As locations immediately surrounding the pecten were successfully imaged up to 10 degrees eccentricity in the X and Y axis directions from the tip of the pecten (Headington et al. (2011), future studies measuring cone density up to 3.5 degrees immediately to the left and right of the pecten tip may be correlated with RNFL, total retinal thickness, and ratio of RNFL/total retinal thickness via the SD-OCT method in the present study. Kisilak et al. (2012) was able to image cone phone receptors without AO via confocal scanning laser ophthalmoscope (CSLO) and may also be an alternative method of

comparing cone density to SD-OCT measurements longitudinally. There has been a trend towards in-vivo techniques of evaluating glaucoma and/or ocular hypertension with evidence that OCT RNFL thickness measurements and/or multifocal VEP might be superior to standard automated perimeter in detecting and monitoring associated visual field defects in humans (Hood et al. (2004); Moschos et al. (2012); Wangsupadilok et al. (2009)). As photopic negative responses and pattern electroretinogram has been shown to detect glaucoma in humans (Preiser et al. (2013), future studies in chickens using these methods to study elevated IOP may potentially be useful. If future studies prove the chicken to be an effective model for elevation of IOP of sustainable duration, development of pharmacological IOP lowering agents, neuroprotective therapy, and possible stem cell transplantation of degenerate RGCs maybe indicated in the chicken.

3.5 CONCLUSIONS

We have demonstrated elevation of IOP in chicken via magnetic microbeads while maintaining a clear visual axis, thus establishing a potential for chicken as an animal model for in vivo studies of ocular hypertension and/or glaucoma. To achieve an elevation in IOP, the data indicates the use of anterior chamber injections of magnetic microbeads (~ 140 million beads per injection) at a minimum injection age of ~ 50 days of age. Studying the retinal effects of elevated IOP in chicken over a longer time period is indicated using advanced imaging methods such as SD-OCT and AO to shed further insights on the pathophysiology of intraocular damage from IOP.

CHAPTER 4: GENERAL DISCUSSION AND CONCLUSIONS

The White Leghorn chicken continues to be an appropriate experimental animal for further understanding of ocular conditions in other species and in particular humans. Although many ocular studies in chickens have studied chicks of 4 weeks or less due to their faster ocular growth rate and responsiveness to experimental manipulation, the present study found the age range 21-107 days to also be an instrumental time period for the normal growth of the eyes. The period between birth and ~ 50 days has been shown by other studies to be a critical time period when chick eyes are more responsive to refractive manipulation and recovery and a period when diet is more critical to growth of ocular structures. Furthermore, in the present study animals younger than ~ 50 days did not result in an elevation of IOP which we believe might be due the continual growth of the major ocular components in the eye suggesting that the eye is less plastic when the major ocular components reach a certain percentage of their expected adult size. Thus, understanding developmental milestones in the eye might help differentiate abnormal from normal ocular disease processes. Furthermore, future studies measuring corneal and lens curvature longitudinally over the age range in the present study may be combined with data in the present study to construct a schematic eye for the chicken during this time period. We have shown the normal course of development of ultrasound biometry parameters as well as SD-OCT parameters to help those that choose to use the chicken for experimental models of ocular conditions and diseases, and in particular glaucoma. We have shown elevation in IOP in two animals as well as reliable SD-OCT imaging of the optic nerve retina, thus the chicken has a potential to be used as an

experimental model of ocular hypertension or glaucoma. Although we were able to elevate IOP, this was only in a small percentage of the animals used and future studies are indicated to show reproducibility. As species differences do exist, it is important to note that although chickens are used to help further understand detrimental eye conditions, inferences between species should be taken with caution as there is always a possibility that this does not occur or even resemble the processes in humans. Furthermore, we hope that the results in the present study will aid investigators in planning and conducting studies utilizing the White Leghorn chicken.

BIBLIOGRAPHY

Agarwal, R., Gupta, S.K., Agarwal, P. Saxena, R, Agrawal, S.S. (2008). Current concepts in the pathophysiology of glaucoma. *Indian J Opthalmol. 57*(4), 257-66.

Atkinson, R.J. (2007). Brain maturation in chicks: biochemical, behavioral and electrophysiological investigations. Thesis, University of New Castle, Australia

Avila, N.V., McFadden, S.A. (2010). A detailed paraxial schematic eye for the White Leghorn chick. *J Comp Physiol A. 196*(11), 825-840.

Banitt, M.R, Ventura, L.M., Feuer, W.J., Savatovsky, E., et al. (2013). Progressive loss of retinal ganglion cell function precedes structural loss by several years in glaucoma suspects. *Invest Ophthalmol Vis Sci*. 54(3):2346-2352.

Bartmann, M. Schaeffel, F. Hagel, G., Zrenner, E. (1994). Constant light affects retinal dopamine levels and blocks deprivation myopia but not lens-induced refractive error in chickens. *Vis Neurosci. 11*(2), 119-208.

Bassnett, S. (1990). Intracellular pH regulation in the embryonic chicken lens epithelium. J Physiol. 431, 445-464.

Bercovitz, A.B., Harrison, P.C., Leary, G.A. (1972). Light induced alterations in growth pattern of the avian eye. *Vis Res. 12*(7), 1253-1259.

Berninger, T.A., Arden, G.B. (1988). The pattern electroretinogram. *Eye (Lond). 2* Suppl, S257-S283.

Brown, N. (1974). The change in lens curvature with age. *Exp Eye Res. 19*(2), 175-183.

Brown, N.P., Koretz, J.F., Bron, A.J. (1999). The development and maintenance of emmetropia. *Eye (Lond). 13* (Pt1), 83-92.

Burdon, K.P. (2012). Genome-wide association studies in the hunt for genes causing primary open-angle glaucoma: a review. *Clin Experiment Opthalmol. 40*(4)358-363.

Campagna, D., Gobba, F., Mergler, D., Moreau, T, et al. (1996). Colour vision loss among styrene exposed workers: neurotoxicological threshold assessment. *Neurotoxicology 17*(2), 367-374.

Campagna, D., Mergler D., Huel, G., Bélanger, S., et al. (1995). Visual dysfunction among

styrene-exposed workers. *Scand J. Work Environ Health.* 21(5), 382-390.

Casson, R.J., Chidlow, G., Wood, J.P, Crowston, J.G., Goldberg, I. (2012). Definition of glaucoma: clinical and experimental concepts. Clin Experiment Ophthalmol. 40(4):341-349.

Castillo, L., Baldwin, M., Sassine, M-P. (2001). Cumulative exposure to styrene and visual function. *Am J Ind Med 39*, 351-360.

Cegarra, M.J., Izquierdo, C. Alsonso, L., Hernandez Gil de Tejada, T., et al. (2001). Consolidating the anatomical relationship between ocular axial length and spherical equivalent refraction. Eur J Anat. 5(3), 145-150.

Chauhan, B.C., Pan, J., Archibald, M.L. LeVatte, T.L. et al. (2002). Effect of intraocular pressure on optic disc topography, electroretinography, and axonal loss in a chronic pressure-induced rat model of optic nerve damage. *Invest Ophthalmol Vis Sci. 43*(9), 2969-2976.

Chen, H., Wei, X., Cho, K.S., Chen, G., et al. (2011). Optic neuropathy due to microbead-induced elevated intraocular pressure in the mouse. *Invest Ophthalmol Vis Sci. 52*(1), 36-44. DOI: 10.1167/iovs.09-5115

Chia, S.E., Jayaratnam, J., Ong, C.N., Nq, T.P., Lee, H.S. (1994). Impairment of colour vision among workers exposed to low concentrations of styrene. *Am J Ind Med 26*(4), 481-488.

Chiu, P.S., Lauber, J.K., Kinnear, A. (1975). Dimensional and physiological lesions in the chick eye as influenced by the light environment. *Proc Soc Exp Biol Med. 148*(4), 1223-1228.

Choi, S.S., Zawadzki, R.J., Lim, M.C.; Brandt, J.D. et al. (2011). Evidence of outer retinal changes in glaucoma patients revealed by ultrahigh-resolution in vivo retinal imaging. *Br J Ophthalmol 95*(1), 131-141.

Cohen, Y., Belkin, M., Yehezkel, O., Avni, I., Polat, U. (2008). Light intensity modulates corneal power and refraction in the chick eye exposed to continuous light. *Vis Res. 48*(21), 2329-2335.

Cook, C.A., Koretz, J.F., Pfahnl, A., Hyun, J., Kaufman, P.L. (1994). Aging of the human

crystalline lens and anterior segment. *Vis Res. 34*(22), 2945-2954.

Coulombre, J.L., Coulombre, A.J. (1965). Regeneration of neural retina from the pigmented epithelium in the chick embryo. *Dev Biol. 12*, 72-92.

Cruzan, G., Cushman J.R., Andrews, L.S., Granville, G.C., et al. (2001). Chronic toxicity/oncogenicty study of styrene in CD-1 mice by inhalation exposure for 104 weeks. *J Appl Toxicol. 21*(3), 185-198.

Ebneter, A., Casson, R.J., Wood, J.P., Chidlow, G. (2012). Estimation of axon counts in a rat model of glaucoma:comparison of fixed-pattern sampling with target sampling. *Clin Experiment Ophthalmol. 40*(6), 626-33.

Eguchi, T., Kishi, R., Harabuchi, I., Yuasa, J. et al. (1995). Impaired colour discrimination among workers exposed to styrene:relevance of a urinary metabolite. *Occup Environ Med. 52*(8), 534-538.

Evans, H.E. (1996). Anatomy of the budgerigar and other birds. In "Diseases of Cage and Aviary Birds" (W.J.) Rosskopf and R.W. Woerpel, eds). Williams & Williams Co., Baltimore.

Fazio, D.T., Heckenlively, J.R., Martin, D.A, Christenson, R.E. (1986). The electroretinogram in advanced open angle glaucoma. *Doc Ophthalmol. 64*, 45-54.

Feng, L., Chen, H., Suyeoka, G., Liu, X. (2013). A laser-induced mouse model of chronic ocular hypertension to characterize visual defects. *J Vis Exp. 14*(78) DOI: 10.3791/50440

Fischer, A.J. (2005). Neural regeneration of the chick retina. *Prog Retin Eye Res. 24*, 161-182.

Frankelson, E.N., Lauber, J.K., Boyd, T.A.S. (1969). The role of angle closure in light-induced avian glaucoma. *Canad J Ophthalmol. 4*(1), 59-63.

Frankfort, B.J., Khan, A.K., Tse, D.Y., Chung, I., et al. (2013). Elevated intraocular pressure causes retinal dysfunction before cell loss in a mouse model of experimental glaucoma. *Invest Ophthalmol Vis Sci. 54*(1), 762-770.

Freddo, T.F., Gong, H. (2009). Etiology of IOP elevation in primary open angle glaucoma. *Optom Glaucoma Soc E J. 4*(1), pii: ogs_0709.htm#article3

Gaasterland, D., Kupfer, C. (1974). Experimental glaucoma in the rhesus monkey. *Invest Ophthalmol. 13*(6), 455-457.

Gaasterland, D., Tanishima, T., Kuwabara, T. (1978). Axoplasmic flow during chronic experimental glaucoma. *Invest Ophthalmol Vis Sci. 17*(9)*:*838-846.

Garcia-Valenzuela, E., Shareef, S., Walsh, J., Sharma S.C. (1995). Programmed cell death of retinal ganglion cells during experimental glaucoma. *Exp Eye Res. 61*(1), 33-44.

Gardiner, S.K. Fortune, B., Wang, L., Downs, J.C., Burgoyne, C.F. (2012). Intraocular pressure magnitude and variability as predictors of rates of structural change in non-human primate experimental glaucoma. *Exp Eye Res. 103*, 1-8.

Garner, L.F., Yap, M.K. Kinnear, R.F. Frith, M.J. (1995). Ocular dimensions and refraction in Tibetan children. *Optom Vis Sci. 71*(4), 266-271.

Genest, R., Chandrashekar, N., Irving , E. (2012). The effect of intraocular pressure on chick eye biometry and its application to myopia. Acta Bioeng Biomech. 14(2), 3-8. DOI: 10.5277/abb12021

Giordano, L., Friedman, D.S, Repka, M.X, Katz, J., et al. (2009). Prevalence of refractive error among preschool children in an urban population: The Baltimore Pediatric Eye Disease Study. *Ophthalmol. 116*(4), 739-746.

Giorgiou, A.L., Guo, L., Francesca Cordeiro, L.G., Salt, T.E. (2013). Electroretinogram and visual-evoked potential assessment of retinal and central visual function in a rat ocular hypertension model of glaucoma. *Curr Eye Res.* 1-15. [Epub ahead of print] DOI:10.3109/02713683.2013.848902

Glasser, A., Murphy, C.J., Troilo, D., Howland, H.C. (1995). The mechanism of lenticular accommodation in chicks. *Vis Res. 35*(11), 1525-1540.

Glickstein, M., Millodot, M. (1970). Retinoscopy and eye size. *Science. 168*(3931), 605-606.

Gobba, F., Galassi, C. Imbriani, M., Ghittori, S., et al. (1991). Acquired dyschromatopsia among styrene-exposed workers. *J Occup Med. 33*(7), 761-765.

Gong, Y., Kishi, R., Katakura, Y., Tsukishima, E., et al. (2002). Relation between colour vision loss and occupational styrene exposure level. *Occup Environ Med. 59*(12), 824-829.

Gordon, M.O. (2002). The ocular hypertension treatment study: baseline factors that predict the onset of primary open angle glaucoma. *Arch Ophthalmol. 120*(6), 714-720.

Gottlieb, M.D., gugate-Wentzek, L.A., Wallman, J. (1987). Different visual deprivations produce different ametropias and different eye shapes. *Invest Ophthalmol Vis Sci. 28*,1225-1235.

Graham, B., Judge, S.J. (1999). Normal development of refractive state an ocular component dimensions in the marmoset *(Callithrix jacchus). Vis Res. 39*(2),177-187.

Groshke, A.C., Anderson, J.O., Briggs, G.M. (1948). Peculiar enlargement of eyeballs in chicks caused by feeding a high level of glycine. *Proc Soc Exp Biol Med. 69*(3),488-491.

Hayes, B.P, Fitzke, W., Hodos, W., Holden, A.L. (1986). A morphological analysis of experimental myopia in young chickens. *Invest Ophthalmol Vis Sci 27*(6):981-991.

Hayes, S., Nelson, B.R, Buckingham, B., Reh, T.A. (2007). Notch signaling regulates regeneration in the avian retina. *Dev Biol. 312*, 300-311.

Hayreh, S.S, Jonas, J.B., Zimmerman, M.B. (1998). Parapapillary chorioretinal atrophy in chronic high-pressure experimental glaucoma in rhesus monkeys. *Invest Ophthalmol Vis Sci. 39*(12), 2296-2303.

Harrison, P.C., Bercovitz, A.B., Leary G.A. (1968). Development of eye enlargement of domestic fowl subjected to low intensity light. *Int J Biometeor. 12*(4)351-358.

Headington, K., Choi, S.S, Nickla, D., Doble, N. (2011). Single cell imaging of the chick retina with adaptive optics. *Curr Eye Res. 36*(10), 947-957.

Hikoya, A., Sato, M., Tsuzuki, K., Koide, Y.M., et al. (2009). Central corneal thickness in Japanese children. Jpn J Ophthalmol. 53(1), 7-11.

Hood, D.C, Thienprasiddhi, P. Greenstein, V.C, Winn, B.J., et al. (2004). Detecting early to mild glaucomatous damage: a comparison of the multifocal VEP and automated perimetry. *Invest Ophthalmol Vis Sci. 45*(2), 492-498.

Hoyt, C.S, Stone, R.D., Fromer, C., Billson, F.A. (1981). Monocular axial myopia associated with neonatal eyelid closure in humans and infants. *Am J Ophthalmol. 91*(2), 197-200.

Hughes, A. (1979). A useful table of reduced schematic eyes for vertebrates which includes

computed longitudinal chromatic aberrations. Vis Res. 19(11), 1273-1275.

Inglis, H., Skalicky, S.E., Horowitz, G. (2013). "Toxic" glaucoma? A case of possible styrene-induced ocular hypertension. *J Glaucoma. 00*, 1-2. [Epub ahead of print]

Irving, E.L., Sivak, J.G, Curry, T.A., Callendar, M.G. (1996). Chick eye optics: zero to fourteen days. *J Comp Physiol A. 179*(2), 185-194.

Jenson, L.S, Matson, W.E (1957). Enlargement of avian eye by subjecting chicks to continuous incandescent illumination. *Science. 125*(3251), 741.

Jeon, C.J, Strettoi, E. Masland, R.H. (1998). The major cell populations of the mouse retina. J Neurosci. 18(21), 8936-8946.

Joos, K.M., Li, C., Sappington R.M. (2010) Morphometric changes in the rat optic nerve following short-term intermittent elevations in intraocular pressure. *Invest Ophthalmol Vis Sci. 51*(12), 6431-40. DOI:10.1167/iovs.10-5212.

Kalvin, N.H., Hamasaki, D.I., Gass, J.D.M. (1966). Experimental glaucoma in monkeys. I. Relationship between intraocular pressure and cupping of the optic nerve and cavernous atrophy of the optic nerve. Arch Ophthalmol.76(1), 82-93.

Karl, M.O. (2013). The potential of stem cell research for the treatment of neuronal damage in glaucoma. *Cell Tissue Res. 353*, 311-325.

Karl, M.O, Reh, T.A., (2010). Regenerative medicine for retinal diseases: activating endogenous repair mechanisms. *Trends Mol Med. 16*, 193-202.

Kendell, K.R, Quigley, H.A, Kerrigan, L.A, Pease, M.E., Quigley, E.N. (1995). Primary open-angle glaucoma is not associated with photoreceptor loss. *Invest Ophthalmol Vis Sci.* 1995, 36(1), 200-205.

Kiely, P.M., Carney, L.G., Smith, G. (1982). Diurnal variations of corneal topography and thickness. *Am J Optom Physiol Optics. 59*(12), 976-982.

Kinnear, A., Lauber, J.K. (1978). Biochemical studies of the chicken vitreous in light-induced avian glaucoma. *Comp Biochem Physiol B*. 61(1), 107-110.

Kinnear, A., Lauber, J.K., Boyd, T.A.S. (1974). Genesis of light-induced avian glaucoma . *Invest Ophthalmol.13*(11), 872- 875.

Kisilak, M.L., Bunghardt, K., Hunter, J., Irving, E.L, Campbell, M.C. (2012). Longitudinal in

vivo imaging of cones in the alert chicken. *Opt and Vis Sci. 89*(4), 644-651.

Koretz, J.F., Rogot, A., Kaufman, P.L. (1995). Physiological strategies for emmetropia. *Trans AM Ophthalmol Soc. 93,* 105-118; discussion 118-122.

Kram, Y.A., Mantey, S., Corbo, J.C. (2010). Avian cone photoreceptors tile the retina as five independent, self organizing mosaics. *PLoS ONE. 5*(2), e8992.

Krishna, R., Mermoud, A., Baerveldt, G., Minckler, D.S. (1995). Circadian rhythm of intraocular pressure: a rat model. *Ophthalmic Res. 27*(3), 163-167.

Kwong, J.M., Vo, N., Quan, A., Nam, M. et al. (2013). The dark phase intraocular pressure elevation and retinal ganglion cell degeneration in a rat model of experimental glaucoma. *Exp Eye Res. 112*, 21-28.

Larsen, J.S. (1971a). The Saggital growth of the eye I. Ultrasonic measurement of the depth of the anterior chamber from birth to puberty. *Acta Ophthalmol (Copenh). 49*(2), 239-262.

Larsen, J.S. (1971b). The Saggital growth of the eye II. Ultrasonic measurement of the axial diameter of the lens and the anterior segment from birth to puberty. *Acta Ophthalmol (Cophenh). 49*(3),427-440.

Larsen, J.S. (1971c). The Saggital growth of the eye III. Ultrasonic measurement of the posterior segment (axial length of the vitreous) from birth to puberty. *Acta Ophthalmol (Cophenh). 49*(3),441-453.

Larsen, J.S. (1971d). The Saggital growth of the eye IV. Ultrasonic measurement of the axial length of the eye from birth to puberty. *Acta Ophthalmol (Cophenh). 49*(3),441-453

Lauber, J.K. (1983) Retinal pigment epithelium: ring mitochondria and lesions induced by continuous light. Curr Eye Res. 2(12), 855-862.

Lauber, J.K. (1987). Review: Light-induced avian glaucoma as an animal model for human primary glaucoma. *J Ocul Pharmacol. 3*(1), 77-100.

Lauber, J.K. (1991). Three avian enlargement protocols as myopia models: effects of pharmacological interventions. J Ocul Pharmacol. 7(1), 65-75.

Lauber, J.K., Boyd, J.E., Boyd, T.A.S. (1970). Intraocular pressure and aqueous outflow facility in light-induced avian buphthalmos. *Exp Eye Res. 9*(2), 181-187.

Lauber, J.K., Boyd, J.E., Boyd, T.A.S. (1972). Aqueous humor inflow in normal and glaucomatous avian eyes. *Exp Eye Res. 13*(1), 77-82.

Lauber, J.K, Kinnear, A. (1979). Eye enlargement in birds induced by dim light. *Canad J Ophthalmol. 14*(4), 265-269.

Lauber, J.K., McGinnis, J. (1966). Eye lesions in domestic fowl reared under continuous light. *Vis Res. 6*(12), 619-626.

Lauber, J.K., Oishi, T. (1987). Lid suture myopia in chicks. *Invest Ophthalmol Vis Sci 28*(11),1851-1858.

Lauber, J.K., Oishi, T., Vriend, J. (1986). Plasma melatonin rhythm lost in preglaucomatous chicks. *J Ocul Pharmacol. 2*(3), 205-213.

Lee, J.B., Javier, J.A. Change, J.H., Chen, C.C., Kato, T. Azar, D.T. (2002). Confocal and electron microscopic studies of laser supepithelial keratomileusis (LASEK) in the White Leghorn chick eye. *Arch Ophthalmol. 120*(12), 1700-1706.

Lessell, S., Kuwabara, T. (1969). Experimental α-chympotrypsin glaucoma. *Arch Ophthalmol. 81*(6), 853-864.

Levitt, P. (2003). Structural and functional maturation of the developing primate brain. *J Pediatr. 143*(4Suppl), S35-S45.

Li, T., Troilo, D, Glasser, A., Howland, H.C, (1995). Constant light produces severe corneal flattening and hyperopia in chickens. *Vis Res 35*(9), 1203-1209.

Lotmar, W. (1976). A theoretical model for the eye of new-born infants. Albrect Von Graefes *Arch Klin Exp Ophthalmol. 198(*2), 179-185.

Mehaffey, L., Hologigian, K., Seiple, W. (1993). Electrooculogram changes in patients with ocular hypertension and primary open-angle glaucoma. *Doc Ophthalmol. 83*(2), 103-110.

Meyer, D.B., May, H.C. (1973). The topographical distribution of rods and cones in the adult chicken retina. *Exp Eye Res. 17*(4), 347-355.

Mittag, T.W., Danias, J., Pohorenec, G., Yuan, H.M., et al. (2000). Retinal damage after 3 to 4 months of elevated intraocular pressure in a rat glaucoma model. *Invest Ophthalmol Vis Sci. 41*(11), 3451-3459.

Mohindra, I. Held, R. (1980). Development of human refraction. In Abstracts of Third International Conference on Myopia, Copenhagen

Montiani-Ferreira, F. Cardosa, F. Petersen-Jones, S. (2004). Postnatal development of central corneal thickness in chicks of Gallus gallus domesticus. *Veterinary Ophthalmol. 7*(1), 37-39.

Moorison, J.C., Johnson, E.C., Cepurta, W, Jia, L. (2005). Understanding mechanisms of pressure-induced optic nerve damage. *Prog Retin Eye Res. 24*(2), 217-240.

Moorison, J.C., Moore, C.G., Deppmeier, L.M., Gold, B.G., et al. (1997). A rat model of chronic pressure-induced optic nerve damage. *Exp Eye Res. 64*(1), 85-96.

Moorison, J.C., Cepurna, W.O., and Johnson, E.C. (2010). Pathophysiology of human glaucomatous optic nerve damage: Insights from rodent models of glaucoma, *Exp Eye Res. 93*(2), 1-9. DOI: 10.1016/j.exer.2010.08.005

Morgan, I.G., Boelen, M.K. (1996). A retinal dark-light switch: a review of the evidence. *Visual Neurosci. 13*(3), 399-409.

Moschos, M.M., Georgopoulos, G., Chatziralli, I.P., Koutsndrea, C. (2012). Multifocal VEP and OCT findings in patients with primary open angle glaucoma: A cross-sectional study. *BMC Ophthalmol.* 12:34. DOI: 10.1186/1471-2415-12-34.

Mutti, D.O., Lynn Mitchell, G., Jones, L.A., Friedman, N.E., et al. (2005). Axial growth and changes in lenticular and corneal power during emmetropization in infants. *Invest Ophthalmol Vis Sci. 46*(9), 3074-3080.

Mutti, D.O, Lynn Mitchell, G. Jones, L.A, Friedman, N.E. et al. (2004). Refractive astigmatism and the toricity of ocular components in human infants. *Optom and Vis Sci. 81*(10), 753-761.

Nickla, D.L., Wildsoet, C, Wallman, J. (1998). The circadian rhythm in intraocular pressure and its relation to diurnal ocular growth changes in chicks. *Exp Eye Res. 66*(2), 188-193.

Nork, T.M., VerHoeve, J.N., Poulsen, G.L., Nickells, R.W., et al. (2000). Swelling and loss of photoreceptors in chronic human and experimental glaucomas. *Arch. Ophthalmol. 118*(2), 235-245.

O'Leary, D.J., Millodot, M. (1979). Eyelid closure causes myopia in humans. *Experientia. 35*(11), 1478-1479.

Papastergiou, G.I., Schmid, G.F., Riva, C.E, Mendel, M.J., Stone, R.A, Laties, A.M. (1998). Ocular axial length and choroidal thickness in newly hatched chicks and one-year-old chickens fluctuate in a diurnal pattern that is influenced by visual experience and intraocular pressure changes. *Exp Eye Res. 66*(22),195-205.

Pediatric Eye Disease Investigator Group, Bradfield, Y.S., Melia, B.M., Repka, M.X., et al. (2011). Central corneal thickness in children. *Arch Ophthalmol. 129*(9), 1132-1138.

Phillips, J.R., McBrien, N.A. (2004). Pressure-induced changes in axial eye length of chick and tree shrew: significance of myofibroblasts in the sclera. Invest Ophthalmol Vis Sci. 45(3), 758-763.

Pickett-Seltner, R.L., Sivak, J.G., Pasternak, J.J. (1988). Experimentally induced myopia in chicks: morphometric and biochemical analysis during the first 14 days after hatching. *Vis Res. 28*(2):323-328.

Portillinha, W., Belfort, R. Jr., (1991). Central and peripheral corneal thickness in newborns. *Acta Ophthalmologica (Copenh). 69*(2), 247-250.

Preiser, D., Lagrèze, W.A., Bach, M. Poloschek, C.M. (2013). Photopic negative response versus pattern electroretinogram in early glaucoma. Invest Ophthalmol Vis Sci. 54(2), 1182-1191.

Price, F.W. Jr., Koller, D.L., Price, M.O. (1999). Central corneal pachymetry in patients undergoing laser in situ keratomileusis. *Opthalmol 106*(11), 2216-2220.

Qiao-Grider, Y, Hung, L., Kee, C., Ramamirtham, R., Smith, E.L. 3rd (2007). Normal ocular development in young rhesus monkeys (Macaca Mulatta) *Vis Res. 47*(11), 1424-1444.

Quigley, H.A., Addicks, E.M. (1980). Chronic experimental glaucoma in primates. I. Production of elevated intraocular pressure by anterior chamber injection of autologous ghost red blood cells. *Invest Ophthalmol Vis Sci*. *19*(2),126-136.

Quigley, H.A., Broman, A.T. (2005). The number of people with glaucoma worldwide in 2010 and 2020. *Br J Ophthalmol. 90*(3), 262-267.

Quigley, H.A., Green, W.R. (1979). The histology of human glaucoma cupping and optic

nerve damage; clinicopathologic correlation in 21 eyes. *Ophthalmology. 86*(10), 1803-1830.

Quigley, H.A., Hohman, R.M. (1983). Laser energy levels for trabecular meshwork damage in the primate eye. *Invest Ophthalmol Vis Sci. 24*(9), 1305-1307.

Quigley, H.C., Nickells, R.W., Zack, D.J., Kerrigan, L.A. et al. (1994). Ganglion cell death in experimental monkey glaucoma and after axotomy occurs by apoptosis. *Invest Ophthalmol Vis Sci. 36*(5), 774-786.

Rasband, W.S, ImageJ, U.S. National Institutes of Health, Bethesda, Maryland, USA, http://imagej.nih.gov/ij/1997-2012

Ray, K., Mookherjee, S. (2009). Molecular complexity of primary open angle glaucoma: current concepts. *J of Genet. 88*(4), 451-467.

Renard, G, Hirsch, M, Savoldelli, M, Pouliquen, Y. (1980). The development of the irido-corneal angle in the chick embryo. *Albrecht Von Graefes Arch Klin Exp Ophthalmol. 212*, 135-142

Rieck, J. (2013). The pathogenesis of glaucoma in the interplay with the immune system. *Invest Ophthalmol Vis Sci. 54*(3) 2393-2409.

Rivera, J.L., Beld, N.P., Feldman, R.M. (2008). Risk factors for primary open angle glaucoma progression: what we know and what we need to know. *Curr Opin Ophthalmol. 19*(2), 102-106. DOI: 10.1097/ICU.0b013e3282f493b3

Reuff, J., Teixeira, J.P., Santos, S.S., Gaspar, J.F. (2009). Genetic effects and biotoxicity monitoring of occupational styrene exposure. *Clin Chim Acta. 399*(1-2), 8-23. DOI: 10.1016/j.cca.2008.09.012

Rostas, J.A.P., Dunkley, P.R. (1992). Multiple forms and distribution of calcium/calmodulin-stimulated protein kinase II in brain. *J of Neurochemistry. 59*(4)1191-1202.

Rymer, J., Choh, V., Bharadway, S., Padmanabhan,V., et al. (2007). The albino chick as a model for studying ocular developmental anomalies, including refractive errors, associated with albinism. *Exp Eye Res. 85*(4), 431-442.

Samsel, P.A, Kisiswa, L, Erichsen, J.T, Cross, S.D, Morgan, J.E. (2011). A novel method for

induction of experimental glaucoma using magnetic microspheres. *Invest Ophthalmol Vis Sci 52*. (3), 1671-1675. DOI: 10.1167/iovs.09-3921.

Sappington, R.M., Carlson, B.J., Crish, S.D., Calkins, D.J. (2010). The microbead occlusion model: a paradigm for induced ocular hypertension in rats and mice. *Invest Ophthalmol Vis Sci. 51*(1), 207-216. DOI:10.1167/iovs.09-3947.

Schaeffel, F. Howland, H.C., (1988). Visual optics in normal and ametropic chickens. Clin *Vis Sci. 3*(2), 83-98.

Schmid, K.L., Hills, T., Abbott, M., Humphries, M. (2003). Relationship between intraocular pressure and eye growth in chick. *Ophthalmic Physiol Opt. 13*(1), 25-33.

Schmid, G.F., Papastergiou, G.I., Nickla, D.L., Riva, C.E., et al. (1996). Validation of laser Doppler interferometric measurements in vivo of axial eye length and thickness of fundus layers in chicks. *Curr Eye Res. 15*(6), 691-696.

Schmid, K., Wildsoet, C. (1996). Breed-and gender-dependent differences in eye growth and form deprivation responses in chick. *J Comp Physiol A. 178*(4),551-561.

Schmucker, C., Schaeffel, F. (2004) A paraxial schematic eye model for the growing C57BL/6 mouse. *Vis res. 44*(16), 1857-1867.

Schuman, J.S., Pedut-Kloizman, T., Pakter, H., Wang, N., et al. (2007). Optical coherence tomography and histologic measurements of nerve fiber layer thickness in normal and glaucomatous monkey eyes. *Invest Ophthalmol Vis Sci. 48*(8), 3645-3654.

Seaman, A.R., Himelfare, T.M. (1963). Correlated ultrafine structural changes of the avian pecten oculi and ciliary body of gallus domesticus. *Am J Ophthalmol. 56*, 278-296.

Shimazawa, M., Nakamura, S., Miwa, M., Tsuruma, K., et al. (2013). Establishment of the ocular hypertension model using the common marmoset. *Exp Eye Res. 111,* 1-8. DOI: 10.1016/j.exer.2013.03.010.

Smith, M.E., Becker, B., Podos, S. (1969). Light-induced angle-closure glaucoma in the domestic fowl. *Invest Ophthalmol. 8*(2), 213-221.

Sommer, A., Katz J., Quigley, H.A., Miller, N.R. et al. (1991). Clinically detectable nerve fiber layer atrophy precedes the onset of glaucomatous field loss. *Arch Ophthalmol. 109(*1), 77-83.

Sorsby, A. Benjamin, B., Sheridan, M. (1961). Refraction and its components during the growth of the eye from the age of three. MRC special report series no 301. London: Her Majesty's Stationary Office

Stone, R.A., Lin, T., Desai, D., Capehart, C. (1995). Photoperiod, early post-natal eye growth, and visual deprivation. *Vis Res 35*(9),1195-1202

Tappeiner, C., Goldblum D, Katsoulis, K, Sarra, G.M., Fruch, B.E. (2011). In vivo measurement of central corneal thickness in normal chicks (Gallus gallus domesticus) with the optical low coherence reflectometer. *Vet Ophthalmol.14*, 257-261.

Torczynski, E. (1979). Survey of changes in the eye. In: Bowden, D.M., editor. Aging in nonhuman primates. New York: Van Nostrand Reinhold, 143-157.

Tripathi, R.C., Tripathi B.J. (1973). The mechanism of aqueous outflow in birds II. An Ultrastructural study of perfused eyes. *Exp Eye Res. 15*(3), 425-434.

Troilo, D. (1990). Experimental studies of emmetropization in the chick. *Ciba Found Symp 155*, 89-102; discussion 102-114.

Troilo, D., Gottlieb, M.D., Wallman, J. (1987). Visual deprivation causes myopia in chicks with optic nerve section. Curr Eye Res. 6(8), 993-999.

Vaegan, S.L., Goldberg, I., Buckland, L., Hollows, F.C. (1995). Flash and pattern electroretinogram changes with optic atrophy and glaucoma. *Exp Eye Res. 60*(6), 697-706.

Ventura, L.M., Prociatti, V. (2006). Pattern electroretinogram in glaucoma. *Curr Opin Ophthalmol 17*(2), 196-202.

Ventura, L.M, Sorokac, N., De Los Santos, R., Feuer, W.J., Prociatti, V. (2006). The relationship between retinal ganglion cell function and retinal nerve fiber layer thickness in early glaucoma. *Invest Ophthalmol Vis Sci. 47*(9), 3904-3911.

Wallman, J., Adams, J.I. (1987). Developmental aspects of experimental myopia in chicks: susceptibility, recovery, and relation to emmetropization. *Vis Res. 27*(7), 1139-1163.

Wallman, J., Adams, J.I., Trachtman, J.N. (1981). The eyes of young chickens grow towards emmetropia. *Invest Ophthalmol Vis Sci. 20*(4), 557-561.

Wallman, J., Winawer, J. (2004). Homeostasis of eye growth and the question of myopia.

Neuron. 43(4), 447-458.

Wangsupadilok, B., Greenstein, V.C, Kanadani, F.N., Grippo, T.M. et al. (2009). A method to detect progression of glaucoma using the multifocal visual evoked potential technique. *Doc Ophthalmologica. 118*(2), 139-150.

Weber, A.J., Zelenak, D. (2001) Experimental glaucoma in the primate induced by latex microspheres. *J Neurosci Methods.111*(1), 39-48.

Weale, R.A. (1982). A biography of the eye: development-growth-age. London, HK Lewis

Weale, R.A. (1983). Ocular anatomy and refraction. *Doc Ophthalmol. 55*(4), 361-374.

Weiss, S., Schaeffel, F. (1993). Diurnal growth rhythms in the chicken eye: relation to myopia development and retinal dopamine levels. *J Comp Physiol A. 172*(3), 263-270.

Werner, J.S, Keltner, J.L, Zawadski, R.J., Choi, S.S. (2011). Outer retinal abnormalities associated with inner retinal pathology in nonglaucomatus and glaucomatous optic neuropathies. Eye (Lond). 25(3)279-289.

Wildsoet, C.F. (1997). Active emmetropization-evidence for its existence and ramifications for clinical practice. *Ophthalmic Physiol Opt. 17*(4), 279-290.

Wildsoet, C, Wallman, J. (1995). Choroidal and sclera mechanisms of compensation for spectacle lenses in chicks. *Vis Res. 35*(9), 1175-1194.

WoldeMussie, E., Ruiz, G., Wijona, M., Wheeler, L.A. (2001). Neuroprotection of retinal ganglion cells by brimonidine in rats with laser-induced ocular hypertension. *Invest Ophthalmol Vis Sci. 42*(12), 2849-2855.

Wygnanski, T. Desarnik, H. Quigley, H.A., Glovinsky, Y. (1995). Comparison of ganglion cell loss and cone loss in experimental glaucoma. *Am J Ophthalmol. 120*(2), 184-189.

Zadnik, K., Manny, R.E., Yu, J.A., Wang, R., et al. (2006). Normal development of refractive state and ocular dimensions in guinea pigs. *Vis Res. 46*(18), 2815-2823.

Zhu, X, Lin, T, Stone, R.A., Laties, A.M. (1995). Sex differences in chick eye growth and experimental myopia. *Exp Eye Res. 61*(2), 173-179.